THE INFLUENCE OF OVERLOADS ON CONSTANT AMPLITUDE FATIGUE CRACK GROWTH IN ALUMINIUM 7050-T7451

A Thesis

Submitted to the Department

of

Mechanical Engineering

at

The University of Adelaide

by

Geoffrey Roland Rohrsheim

B.E. (Aerospace)(HONS), AssDip CompApp

In Partial Fulfilment of the Degree

of

Master of Engineering Science

(1/3 course work, 2/3 research)

August 1995

TABLE OF CONTENTS

LIST OF FIGURES

LIST OF TABLES

ABSTRACT

The research presented is aimed at investigating current methods in Linear Elastic Fracture Mechanics for their suitability to predict crack growth in aluminium 7050-T7451, when a compressive residual stress field has been introduced by an overload.

A comparative study has been made on the effect of various levels of tensile overload on the crack growth rate in aluminium 7050-T7451. Experiments were performed on centre cracked tension specimens at two separate values of stress intensity factor range (ΔK): 300 MPa $\sqrt{mm}$ and 400 MPa $\sqrt{mm}$. Overload ratios of 1.4, 1.6 and 1.8 were investigated for each ΔK level using load shedding to maintain the ΔK value required.

Crack growth measurements were performed using crack propagation gauges (Micro-Measurements CPA series) able to detect a change in crack length of 0.25 mm and a travelling microscope accurate to 0.01 mm displacement. The propagation gauges were used to obtain average crack growth rates (da/dN) for a change in crack length of 0.25 mm. The average da/dN was used to determine an effective ΔK value for each interval using the fatigue crack propagation curve for the above aluminium alloy. The travelling microscope was used to measure the increase in crack length observed during the application of each overload. After the overloads the propagation gauges revealed a period of significant retardation before the crack growth rates returned to their baseline levels.

The total number of cycles required to return to baseline crack growth rates after the application of the overloads were compared to the number of cycles expected in the absence of an overload at the relevant ΔK level. The difference was recorded as the number of retarded cycles for the relevant ΔK level and overload ratio combination. The number of retarded cycles was found to increase with increased overload ratio and decrease with increased ΔK level.

Periodic overloads were applied during a constant amplitude fatigue test to demonstrate possible life enhancement. A single overload (ratio = 1.8) was applied every 5×10^4 cycles producing a significant increase in specimen life.

A Finite Element Analysis was used to model the M(T) specimens under consideration and to determine the value of the Mode-I stress intensity factor (K_I) at various crack lengths. These values were compared with values obtained from available literature, to the output of an established equation and to values calculated using the weight function method.

An advanced crack growth computer model (CG90ARL), provided by the Aeronautical and Maritime Research Laboratory was used to predict crack growth in the specimens. The CG90ARL program is a modified version of a computer program written by McDonnell Douglas Aircraft Company. The predictions were compared with the obtained experimental results and indicate that the CG90ARL program produces conservative results for both constant amplitude crack growth and overload induced retarded growth. A computer program utilising the Wheeler retardation algorithm was developed and a value for the Wheeler exponent obtained from experimental results.

ORIGINALITY STATEMENT

This work contains no material which has been accepted for the award of any other degree or diploma in any university or other tertiary institution and, to the best of my knowledge and belief, contains no material previously published or written by another person, except where due reference has been made in the text.

I give consent to this copy of my thesis, when deposited in the University Library, being available for loan and photocopying.

G.R. ROHRSHEIM
25 August 1995

ACKNOWLEDGMENTS

The author wishes to thank two of his supervisors Dr. Muhammad Wahab (University of Adelaide) and Dr. Jack Finney (AMRL) for their invaluable guidance and encouragement. Their advice, suggestions and editorial corrections are gratefully appreciated.

There also many others to whom special thanks are due: Mr. Ian Brown for his many hours of assistance in conducting the experimental work and the associated photographic documentation; Mr. George Osborne for preparing the required instrumentation and for installing the crack propagation gauges to the specimens; the workshop technicians for preparing experimental apparatus; Mr. Ninh Nguyen for his enthusiastic support and suggestions; Mr. Matthew Richmond at AMRL for his assistance in using the CG90ARL crack growth model; and my younger brothers Andrew and David for their help in publishing this document.

The test material used in this research was provided by the Aeronautical and Maritime Research Laboratory in Melbourne.

CHAPTER 1

INTRODUCTION

1.0. Introduction

Economic and market forces have resulted in an increasing number of aircraft being operated beyond their original design life. Research has shown that the most limiting factor in extending aircraft life has been the fatigue performance of the critical locations of the aircraft structure [Jones and Miller (1991)]. Fastener holes and other circular cut outs are examples of the identified critical locations which act as stress raisers, often resulting in fatigue cracking. Aircraft manufacturers are continuously investigating ways to lower the fatigue susceptibility of these areas. Realising that complete removal of fatigue initiation is impossible, the industry, and particularly the aircraft operators, is also interested in methods which slow down the growth of an existing crack or even stop the process of fatigue crack propagation.

One method of fatigue life enhancement is to introduce compressive residual stresses by controlled yielding of the material ahead of the crack tip . It is well known that such compressive stresses can significantly increase the fatigue life of a component [Reid (1991), Meguid (1989), Broek (1986), Averbach *et al* (1984), Nelson (1982)]. Meguid *et al* (1989) believes that the application of fracture mechanics methodology, to assist in understanding the influence of residual stresses on fatigue fracture, has not yet been given its due attention.

Work has shown that after applying an overload in a constant amplitude fatigue test the crack growth rate during subsequent constant-amplitude cycling will be reduced [Ward-Close *et al* (1988), Robin *et al* (1984)]. An overload, as depicted in Figure 1.1, is defined as any single loading event applied in a constant amplitude fatigue test which exceeds the maximum load level of the baseline constant amplitude cycles.

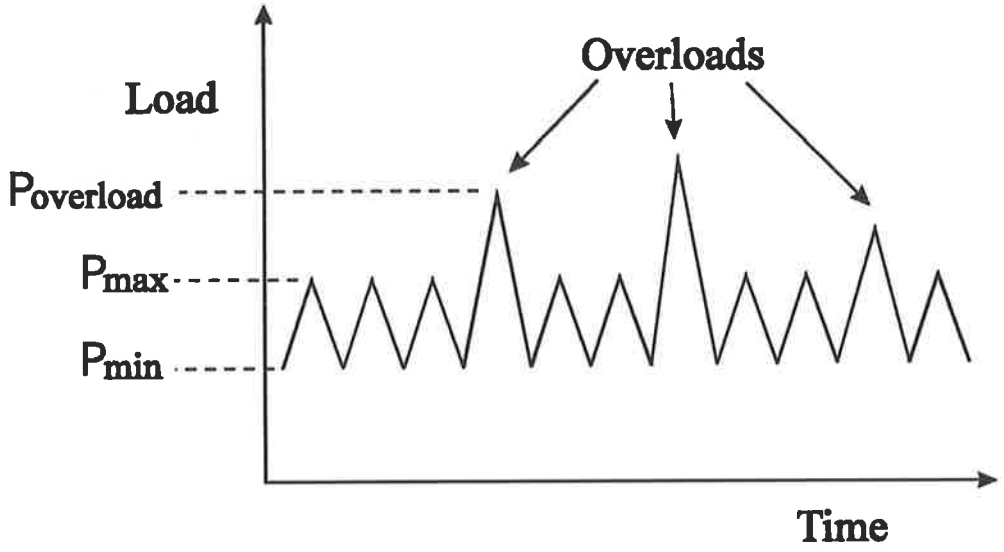

Figure 1.1 Definition of an overload

The magnitude of the overload is normally expressed as a non-dimensionalised ratio of the overload level divided by the maximum load level in the baseline constant amplitude cycles:

$$\text{overload ratio} = \frac{P_{\text{overload}}\ (\text{Newton})}{P_{\text{max load}}\ (\text{Newton})} \tag{1.1}$$

The resulting delay in crack propagation depends on the magnitude of the overload ratio while multiple overloads have been found to cause additional retardation. In some instances, application of an overload may totally arrest crack growth at subsequent low amplitude cycling [Broek (1986), Ranganathan *et al* (1984)].

This research presented here is aimed at investigating current methods in Linear Elastic Fracture Mechanics (LEFM), for their suitability to predict crack growth in aluminium 7050-T7451, when a compressive residual stress field has been introduced by an overload.

Aluminium 7050-T7451 is used extensively in the structure of modern Fighter Aircraft, operated by the Royal Australian Air Force (RAAF). When a crack is found in an aircraft,

the RAAF requires a method of prediction of the subsequent crack growth rate. This enables the operator to:

(i) effectively plan for the repair or replacement of the fatigued component;

(ii) to determine maintenance intervals for components; and

(iii) monitor airframe fatigue life to plan for the replacement of an aircraft type.

The fatigue life of a component comprises both crack initiation and propagation (growth) stages. In the damage tolerance design philosophy used in modern aircraft development, the designer must assume pre-existence of cracks, flaws and stress concentrations. Components designed using this philosophy must be able to sustain the design number of fatigue cycles before these flaws grow to the critical length at which failure is likely to occur. Initial flaws include stress risers due to manufacturing errors, maintenance damage, or corrosion. Stress concentrations occur due to poor design details including abrupt changes in thickness and geometry and the use of adjacent members of incompatible stiffness [Polakovics (1991)].

The RAAF, as operators of aircraft developed using the damage tolerance philosophy and sponsors of this research, is primarily interested in the nature of the fatigue crack propagation which will occur during the life of an aircraft due to the existence of initial flaws.

M(T) type specimens (previously known as CCT type specimens) were used in this work and a flaw was introduced in each specimen by cutting a very fine notch in the centre of each specimen. This provided areas of stress concentration at each end of the notch which ensured the development of a through-the-thickness crack at the centre of each specimen. The complete specifications of each specimen tested are mentioned in Chapter 5 of this report.

1.1. Scope of the Report

Chapter 2 contains a summary of the background to the problem investigated and the literature review conducted in this work. Previous work on overload induced compressive residual stresses was investigated as well as the models developed and proposed to account for the reduced crack growth rates following application of one or more overloads. The concepts of fatigue crack growth and the concept of linear elastic fracture mechanics are reviewed in chapter 3 with emphasis placed on the calculation of the mode I stress intensity factor K_I. Chapter 4 investigates two computer models used in crack growth prediction. An advanced computer model provided by AMRL is compared to a program developed by the author using the theory discussed in chapter 3. The experimental methods used in this study are outlined in chapter 5 while chapter 6 details the results of the experiments conducted. Chapter 7 concludes the work presented in this study and provides recommendations for future work.

CHAPTER 2

BACKGROUND AND LITERATURE REVIEW

2.1. Introduction

Residual stresses (or self induced permanent stresses) are produced when one region of a part or specimen experiences permanent plastic deformation while other regions of the same part or specimen either remain elastic or are plastically deformed to a different degree [Fuchs and Daly (1987)]. Residual stresses are introduced in metals either intentionally by surface treatments such as shot-peening, hammering, carburising, or induction hardening, or unintentionally by most manufacturing processes such as forging, rolling, welding, grinding, and other machining processes. It is well known that residual stresses have a marked influence on the fatigue life of engineering components. The residual stresses effectively add a mean stress to the fatigue cycle. In metal fatigue it is the tensile stresses which produce fatigue damage (crack growth etc.) whereas applied compressive stresses have little effect. It is therefore recognised that adding compressive *residual* stresses can retard (reduce) fatigue crack growth and in some instances even stop crack growth, while tensile residual stress regions produce the opposite effects. The aim of this research was to investigate the phenomenon of compressive residual stresses and their effect on fatigue crack growth in aluminium 7050-T7451.

The fundamental principle of LEFM is the use of the stress intensity factor as the characterising parameter for crack extension [Ewalds *et al* (1991)]. The determination of the fatigue crack propagation curve is an essential part of the fracture mechanics design approach, as the rate of fatigue crack propagation (da/dN) is governed by the range of stress intensity factor (ΔK) [Broek (1986)]. In accordance with ASTM E647-88a, a fatigue test was carried out to obtain the relationship between ΔK and da/dN for aluminium 7050-T7451. The results were compared to data published for the same type of aluminium alloy.

The stress intensity factor for a centre cracked plate can be found from tables [Rooke and Cartwright (1976)] or from equations developed for a number of common geometries [ASTM E647-88a, Broek (1986), Ewalds *et al* (1991)]. Crack propagation curves produced in the above procedure provide a method of predicting crack growth rates in components made of the same material. This method of crack growth prediction however, is not valid when retardation is considered due to interaction effects relating to the history of the preceding crack growth. The crack geometry, the magnitude of the upper and lower limits of the load cycles and the condition of the crack-tip material are all factors to be considered in the study of crack propagation. A simple summation procedure using constant amplitude crack growth data will usually produce conservative results [Meguid (1989)]. For an accurate crack growth prediction the crack growth retardation effect caused by compressive residual stresses induced into the material must be considered.

2.2. Retardation due to Residual Stresses

There has been a great deal of work done into retardation of crack growth due to compressive residual stress fields [Lai *et al* (1992), Reid (1991), Heller *et al* (1991), Meguid (1989), Broek (1986), Averbach and Bingzhe (1984), Fleck and Smith (1984), Nelson (1982)]. There are a number of methods of inducing compressive residual stress fields into a component. Shot peening [Fuchs and Daly (1987)] has long been used by the aircraft industry to induce such stresses at the surface of aircraft components. Cold working techniques such as the split sleeve method and the ballised hole method, are widely used to enhance the fatigue life of holes in aircraft structures [Lam (1991), Reid (1991), Saunder (1991)].

Earlier work has shown that after applying an overload in a constant amplitude fatigue test, the crack growth rate during subsequent constant-amplitude cycling will be reduced. The

overload introduces a large plastic zone in which the material experiences permanent deformation. Upon unloading, the surrounding elastic material attempts to resume its original size (the plastic zone is permanently deformed) and by doing so exerts compressive stresses on the plastically deformed material at the crack tip. This stress interaction and the resulting residual stress system are reported by Broek (1986) and shown in Figure 2.1.

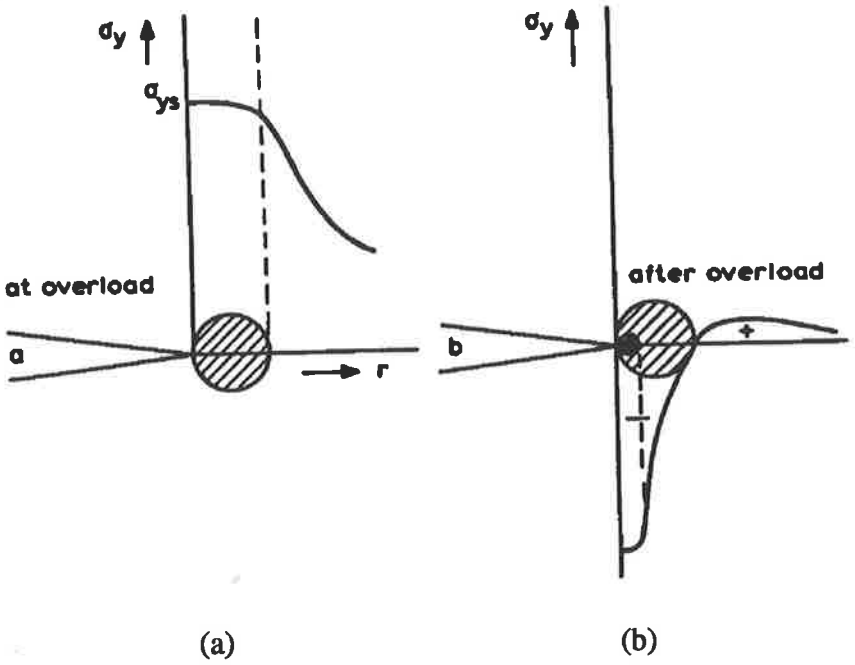

Figure 2.1. Residual compressive stresses at the crack tip as a result of overload

The residual compressive stresses (represented by the minus sign in part b of figure 2.1) tend to close the crack tip and retard crack propagation. When the crack has grown through the region of residual stresses after a further period of fatigue loading, crack growth resumes at the propagation rate expected under constant amplitude fatigue testing. The concept of crack growth and retardation interaction is discussed later in this chapter and again in chapter 4.

Work done by a number of researchers has shown definite crack growth retardation following the application of an overload but has had little success in quantifying the reduced

crack growth. In order to quantify the effect of residual stresses upon fatigue crack growth, it is necessary to know:

(i) the magnitude and shape of the residual stress field;

(ii) the combined effect of the residual and applied stresses upon fatigue crack growth rate; and

(iii) how the existing residual stress field changes as the crack grows under the influence of service loads.

2.3. The Residual Stress Field

Residual stress distribution is difficult to measure accurately and is therefore usually based on an approximate stress field. Common methods used include the hole-drilling technique [Meguid (1989), ASTM E837] and X-ray diffraction [Hauk (1987)]. Taira and Tanaka (1978) used the X-ray microbeam diffraction technique to measure the local stress near the tips of fatigue cracks after the application of single and multiple overloads. Their theoretical prediction of the growth rate of a fatigue crack based on information on the local residual stress distribution near the tip agreed with their experimental results. Measurements of residual stress distribution using strain gauges or X-ray diffraction technique only provide residual stress values at specific locations and were therefore deemed unsuitable for use in this work. Lam and Lian (1989) recently used grid lines laid on the surface of the specimens using the photoresist technique. The measured displacements of the grid points, following introduction of a residual stress field, were used as the boundary conditions for a finite element model of the specimen. The method provided residual stress distribution over the entire region of interest [Lam and Lian (1989)]. This method was unavailable for use in this work.

Accurately modelling residual stress fields has proved to be difficult. There is a lack of agreement between residual stress models and those measured experimentally [Saunder (1991)]. In this work, an estimate was derived experimentally for the average residual stress field over a set distance beyond the location of the application of the overload. Chapter 5 describes how a value for the average residual stress field produced by the application of an overload, was found experimentally.

2.4. Combined Effect of Applied Stresses and Residual Stresses

The theory of linear superposition has been used by many researchers [Lam and Lian (1989), Averbach and Bingzhe (1984), Skalli and Flavenot (1984), Fleck and Smith (1984), Nelson (1982)] to combine the effect of the residual and applied stresses upon fatigue crack growth rate. For example, Averbach *et al* (1984) used the superposition approach and associated the internal stresses with an internal stress intensity factor, K_i, which was added to the applied stress intensity factor, K_a. Thus the net or effective stress intensity, K_e, became:

$$K_e = K_a + K_i$$

where, K_e = the effective stress intensity factor

K_a = the applied stress intensity factor, calculated from the applied load P, the crack length, and the specimen geometry

K_i = the internal stress intensity factor introduced by other factors such as internal stress, side loads etc.

This superposition principle is illustrated in figure 2.2 [Ewalds *et al* (1991)]:

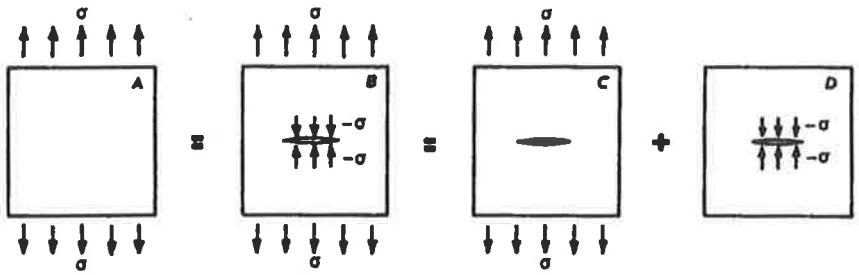

Figure. 2.2. Illustration of the superposition principle

They assumed a residual stress pattern inferred from data which were taken from a flat surface which was carburised at the same time. Their work was a qualitative exercise as notch effects were not considered nor the redistribution of residual stresses which takes place as the crack propagates through the residual stress zone.

Fleck and Smith (1984) investigated the effect of periodic overloads and periodic underloads in low strength steels and an aluminium alloy. By correlating crack growth with that part of the applied stress range for which the crack is open (ΔK_{eff}), they were able to account for both retarded and accelerated growth. Fleck *et al* (1984) also sited the major disadvantage with the ΔK_{eff} approach ie. there is no simple design rules to enable ΔK_{eff} to be calculated from material properties and extensive testing is required before the method can be used effectively. Lam (1989) noted the need for extensive testing to calibrate ΔK_{eff} models for specific materials and expressed the need for further investigations. Finney and Deirmendjian (1992) examined equations developed for ΔK_{eff} and noted that the formulas were material dependant.

The residual stress fields described above are assumed to remain constant and do not redistribute as the crack propagates. In reality the internal stresses in a component change

as the crack propagates in order to meet the requirement of equilibrium on the crack line. For the superposition theory to accurately predict crack retardation due to a change in the ΔK (ΔK_{eff}), it is important to know how the residual stress field changes as crack growth continues after the overload. Lam (1989) showed that if stress redistribution is not accounted for it can lead to non-conservative life prediction. Despite this the effect of residual stress redistribution as the crack propagates is often not taken into account [Lam and Lian (1989)]. To measure the stress field using either the X-ray diffraction method or the hole-drilling method at very small crack growth intervals would be a long and labour intensive procedure. Hence in this work an average value was obtained for the length of crack growth which experienced retardation. Chapter 5 describes in detail how this was achieved.

To effectively and viably implement in practice the theory demonstrated by researchers it is necessary to develop models which describe their work. These models can then form the basis for computer programs which can be used to predict crack growth. Any model should obviously be rigorously validated with experimental results before being used to predict crack growth in any practical situation.

2.5. Retardation Models

There have been a number of crack growth models developed which have endeavoured to account for load interaction effects. These models are of two types [Broek (1986)]:

(i) models based on crack tip plasticity ("first generation" models)

(ii) models based on crack closure ("second generation' models)

Wheeler [Meguid (1989), Broek (1986)] used a retardation parameter, phi in his first generation model based on the ratio of the current plastic zone size and the size of the plastic enclave formed at an overload to predict reduced crack growth due to residual stresses. These models rely completely on material specific empirical constants which can be adjusted to fit experimental results. The model proposed by Wheeler has become popular due to its use of a single retardation constant. The Wheeler model is discussed in detail in chapter 4 where it is used as the basis for a Pascal program developed in this study.

Elber (1968) introduced the notion of the crack opening load, which is defined as the load level at which the crack surfaces have lost contact along the entire crack. de Konig *et al* (1992) reviewed a computer model which incorporated this concept and which has been applied in practice. Once again, however, they noted that the weakness of the approach was that it relied on empirically obtained "material" parameters. This, therefore, introduced the need for extensive test programs to determine these parameters for each new material under investigation.

More recent crack growth models have attempted to incorporate the concept of crack closure [Ewalds *et al* (1991)]. In such models the level of stress at which the crack begins opening (σ_{op}) is required. This method again relies on extensive experimental testing to obtain required parameters and in addition uses large complex computer programs to implement the models. Robin *et al* (1984) in their work on the influence of multiple overloads concluded that the crack closure concept could not satisfactorily explain retardation but rather suggested using a residual stress model of crack growth retardation.

Crack growth models which are based on crack tip plasticity rely heavily on formulas derived for the size of the plastic zone created by each load cycle. These models assume that the length of retardation caused by the application of an overload is directly related to

the length of the overload plastic zone. The size of the plastic zones created by subsequent loading cycles will determine for how many cycles the retardation will occur.

2.6. Plastic Zone Size

Crack growth models based upon crack-tip plasticity, like Wheeler [Meguid (1989), Broek (1986)] and to a degree CG90ARL [McDonnell Douglas Aircraft Company (1991)] rely on using a formula for calculating the plastic zone size created by a load (equation 2.1). For an overload, the plastic zone size calculation will determine the length over which crack growth retardation occurs. The number of load cycles which are retarded will be determined by the plastic zone size produced by each load cycle. Crack growth retardation ceases if the calculated plastic zone size at a given crack length extends beyond the edge of the original overload plastic zone region. This interaction of plastic zones following an overload will be discussed in detail in Chapter 4.

The general equation for the plastic zone size is of the following form:

$$r_p = C_{pz} \frac{K_I^2}{\sigma_{ys}^2} \tag{2.1}$$

where

	r_p	=	plastic zone size
	C_{pz}	=	constant
	K_I	=	Mode-I stress intensity factor
	σ_{ys}	=	yield stress of the material

The value of the above constant C_{pz} is dependant on the state of stress in the component. The plane strain plastic zone is significantly smaller than the plane stress plastic zone. Plain strain conditions exist in this work and according to Irwin [Broek (1986)] the value of C_{pz}

= $1/6\pi$ is commonly taken but not universally used for plane strain conditions. An examination of the source code for the CG90ARL crack growth program (a modified version of a computer program written by the McDonnell Douglas Aircraft Company) indicated that the value of C_{pz} used in that program was:

$$C_{pz} = \frac{Beta}{\pi} \tag{2.2}$$

where:

$$Beta = 0.333333 + 0.5 * Alpha + 0.166667 * Alpha^2 \tag{2.3}$$

The value of *Alpha* referred here as the retardation parameter [McDonnell Douglas Aircraft Company (1991)] was by default equal to zero resulting in a value of $C_{pz} = 1/3\pi$. This is exactly twice the value suggested by Irwin and recommended by Broek ($1/6\pi$). This is a major difference in a factor which plays a major role in determining retarded crack growth due to the interaction of plastic zone sizes (The CG90ARL program is discussed in more detail in Chapter 4).

Models such as the one proposed by Wheeler [Broek (1986)] assume that crack retardation occurs over the length of the plastic zone created by the overload. The work done by Ward-Close *et al* (1988) indicated that the distance over which crack growth was retarded by the overloads was well in excess of the *computed* maximum extent of the overload plastic zone size. The investigations by Ward-Close *et al* revealed a potential for error in retarded crack growth predictions based on plastic zone sizes. The following section will discuss other sources of error identified by researchers of crack growth prediction methodology.

2.7. Accuracy of Crack Growth Prediction

Experimentally obtained crack growth data for most materials produces considerable scatter. Repeat experiments for the same material, using identical specimens, in controlled environments, and applying the same constant amplitude loading, can produce vastly different results. Finney and Deirmendjian (1992) cited that the known variability in crack growth rate data may be of the order of two. This suggests that material anomalies play a large part in determining crack growth. If a crack growth model fails to exactly predict crack growth subsequently found during experiments or under working conditions, it does not therefore prove that the predictive method is unsound.

Broek (1986) lists the following factors which can affect the accuracy of any crack growth prediction model:

(i) uncertainty in the local [residual] stress level;

(ii) uncertainty in the stress intensity calculation;

(iii) insufficient knowledge of the load spectrum applied;

(iv) possible environmental effects; and

(v) the quality of the constant amplitude crack growth rate data used.

The extent of each of these factors and their relevance to this work will be discussed in later chapters. Taking into account all the errors that can enter throughout in such a complex analysis it appears that a substantial safety factor should be applied to crack growth predictions. Instead of applying individual safety factors to each potential source of error a safety factor is normally applied to the final result obtained. In practice this means dividing the number of cycles to a certain crack length by a constant safety factor.

Before embarking on an experimental program to observe both constant amplitude fatigue crack growth and crack growth retardation due to the application of an overload a review of experimental procedures was carried out. Fleck and Smith (1984) noted that load

interaction studies are complicated and require highly developed experimental techniques to see each of the phenomena involved.

2.8. Experimental Techniques

Taylor and Knott (1984) investigated the effect of load cycling frequency on fatigue crack propagation rate da/dN. They tested at frequencies between 0.1 Hz and 100 Hz and found that crack growth rate per cycle increased as the frequency decreased. Within the range of frequencies studied a change in frequency by a factor of 10 caused a change in da/dN by a factor of 1.3. It is important to be aware of this effect if predictions of fatigue life in service are to be made using the results of laboratory tests accelerated by increasing frequency.

Ranganathan *et al* (1984) studied the influence of the initial range of stress intensity factor (ΔK) level on the fatigue crack retardation process in 2024-T351 aluminium alloy following an overload. The test frequency was 20 Hz in air, the load ratio (R = min load/max load) was 0.1 and the overload ratio was very near 2. After the tests the specimen surfaces were examined under interferential contrast to analyse the development of the plastic zones and the behaviour of the crack in the overload affected region. Their experimental results showed that several types of delay behaviour were observed according to the initial ΔK level for the same overload ratio. The conditions for their occurrence and the governing factors were:

(i) Low ΔK region: high delay and even crack arrest, under plain strain condition, the microstructural factors playing an important role;

(ii) Mid ΔK region : minimum delay corresponding to a predeformed fatigue zone of the order of 1 grain and to the

transition from plane strain to plane stress conditions at the crack tip; and

(iii) High ΔK region: more pronounced delay associated with the plane stress conditions developed at the crack tip and residual stress effect.

Robin *et al* (1984) studied the influence of applying multiple overloads on fatigue crack growth. They noted that the distance affected by overload was independent of the number of overloads but the number of cycles to propagate that distance did increase with increased number of overloads. This suggests that the intensity or magnitude of the compressive residual stress is increased by the increase in number of overloads while the size of the plastic zone, which determines the length over which retardation occurs, is not affected by the increasing number of overloads.

The accurate measurement of the crack length at any time is the most important factor to be considered in any experimental work designed to investigate crack propagation rates. The three most common methods used by the other researchers were:

(i) travelling microscope;
(ii) the DC potential drop method; and
(iii) the compliance method.

No crack growth measurement method was available in the Department of Mechanical Engineering at the start of this work. One of the objectives of this work was therefore to develop methods of fatigue crack growth measurement.

2.9. Research Objectives

The main objective of this work was to determine the stress intensity arising from residual stress distribution at a fatigue crack tip. To achieve this the following work was undertaken:

(i) investigate Mode I stress intensity factor values in the specimens under consideration, using FEM calculations;

(ii) develop methods of measuring crack growth during fatigue testing;

(iii) produce a da/dN vs ΔK curve for aluminium Alloy 7050-T7451;

(iv) demonstrate crack growth retardation following application of a single overload;

(v) quantify ΔK_{eff} values in the overload affected area;

(vi) compare the ability of computer models to predict both constant amplitude fatigue crack growth and crack growth following an overload; and

(vii) demonstrate the increase in fatigue life attainable using periodically applied overloads.

CHAPTER 3

THEORETICAL ANALYSIS

3.0. Introduction

In this chapter the theory of linear elastic fracture mechanics (LEFM) will be reviewed with particular emphasis placed on the role of the stress intensity factor. Various methods for determining the value of the stress intensity factor at different crack lengths, for the centre-cracked flat plate specimens are described and finally compared in the last section (3.3.5) of this chapter.

3.1. Linear Elastic Fracture Mechanics

Failures under loading conditions well below the material yield stress often occur in structures with small cracks or material flaws. Such failures have highlighted that conventional static strength studies are not always sufficient to guarantee structural integrity under operational conditions. The field of study which considers crack-extension behaviour as a function of applied loads is known as fracture mechanics [Dally and Riley]. When flaws such as cracks exist in a body, elastic theory is not sufficient to completely predict the onset of failure due to the geometry of the crack tip. The crack tip is sharp with a radius of curvature approaching zero which leads to the prediction of local stresses which tend to infinity. Fracture mechanics treats this singular state of stress at the crack tip by using a quantity known as the stress intensity factor K, defined as:

$$K_I = \lim_{r \to 0} (\sqrt{2\pi\ r\sigma_{yy}}) \qquad (3.1)$$

Equation (3.1) provides a stress intensity factor that is a linear function of the loads applied to the body and provides a means of determining the critical load condition. Chapter 2

discussed the existence of the plastic zone formed at the crack tip during fatigue loading. The radius of the plastic zone is small enough in relation to the entire crack length to justify using the theory of linear elastic fracture mechanics in all cases.

A crack in a solid can be stressed in three different modes leading to three different stress intensity factors. Normal stresses produce the "opening mode" or Mode I loading in which the displacements of the crack surfaces are perpendicular to the plane of the crack as shown in figure 3.1. Mode I is the most predominant stress situation in many practical situations and consequently this work will only deal with the corresponding stress intensity factor, K_I.

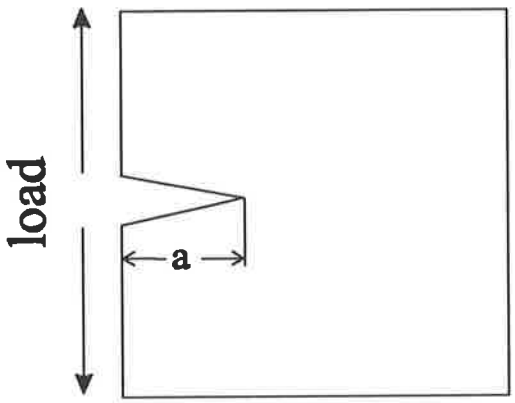

Figure 3.1 Mode I loading definition

The stress intensity factor determines the rate of fatigue crack growth per load cycle. If a constant amplitude fatigue load varies between zero and some positive value, the stress intensity cycles over a range $\Delta K = K_{max} - K_{min}$, where $K_{min} = 0$. It follows that the rate of fatigue crack propagation per cycle (da/dN) must therefore depend upon the stress intensity range ΔK . It has been found experimentally that provided the stress ratio, $R = \sigma_{min}/\sigma_{max}$, is the same then ΔK correlates fatigue crack growth rates in specimens of different geometry. Although researchers have noted that crack growth rates under such controlled conditions, may vary by as much as a factor of 2 [Finney and Deirmendjian (1992)]. The two most widely used formulae for describing crack growth rate curves are [Broek, Wanhill]:

$$\frac{da}{dN} = C(\Delta K)^n \qquad \text{- Paris' equation} \qquad (3.2)$$

$$\frac{da}{dN} = \frac{C(\Delta K)^n}{(1-R)K_c - \Delta K} \qquad \text{- Forman's equation} \qquad (3.3)$$

where a = half of crack length

N = number of load cycles applied

C, n = material constants

ΔK = range of stress intensity factor ($\Delta K = K_{max} - K_{min}$)

The initial concept proposed by Paris was that for an elastic body with only a small amount of plasticity at the crack tip if K_{crit} was a universal indicator of the onset of fracture then ΔK might be a measure of fatigue crack growth. Paris' equation describes a linear relationship between ΔK and da/dN (log/log scale) while Forman later modified the equation to more accurately describe the sinusoidal relationship found experimentally . The straight line assumption was found to be inappropriate at very low crack growth rates and at very high crack growth rates. This work was restricted to crack growth rates which are adequately described using a straight line approximation and hence Paris' equation was used in all theoretical calculations. To obtain the constants C and n needed in Paris' equation experimental data must be obtained for the material required. In a double-logarithmic plot, the da/dN versus ΔK often fall on a straight line, allowing the calculation of the constants C and n using any two points.

The stress intensity factor for mode-I has the following form:

$$K_I = Y\sigma\sqrt{\pi a} \qquad (3.4)$$

where Y = dimensionless configuration factor expressed as a function of crack length and specimen geometry

σ = remotely applied nominal stress

The value of Y can be found experimentally, or for common geometries is also available from tables. For the case of a centre cracked flat plate Broek (1986) suggests the following formula for Y which the ASTM-E647 also recommends:

$$Y = \sqrt{\sec\left(\frac{\pi a}{W}\right)} \tag{3.5}$$

where W = width of the cracked plate

Combining equations (3.2), (3.4) and (3.5) provides a useful relationship between crack growth rate, da/dN, and the crack length, a:

$$\frac{da}{dN} = C\left(\sigma\sqrt{\pi a \sec\left(\frac{\pi a}{W}\right)}\right)^n \tag{3.6}$$

where C and n are both material specific constants. See figure 3.3 for the definition of the crack length terminology used in equation (3.6).

3.2. Prediction of Fatigue Crack Growth - Constant Amplitude Loading

The main purpose of crack growth predictions is to construct a crack growth curve: crack length 'a' versus number of loading cycles 'N'. It is possible to predict crack growth from any da/dN versus ΔK curve, provided the relationship between crack length, a, and ΔK is known and the material constants, C and n in equation (3.6), have been calculated. The crack length "a" versus number of cycles "N" curve is then obtained by integrating equation (3.6):

$$N = \int_{a_i}^{a_f} \frac{da}{C\Delta K^m} \tag{3.7}$$

Equation (3.7) is often calculated numerically using computer programs. Wanhill *et al*, provides a description of the algorithm used in such programs:

a. choose a suitable increment of crack growth, $da_i = a_{i+1} - a_i$;
b. calculate ΔK (in this case using equations 3.4 and 3.5) for the crack length corresponding to the mean of the crack growth increment, ie. $(a_{i+1} + a_i)/2$;
c. determine da/dN for this value of ΔK (using equation 3.6);
d. calculate dN_i from $da_i/(da/dN)_i$;
e. repeat the previous steps over the required range of crack growth and sum the values of dN_i.

Chapter 5 describes the experiment conducted and the data reduction method used to construct the da/dN versus ΔK curve for aluminium 7050-T7451, and to calculate the material constants C and n. Chapter 6 shows the results of a computer model written by the author to numerically integrate equation (3.6).

Equations (3.1) through to (3.6) have been found to provide reasonable predictions for fatigue crack propagation in a wide range of materials. The equations however, ignore a number of parameters which have been shown to affect crack growth such as the applied stress ratio, and the effect of residual stresses (as discussed in chapter 2). Researchers have therefore modified Paris' equation (equation 3.2) by replacing the stress intensity factor range ΔK with an effective stress intensity factor range ΔK_{eff}. The concept of ΔK_{eff} was described in chapter 2 and its role in this work is discussed in chapter 5.

3.3. The Stress Intensity Factor K_I

As highlighted in section 3.1, the stress intensity factor is the most critical part of LEFM and therefore warranted thorough investigation in this work. Some of the currently available methods for determining K_I for the geometry shown at figure 3.2 are described in the following sections 3.3.1 through to 3.3.4.

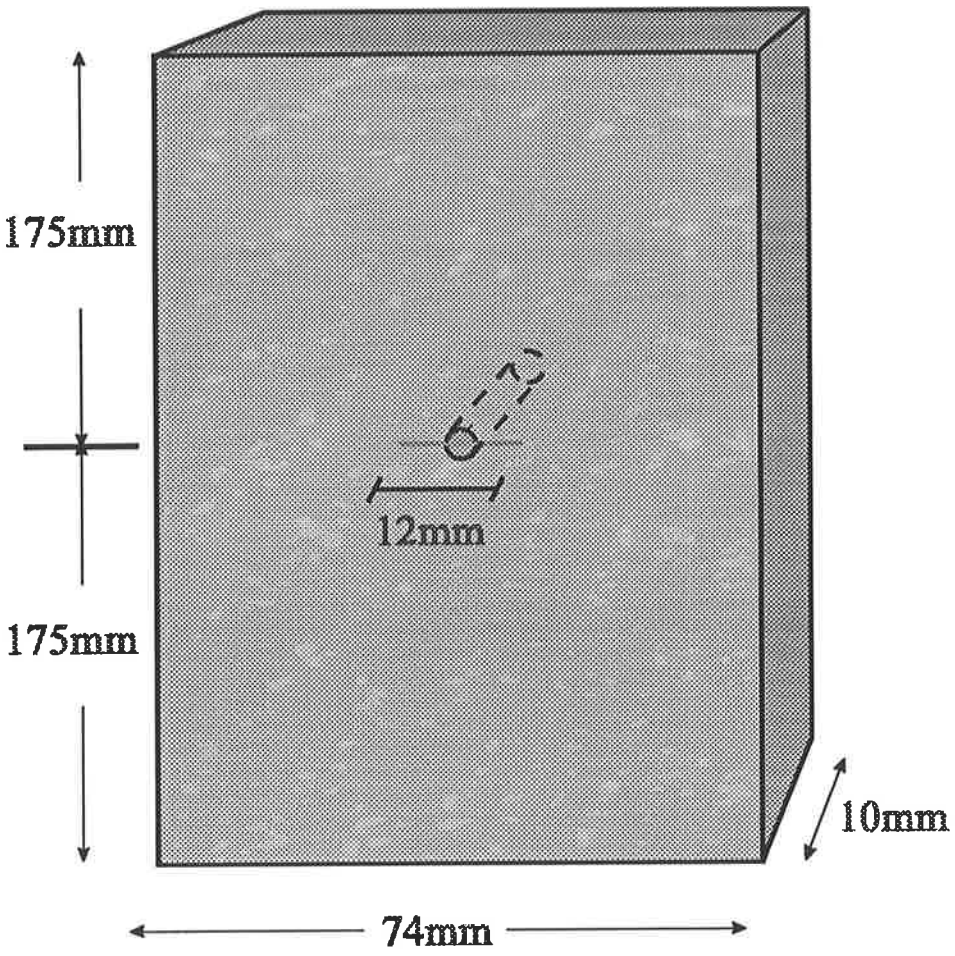

Figure 3.2 Specimen dimensions

The results obtained from each method are displayed graphically and compared to one another in section 3.3.5. The crack length definitions used in the following sections are represented at figure 3.3:

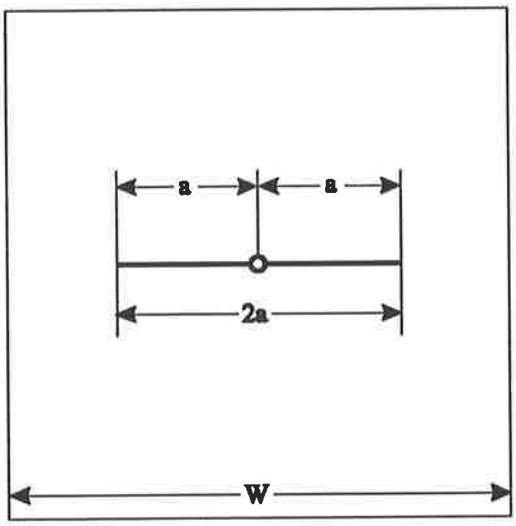

Figure 3.3 Crack length definition for M(T) specimen

Figure 3.2 shows that the specimens provided by AMRL contained starter notches 12 mm in length. In the following sections the first value of stress intensity factor K_I was therefore calculated at crack half length a (see figure 3.3) of 6 mm. The final value of K_I was calculated for a = 35 mm which is roughly 0.95 W after which the equations used are deemed invalid [ASTM-E647].

3.3.1. Handbook values for K_I

The Compendium of Stress Intensity Factors [Rooke and Cartwright (1976)] is a compilation of solutions to static crack problems, presented in a simple graphical form. Solutions for the plate in this work were extracted from Table 1.3.1 "Two cracks at a circular hole in a rectangular sheet: uniform uniaxial tensile stress" (see Appendix M). The case modelled in Table 1.3.1 is a rectangular sheet of width 2b and height 4b containing a central hole of radius "r" with two equal length cracks perpendicular to the applied stress σ. For a range of a/b values (a = half crack length) and for three values of r/b, the ratio of K_I/K_0 are plotted, where:

$$K_0 = \sigma\sqrt{\pi a} \qquad (3.8)$$

Unfortunately the plate used in this work did not have a height/width ratio of 2 and the r/b value of 0.054 was not plotted in the figure provided at Table 1.3.1. r/b=0.0 and r/b=0.25 were plotted but the dramatic difference in the shape of the respective curves prevented interpolation for r/b=0.054. Two assumptions were therefore made before Table 1.3.1 was used:

a. That the plate had a height/width ratio of 2 (no other table exists); and

b. That r/b=0.0.

At r/b=0.0 the values in Table 1.3.1 are identical to Table 1.1.1 (see Appendix N) "Central crack in a rectangular sheet: uniform uniaxial tensile stress" (ie. no hole). However, the K_I/K_0 values were obtained from Table 1.3.1 as it contained a longer range of a/b values than did Table 1.1.1. The K_I/K_0 values and the corresponding K_I results using equation (3.4) are presented in Table 3.1.

half crack length a (mm)	K_I/K_0	K_I (MPa $\sqrt{mm}$)
6	1.01	118.5
7.5	1.025	134.5
10	1.05	159.1
12.5	1.06	179.5
15	1.10	204.1
17.5	1.15	230.5
20	1.22	261.4
22.5	1.31	297.7
25	1.42	340.1
27.5	1.60	401.9
30	1.85	485.4
32.5	2.30	628.1
35	not available	not available

Table 3.1 K_I values obtained from Compendium of Stress Intensity Factors

3.3.2. Standard for crack growth rate determination

ASTM E647-88a describes the standard test method for measurement of fatigue crack growth rates (see Chapter 5 for details of this standard). Results are expressed in terms of the crack-tip stress intensity factor range (ΔK), for which the standard provided the following expression:

$$\Delta K = \frac{\Delta P}{B}\sqrt{\frac{\pi\alpha}{2W}\sec\frac{\pi\alpha}{2}} \qquad (3.9)$$

where α = 2a/W; expression valid for 2a/W < 0.95 (ie a = 35 mm for this work).

The values produced from equation (3.9) are good approximations to those obtained from the handbook in Table 3.1, making the equation ideal for computerised data reduction as described in ASTM E647. It is important to note that in equation (3.9) there is no attempt to account for the presence of the hole in the plate, which was not meant to be part of the model but was placed there so that the starter notches could be cut. The resulting K_I values obtained using equation (3.9) are tabled below in Table 3.2:

half crack length a (mm)	K_I (MPa $\sqrt{mm}$)
6	119.3
7.5	134.6
10	158.7
12.5	182.4
15	206.9
17.5	233.5
20	263.6
22.5	299.0
25	343.0
27.5	401.0
30	484.9
32.5	626.7
35	973.2

Table 3.2 K_I results using equation (3.9)

3.3.3. Finite Element Analysis

Finite Element Methods (FEM's) are a widely used structural analysis tool. The Mechanical Engineering Department at the University of Adelaide uses the ANSYS package for FEM analysis. To gain experience in using FEM software, and to investigate the extent of their use in Fracture Mechanics problems, the specimens tested were modelled using Version 5.0 of ANSYS running on a DEC UNIX machine.

ANSYS was used to calculate the Opening Mode Stress Intensity Factor (K_I) at the crack tip. The recommended element type [ANSYS User's Manual (1992)] for a two-dimensional fracture model was the PLANE2 element. The element was defined by six nodes, each having two degrees of freedom at each node. The Young's Modulus for the elements of aluminium 7050-T7451 was entered as 68900 MPa and Poisson's ratio as 0.33.

Due to the symmetry in both the X and Y directions of the plate investigated, only one half of the plate and one edge of the crack was required to be modelled. Effectively, only one quarter of the specimen was modelled as in figure 3.4.

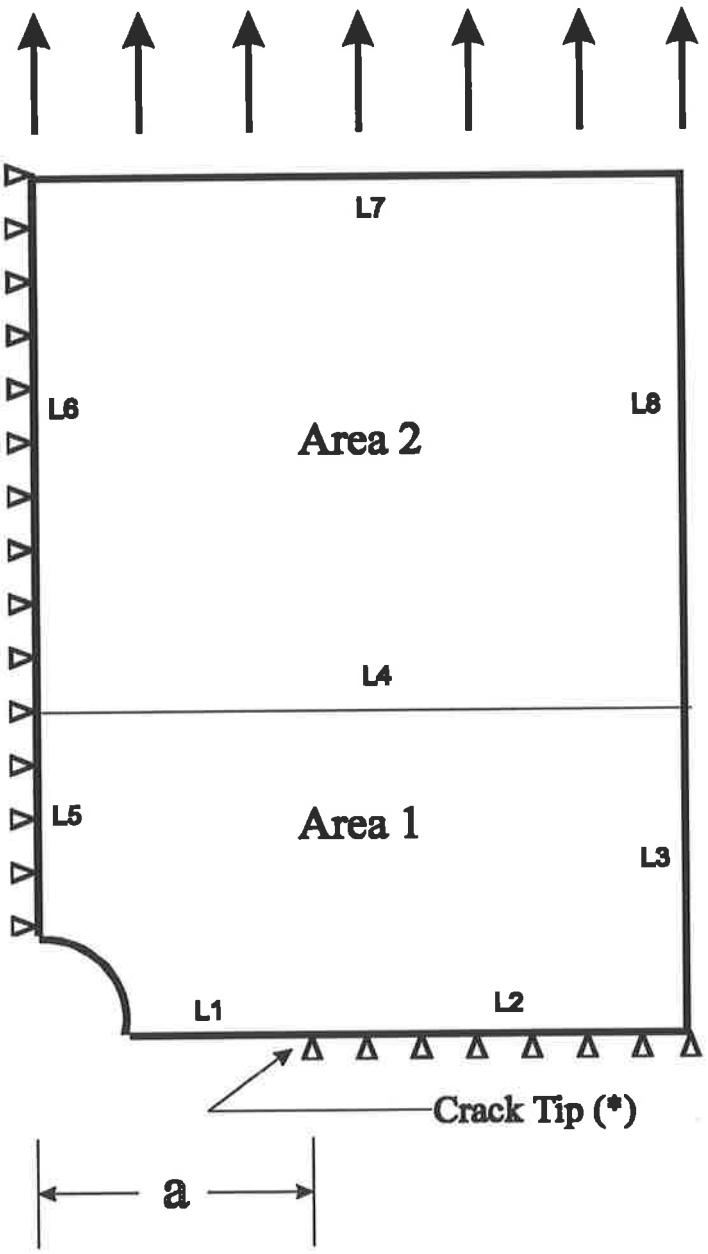

Figure 3.4 Schematic of ANSYS model used

The main area of interest on the model was at the simulated crack tip, shown on figure 3.4. To obtain accurate results for K_I the model required concentrated meshing at that point. Such fine mesh control was not needed for the remainder of the model. To significantly reduce mesh generation times and therefore solution times, the model was divided into two parts. The two parts were named areas 1 and 2 and are also shown on figure 3.4. Figure

3.5a shows an example of the mesh automatically generated by ANSYS for the specimen under consideration. Figure 3.5b is a close up of the mesh at the simulated crack tip indicating the concentration at that point.

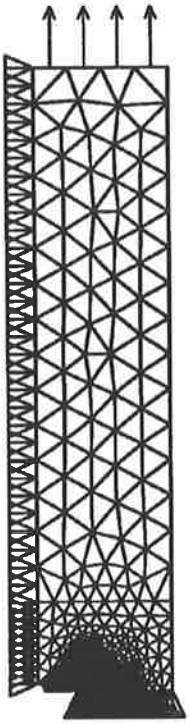

(a)

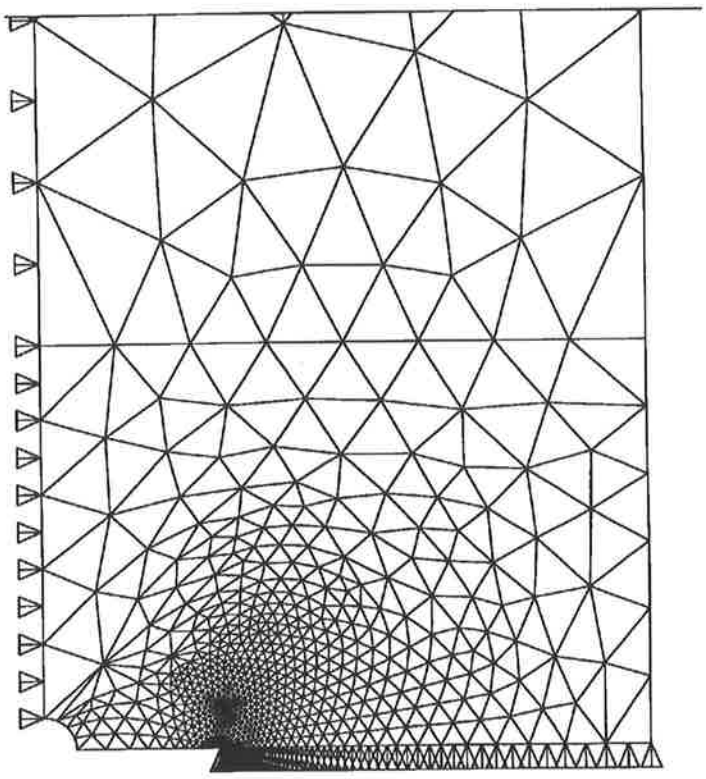

(b)

Figure 3.5 Example of ANSYS mesh used - (a) overall and (b) close up of crack tip

Constraining loads were applied to define the symmetry planes for the model. Line numbers 2, 5 and 6 of figure 3.4 were constrained, leaving line 1 and the quarter hole unrestrained to model the hole in the plate, and the crack length at a given time. The crack tip, at the point which divided lines 1 and 2, was moved to obtain each required crack length and subsequent calculation of K_I. A surface pressure load of -27.027 MPa (corresponding to a +20 kN load applied to an area 10 mm by 74 mm) was applied to line 7.

The ANSYS command KCALC determined the stress intensity factor (K_I) at each crack length using a linear elastic fracture mechanics analysis. The analysis uses a fit of the nodal displacements in the vicinity of the crack , as shown in figure 3.6.

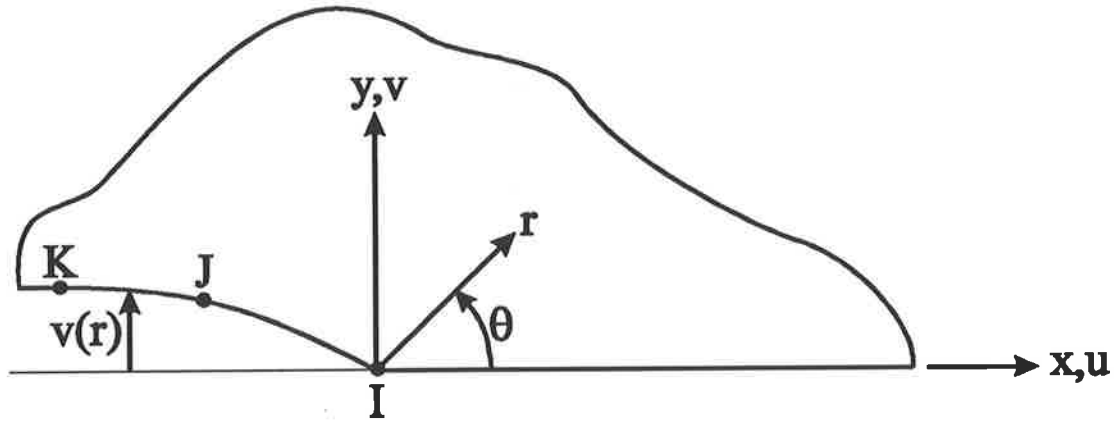

Figure 3.6 Nodes used for the approximate crack tip displacements (half-crack model)

The actual vertical displacements at and near a crack for a linear elastic material, for theta = +/-180 degrees and neglecting higher order terms [ANSYS theory manual], can be expressed as:

$$v = +\frac{K_I}{2G}\sqrt{\frac{r}{2\pi}}\,(1+x) \qquad (3.10)$$

where v = displacement in the y direction

G	=	shear modulus
r	=	coordinate in the local coordinate system
v	=	Poisson's ratio
x	=	3-4v

Equation (3.10) is rearranged to give an expression for K_I:

$$K_I = \sqrt{2\pi}\,\frac{2G}{1+x}\,\frac{|v|}{\sqrt{r}} \tag{3.11}$$

The final factor in equation (3.11), $|v|/\sqrt{r}$, was evaluated based on the nodal displacements at locations I, J, and K shown in figure 3.6. The vector v was normalised so that v at node I was zero. As K_I was required at the crack tip, ie. when r=0, the value A was determined from:

$$\lim_{r\to 0}\frac{|v|}{\sqrt{r}} = A \tag{3.12}$$

Hence equation (3.11) becomes:

$$K_I = \sqrt{2\pi}\,\frac{2GA}{1+x} \tag{3.13}$$

Stipulating plane strain conditions and utilising the KCALC command discussed above, the results obtained using the ANSYS package are tabulated at Table 3.3.

half crack length a (mm)	K_I (MPa $\sqrt{mm}$)
6	136.2
7.5	152.7
10	179.1
12.5	205.4
15	232.7
17.5	262.5
20	296.3
22.5	336.5
25	386.8
27.5	453.6
30	550.9
32.5	711.7
35	1122.5

Table 3.3 Results obtained for K_I using ANSYS version 5.0

An equation was fitted to the K_I data produced by ANSYS (see Table 3.3) so that values could be determined at any crack length between 6 mm and 35 mm. This could then be used in place of equation (3.9) in the crack growth routines discussed in chapter 4 to see the resulting change in fatigue life predicted.

$$K_1 = \frac{(a + cx + ex^2)}{(1 + bx + dx^2)} \tag{3.14}$$

where

a = 9.6739

b = 0.0725

c = 30.3227

d = -0.0025

e = -0.4725

An example of the output produced by the KCALC command, including the node numbers used, their displacements (v), and the resulting K_I value, is shown at Appendix A.

3.3.4. Weight Function

The stress intensity factor for a non-uniform but symmetric loading can be obtained from the stress intensity for another simple case of symmetric loading using weight functions [Broek (1986)]. A weight function is unique to a given geometry and is independent of the loading from which it was derived. Stress intensity factor solutions can be obtained from the following general expression [Parker (1981)]:

$$K_1 = \int_a p(x)m(x,a)\,dx \tag{3.15}$$

where p(x) = the stress distribution along the x-axis in the *uncracked* structure

m(x, a) = the weight function

Kanazawa [Nelson (1982)] developed a weight function for the centre cracked plate used in this work. His weight function m(x,a) is as follows:

$$m(x,a) = \sqrt{\frac{2\sin\frac{\pi(a+x)}{W}}{W\sin\frac{2\pi a}{W}\sin\frac{\pi(a-x)}{W}}}\,dx \tag{3.16}$$

Figure 3.10 is a graph of Kanazawa's weight function when a = 15 for -a <x < a. Note that equation (3.15) is undefined at x = a due to the $[\sin(\pi(a-x))]^{-1}$ term, so m(x,a) at x = a was not plotted.

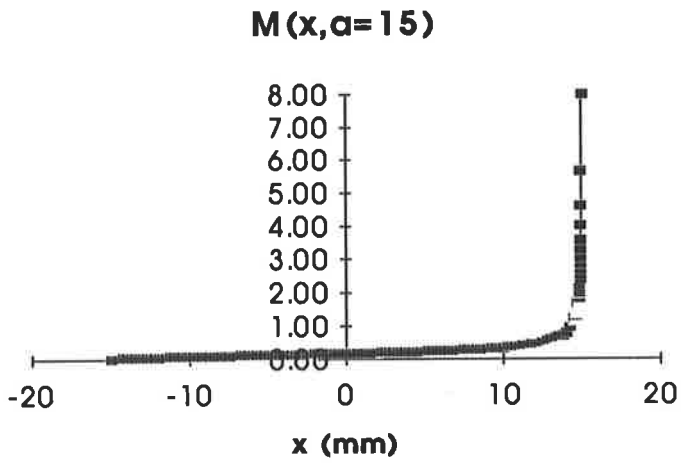

Figure 3.7 Kanazawa's Weight Function m(x,a=15)

Kanazawa's weight function is applicable to centre cracked plates only and therefore does not take into account the effect the hole would have on the solution in this case. In order to use Kanazawa's function, the hole was ignored in the geometry (and hence the weight function) and accounted for in the applied stress distribution. The stress distribution along the axis of the uncracked structure was obtained from ANSYS. For an applied stress of 27.0 MPa, the finite element solution for the stress in the Y direction, from the edge of the hole to the edge of the plate was obtained. A least squares package was used to fit an exponential equation to this stress distribution. The curve was divided into four sections to enable a precise curve fit with correlation factors (r^2) equal or better than 0.999. The results are shown at figure 3.8. Note that the maximum stress appears at the edge of the hole and is very close to the 3.σ value that theory predicts, and the value levels out at approximately the level of the applied stress.

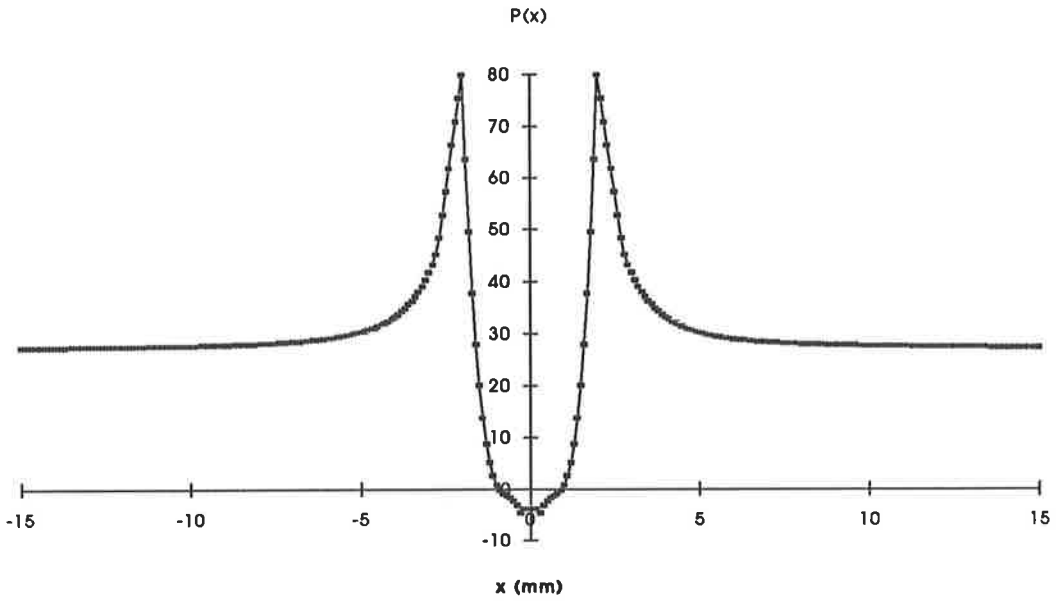

Figure 3.8 ANSYS stress distribution for the plate with hole but no crack

The complete formula for p(x) was:

$0 \le |x| \le 0.25$: p(x)= -3.8964

$0.25 \le |x| \le 2.0$: p(x)= -14.2559+49.0957*|x|-66.9986*|x|^2+32.9991*|x|^3

$2.0 \le |x| \le 2.72917$: p(x)= -45.1664 * (|x| - 2) + 79.906

$|x| \ge 2.72917$: p(x)= 26.791006+7.450222/(|x|-2)+20.169341*exp(-(|x|-2))

(3.17)

Equations (3.16) and (3.17) were substituted into equation (3.15) and numerically integrated for each crack length required. A Fortran program was written to perform the integration required in equation (3.15). Open integration was required as equation (3.15) was undefined at x=a. To obtain the most accurate result the integration routine was divided into two parts. Figure 3.9 shows the product of the functions p(x) and m(x,a), for a = 15 mm. Closed integration, utilising the Trapezoidal algorithm [Numerical Recipes], was

performed for x from -a to (a-0.1). Open integration, utilising the Rhomberg algorithm [Numerical Recipes], was used to evaluate the integral from x = (a-0.1) to x =+a.

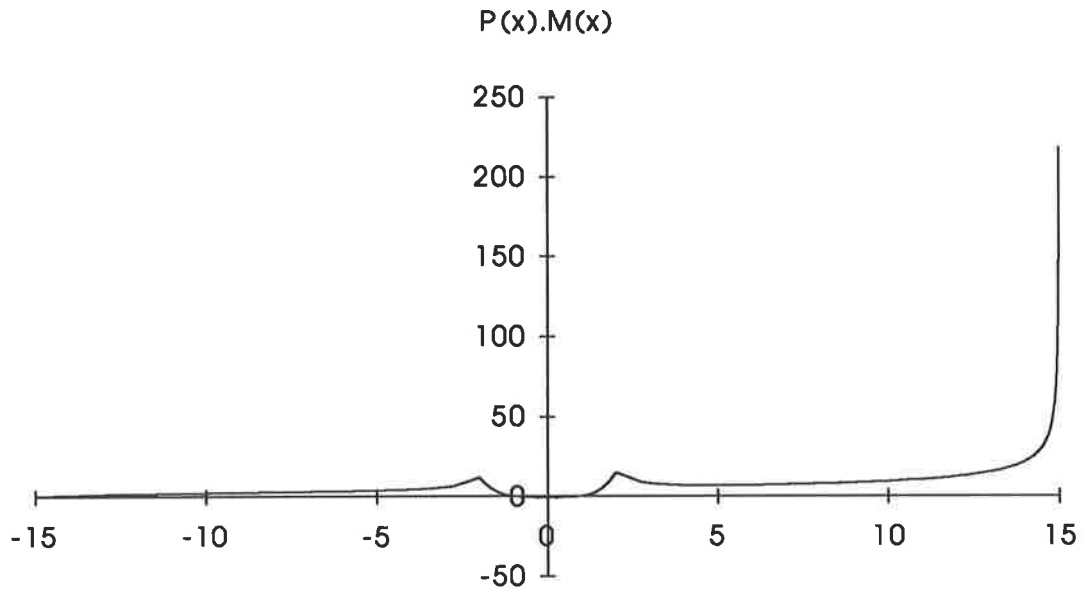

Figure 3.9 Weight Function: p(x) multiplied by m(x,a)

A subroutine called Kanazawa was used to multiply p(x) by m(x,a) at each of the function evaluations performed. Appendix B is a listing of the Fortran program kanazawa.f (main program) used to perform the integration at each crack length. The subroutine "integrate" was taken from literature [Numerical Recipes] and was incorporated into Kanazawa.f using the 'include' command in Fortran. The program was compiled using the SUN Fortran compiler for UNIX and the results are listed in Table 3.4 below. Figure 3.9 shows that the magnitude of K_I predicted by this method would depend on the largest value of x used in the integration routine. As x approached "a" (but was never equal to "a"), the value of p(x).m(x,a) increased dramatically resulting in an increase in the value of K_I.

crack length (mm)	Mode I Stress Intensity Factor, K_I
6	132.4
7.5	145.5
10	166.7
12.5	187.7
15	209.0
17.5	231.7
20	256.6
22.5	285.4
25	320.4
27.5	366.0
30	431.6
32.5	542.8
35	818.1

Table 3.4 K_I values calculated using Kanazawa's Weight Function

Bueckner [Parker(1981), Broek (1986)] developed a weight function for an edge crack in a plate. Bueckner's function was investigated as an exercise. The stress profile for the plate with a hole p(x) was already obtained from ANSYS. Of course in the case of an edge crack, the applied constraints at lines 2, 5, and 6 of figure 3.4 are not valid and as expected, the resulting K_I values were considerably higher than those predicted by Kanazawa's function and the ANSYS package.

3.3.5. Comparison of results

The K_I values in Tables 3.1 and 3.2 are very close and produced nearly identical curves when graphed. This result was expected because the equation recommended by the ASTM, equation (3.9), is an approximation to the data available in tables such as the Compendium of Stress Intensity Factors.

Figure 3.10 shows that the values predicted by equation (3.9) as recommended by the ASTM, were consistently below those predicted by the ANSYS v5.0 package. As

mentioned in section 3.3.2, equation (3.9) was an approximation to data provided by published literature. Equation (3.9) was found to provide K_I values nearly identical to those presented for the case of a centre-cracked plate in the Compendium of stress intensity factors (see section 3.3.1). The equation therefore assumes, in accordance with Table 1.3.1 of the Compendium, that the plate had a height/width ratio of 2 and that there was no hole present. Neither of these assumptions was valid in the plate investigated in this work (see figure 3.2).

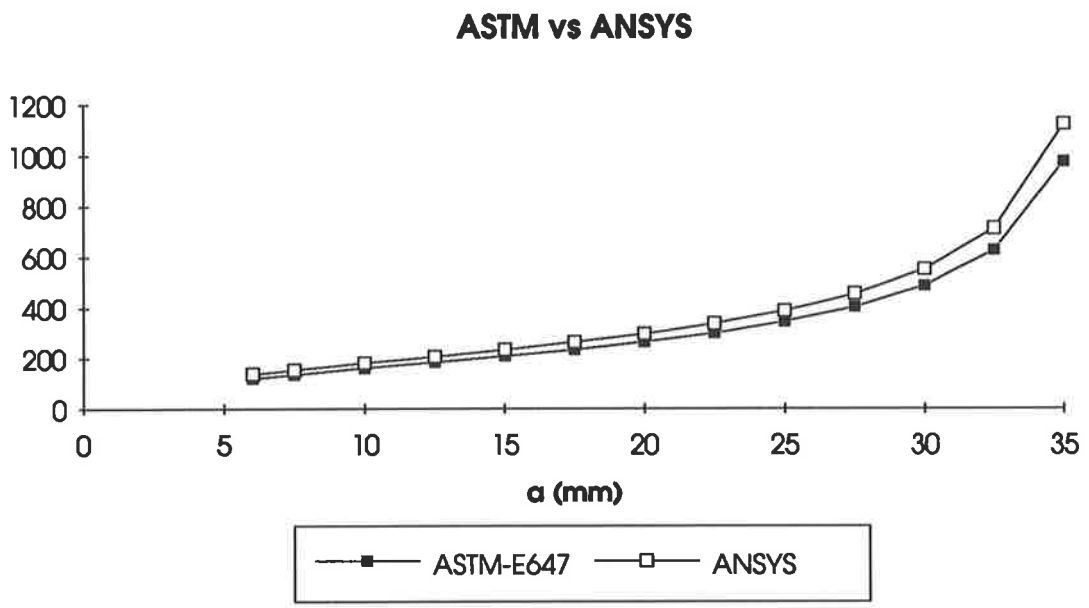

Figure 3.10 Comparing ASTM formula with ANSYS results

Figure 3.11 compares the results obtained from equation (3.9) shown in Table 3.2 and the results from Kanazawa's weight function shown at Table 3.4. As expected, the Kanazawa results are higher at crack tip locations closer to the hole (6 mm < a < 12.5 mm), due to the magnitude of the stress profile at the hole (see figure 3.8). The effects of this non constant stress profile gradually decrease until at a=20 mm, where the curves begin to depart. Figure 3.11 indicates that Kanazawa values could be assumed to be valid to the point where a = 22.5 mm, or a=0.6W in this case.

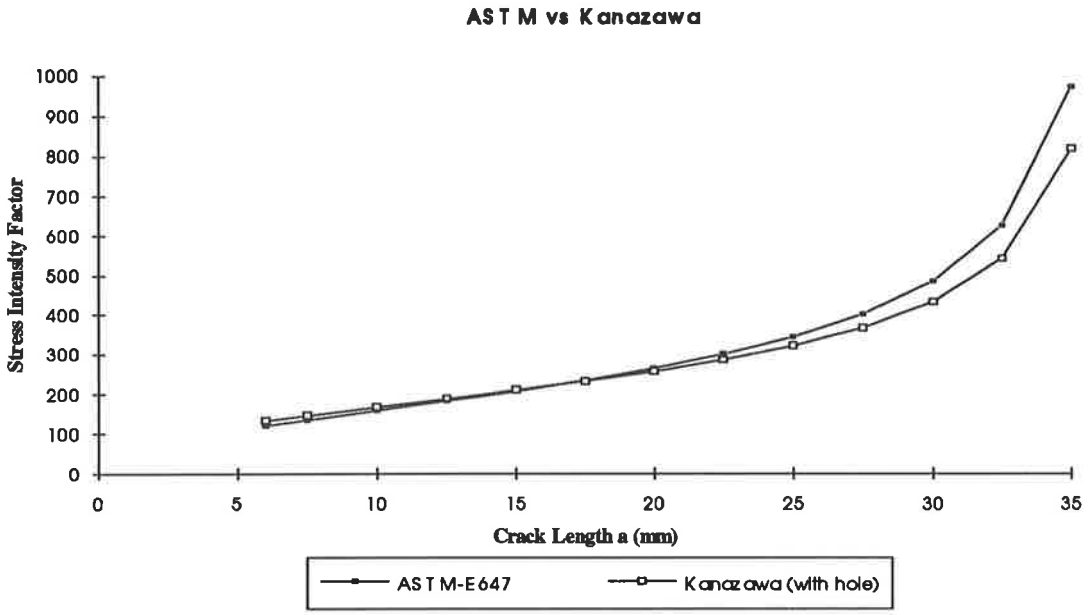

Figure 3.11 Comparing ASTM formula with Kanazawa results

Figure 3.12 compares the values obtained from ANSYS, Kanazawa's weight function, and equation (3.9). For crack lengths up to about 12.5 mm, the Kanazawa results were within 9% of those obtained using the ANSYS package and the ASTM values were within 11%. After that point both the Kanazawa's results and those produced using the ASTM recommended formula (equation 3.9), were found to be lower than those predicted by the finite element package ANSYS. At a simulated crack length of 22.5 mm the Kanazawa result was 15% less than the ANSYS value and the ASTM-E647 result was 11% less than the figure predicted by ANSYS. The differences increased to 27% and 13% respectively at the final crack length investigated of 35 mm.

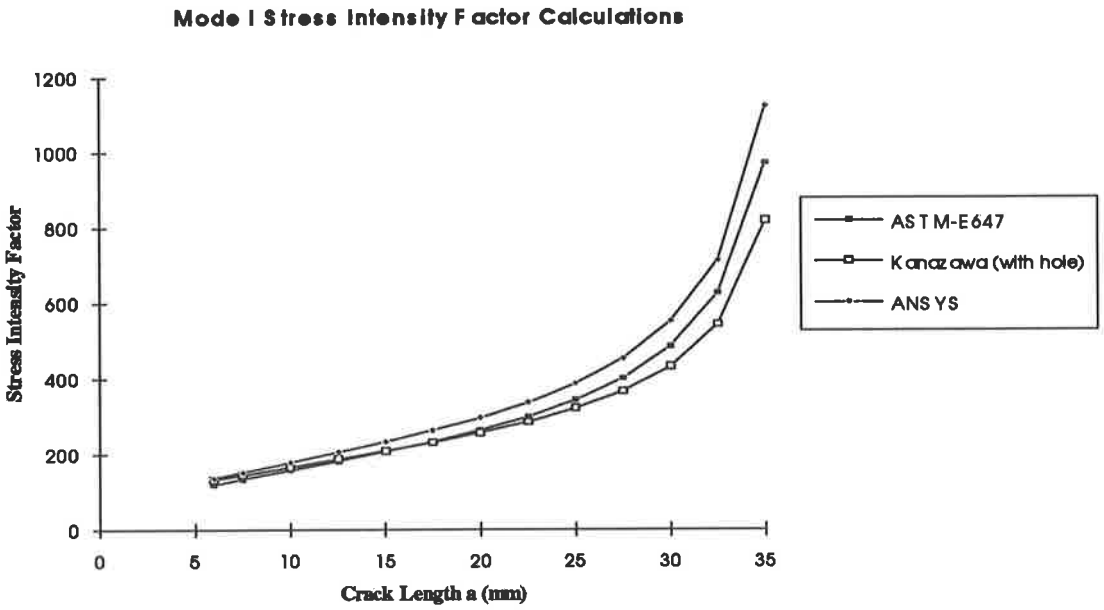

Figure 3.12 Comparing ASTM formula, ANSYS, and Kanazawa results

CHAPTER 4

COMPUTER MODELS FOR CRACK GROWTH ANALYSIS

4.1. CG90ARL

4.1.1. Introduction

In November of 1991 AMRL received source code and user information for a program written and developed by McDonnell Douglas Aircraft Company (McAir) which had been used for the damage tolerance analysis of several of the company's aircraft programs. The program, called CG90, was used for crack growth predictions for the F/A-18 aircraft, which is currently in service with the RAAF. AMRL is undertaking further research into the damage tolerance of the F/A-18 aircraft under RAAF flying conditions. AMRL has reviewed the CG90 program and subsequently made several modifications to correct prediction trends that were inconsistent with experimental observations. The modified program was named CG90ARL.

A copy of the CG90ARL program was provided by AMRL to the author under strict conditions due to the intellectual property of the program. Consequently, this report will not mention the algorithms used in the program or any details of the way the source code was structured. Studies done on the program by Bos (1991) and Potts (1992) are available for those authorised to view them.

The CG90ARL program was used during this research to predict crack growth in aluminium 7050 - T7451 and the results compared to fatigue experiments conducted in this study. The code was modified to include an extra output file which contained only the crack length and number of cycles information, to streamline the plotting of results in the Excel spreadsheet package.

4.1.2. CG90ARL Material Data File

The material data file contains mechanical properties, fracture toughness, and constant amplitude crack growth rate data for load ratio R=0. The file is read by the CG90ARL program during run time and the format of the file is as shown in Table 4.1. AMRL provided the material data file 7050SI.ANL which contained the relevant material properties and da/dN versus ΔK data for aluminium 7050-T7451, in S.I. units. Figure 4.1 is a log/log plot of that da/dN versus ΔK data and a copy of the 7050SI.ANL material file used in this work is shown at Appendix C.

Title		
Modulus of Elasticity	Poisson's ratio	
Cyclic Proportional Limit (elastic yield limit)	Cyclic 0.2% Offset Yield Stress	Monotonic 0.2% Offset Yield Stress
Ultimate Strength	Ultimate Strain	
Critical Stress Intensity (K_{1c})	Number of ΔK v da/dN pairs (npts)	
ΔK1	da/dN1	}
.		} ΔK v da/dN data
.		}
ΔKnpts	da/dNnpts	}
0 (end of file flag)		

Notes.

1. The ΔK values must be monotonically increasing or decreasing.
2. The largest ΔK value should be just less than the critical stress intensity factor.
3. The last line of the file should be 0 unless the material is titanium where it should be 1.

Conditions.

Young's Modulus	>	0		
Poisson's ratio	>	0		
Elastic limit	>	0	<	0.2% limit
Elastic limit	<	Ultimate limit		
Cyclic yield	>	0	<=	Ultimate Yield
Yield Strain	>	Proportional Strains		
ΔKmin	>	0		

Table 4.1 CG90ARL Material data file format and criteria

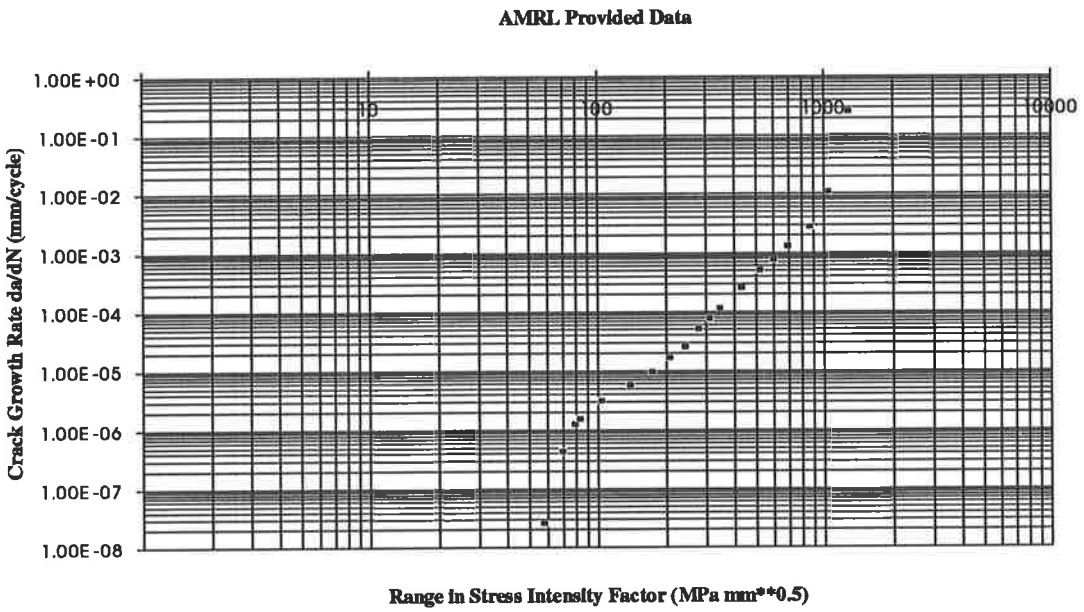

Figure 4.1 da/dN vs ΔK provided in 7050SI.ANL

4.1.3. CG90ARL Spectrum File

The spectrum file defines the simulated load variations which are to be applied by CG90ARL allowing the user to describe the exact load conditions and number of applied cycles which are required. A sequence file may consist of a number of blocks of varied loads or may simply consist of a single block. In either case, the load sequence described in the file will be repeated until the program has reached one of the following stopping criteria:

(i) user specified maximum crack length exceeded;

(ii) user specified maximum number of cycles exceeded;

(iii) K_{max} specified in material data file exceeded; and/or

(iv) any program run time error.

A cycle of loading is defined by a peak and a valley (dimensionless quantities) which, when multiplied by the fatigue reference stress at the location under consideration, give the maximum and minimum stress in the cycle.

The spectrum file is organised as follows:

Comment line 1	- printed in output file		
Comment line 2	- information only	: not printed	
Comment line 3	- information only	: not printed	
No. of load levels in the spectrum	No. cycles represented by spectrum		
maximum peak factor	minimum valley factor		
$peak_1$	$valley_1$	no. cycles	}
.	.	.	} load levels
.	.	.	} in block
$peak_n$	$valley_n$	no. cycles	}
0 (end of file flag)			

Notes.
1. The fatigue reference stress is always a positive quantity; the sense of the loading is specified by the sign of the spectrum peaks and valleys.

Table 4.2 CG90ARL Load spectrum file format

Two examples of load spectrum files developed for this work were as follows:

a. filename = CAR00P20.SEQ

where:

CA = constants amplitude.

R00 = load ratio R = 0.

P20 = load = 20 kN.

```
Constant Amplitude Loading, 0-20 kN
R = 0.0
G.R. Rohrsheim      Date
1       1
1.0     0.0
1.0     0.0     1
0
```

Figure 4.2 File CAR00P20.SEQ

The type of load sequence file shown at figure 4.2 was used for simulating constant amplitude fatigue loading at a load ratio of R = 0.0. The file describes a single block with a single load cycle described by a valley of 0.0 x reference stress and a peak of 1.0 x reference stress. This block is repeated until one of the stopping criteria are met; the reference stress value was supplied at program run time.

b. filename = OL.SEQ

where:

OL = overload.

```
Overload Sequence. Pol = 1.5 x Pmax
R = 0.0; 1 overload cycle followed by constant amplitude loading
G.R. Rohrsheim      Date
2       1000000
1.5     0.0
1.5     0.0     1
1.0     0.0     999999
0
```

Figure 4.3 File OL.SEQ

The type of load sequence file shown at figure 4.3 was used for simulating the application of a single overload followed by constant amplitude loading at load ratio R = 0.0. The block was repeated every 1 million cycles until the program was ended by any of the stopping criteria. Different overload ratios were simulated by simply replacing all occurrences of "1.5" in figure 4.3 with the required overload ratio.

4.1.4. CG90ARL Crack Growth Integration

The CG90ARL crack growth model uses the concept of an effective crack opening load as proposed by Elber (1971) to describe retardation and acceleration of nominal constant amplitude crack growth rates when variable amplitude loading occurs. The loading is

represented as a series of constant amplitude load blocks stored in an external sequence file as discussed in the previous section. In this work, an overload was applied (represented as a one cycle load block) and the resulting retarded crack growth investigated. The factors affecting the crack opening stress intensity are dependent on the stress state (in this case plane strain), the cyclic behaviour of the material, the applied loading, and the stress ratio R.

Once the effective stress intensity change has been determined the cyclic crack growth rate is found from another external file, the material data file (see section 4.1.2). The resulting crack increment is added to the crack length and the number of cycles incremented by one. The crack opening load for the next cycle (in accordance with the load sequence file) is determined. The maximum and minimum loads are compared to the previously recorded effective maximum and minimum loads and the progress of the crack through the plastic zone created by the effective maximum load is monitored. If any of the conditions for setting a new effective maximum or minimum load are met, then the opening load is updated. This process is repeated for each cycle in the load block and for each load block in the spectrum until failure occurs or the required number of cycles has been performed. When the end of the spectrum file is encountered it is rewound and repeated [Bos (1991)].

The program was used in the first instance to provide an estimate of the crack growth and the number of cycles until K_{max} was exceeded under constant amplitude loading. For a starting crack length of 7.0 mm (assuming a notch of 6 mm and fatigue precrack of 1 mm), and using the sequence file CAR00P20.SEQ with a reference through stress of 27 MPa [20000N/(10 mm * 74 mm)], the results shown in Figure 4.4 were obtained.

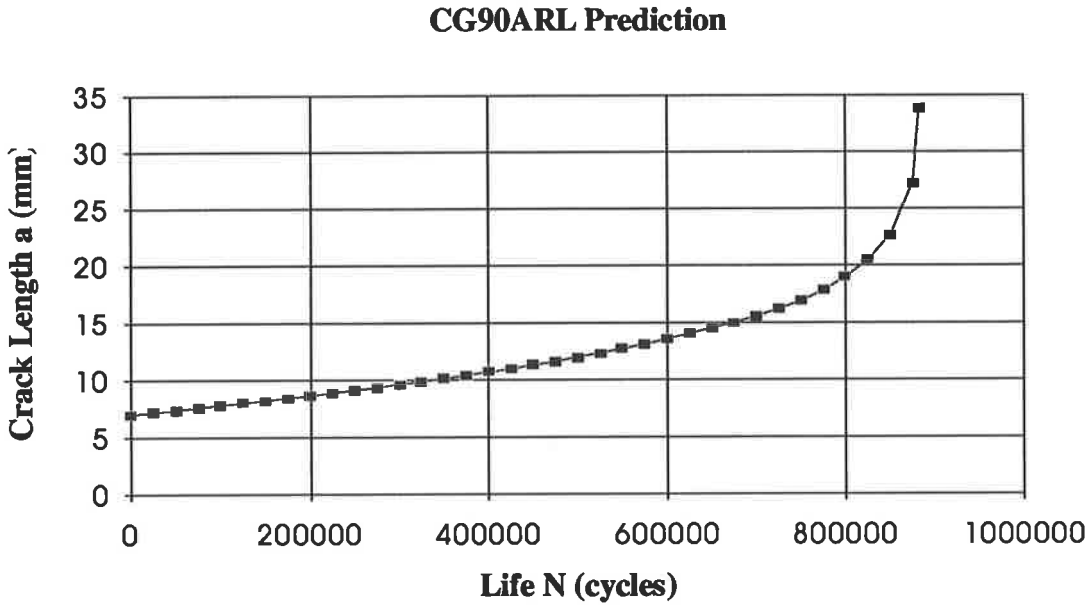

Figure 4.4 CG90ARL crack growth prediction for constant amplitude loading

The program ended after 882,441 cycles at a crack length of 33.8 mm when K_{max} was exceeded.

4.1.5. CG90ARL Retardation Prediction due to Single Overload

A preliminary investigation into the CG90ARL program's ability to predict crack growth retardation due to the application of an overload was carried out. A single overload applied after 25000 cycles was simulated in a constant amplitude fatigue test and compared to the results obtained in section 4.1.4. CG90ARL applies the maximum load first so the overload test was conducted with an initial crack length of 7.18595 mm which was the value of the crack length after 25000 cycles in the above constant amplitude fatigue test. The CG90ARL program provided a life shift option at the end of a program run which was used to add 25000 cycles to each crack length "a" vs life "N" point before the data were written to file. Figure 4.5 shows that a simulated single overload at N=25000 cycles produced a

6.78% increase in life to 942,294 cycles before the critical stress intensity factor (K_{max}) value in the 7050SI.ANL file was exceeded:

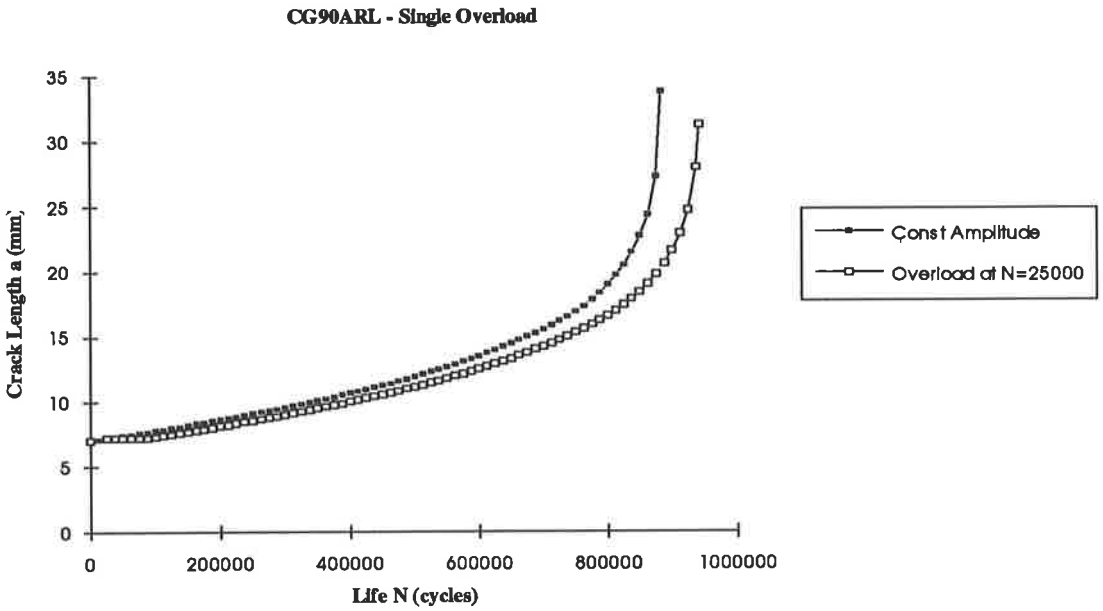

Figure 4.5 Retardation due to single overload - CG90ARL

The diagram above clearly shows a flattening of the crack growth curve after the overload was applied after 25000 cycles. This was followed by a return to the crack growth rate predicted by CG90ARL for constant amplitude loading resulting in an overall increase in specimen life.

To investigate the effects of the overload more closely, the crack growth data immediately before and after the overload application was investigated using Figure 4.6.

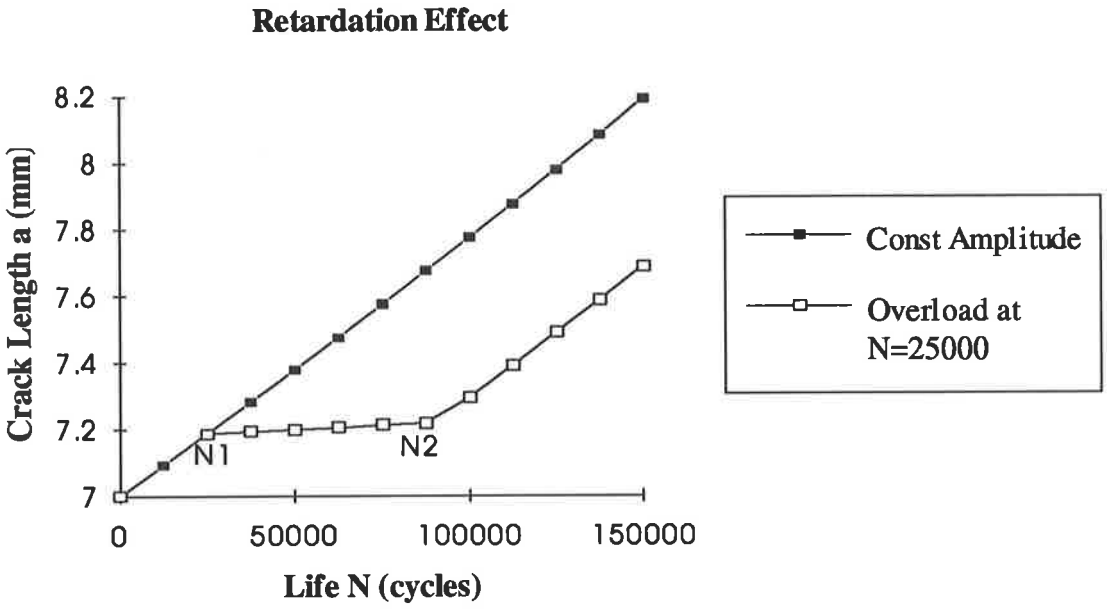

Figure 4.6 Number of cycles effected by overload

The overload was applied at N_1=25000 cycles and normal crack growth rates appear to have resumed at roughly N_2=89500 (taken from actual data). The number of cycles for which crack growth was retarded was therefore calculated as:

$$N^* = N_2 - N_1 = 64500 \text{ cycles} \qquad (4.1)$$

The crack length values at N_1 and N_2 were: $a_1 = 7.18595$, and $a_2 = 7.218505$ respectively. The length over which crack growth retardation occurred was therefore:

$$a^* = a_2 - a_1 = 0.032555 \text{ mm} \qquad (4.2)$$

The above exercise suggests that the distance over which crack retardation occurred was roughly 0.032555 mm or a*. Chapter 2 discussed crack growth models which use the size of the plastic zone caused by the overload to determine the length for which retardation occurs. Equation (2.1) was the general equation for the plastic zone size and equation (3.9)

was the ASTM recommended formula for the calculation of K_I. The relevant values for the required variables to compute the size of the plastic zone for the above overload are shown below:

Overload (P_{ol})	=	36 kN	
crack length (a)	=	7.18595 mm	
K_I	=	236.741	equation (3.9)
Cpz	=	$1/3\pi$	CG90ARL for alpha = 0
σ_{ys}	=	427.2 MPa	7050SI.ANL

resulting in a computed plastic zone size of

$$r_p = C_{pz}\frac{K_I^2}{\sigma_{ys}^2} \quad = \ 0.032585 \text{ mm} \qquad (4.3)$$

This shows that a* (see equation 4.2) is essentially equal to r_p which confirms that the CG90ARL program uses the plastic zone size created by an overload to determine the length over which crack retardation occurs. Once again it highlights the importance of calculating a precise plastic zone size if programs like these are to be used to predict retarded crack growth rates.

4.1.6. CG90ARL Retardation Prediction due to Multiple Overloads

Using the information obtained in section 4.1.5, the CG90ARL program was used to investigate the effect of multiple overloads on crack growth rates. In the first case a single overload of ratio 1.8 was applied every 64500 cycles (N* calculated above) and crack growth was found to virtually stop. This was in line with expectations as each subsequent overload was being applied just as the retardation effects of the previous overload had subsided, producing continuing crack growth retardation. As the crack length increases so too does the value of K_I which in turn leads to a larger plastic zone size. In theory, the

number of cycles between overload applications could therefore increase throughout such a test with no loss of retardation advantage.

A second case was investigated where an overload also of ratio 1.8 was applied every 100,000 cycles during a constant amplitude fatigue test (0-20 kN) and the results shown at Figure 4.7. The test indicated that significant fatigue life enhancement could be obtained (in theory) using periodically applied single overloads.

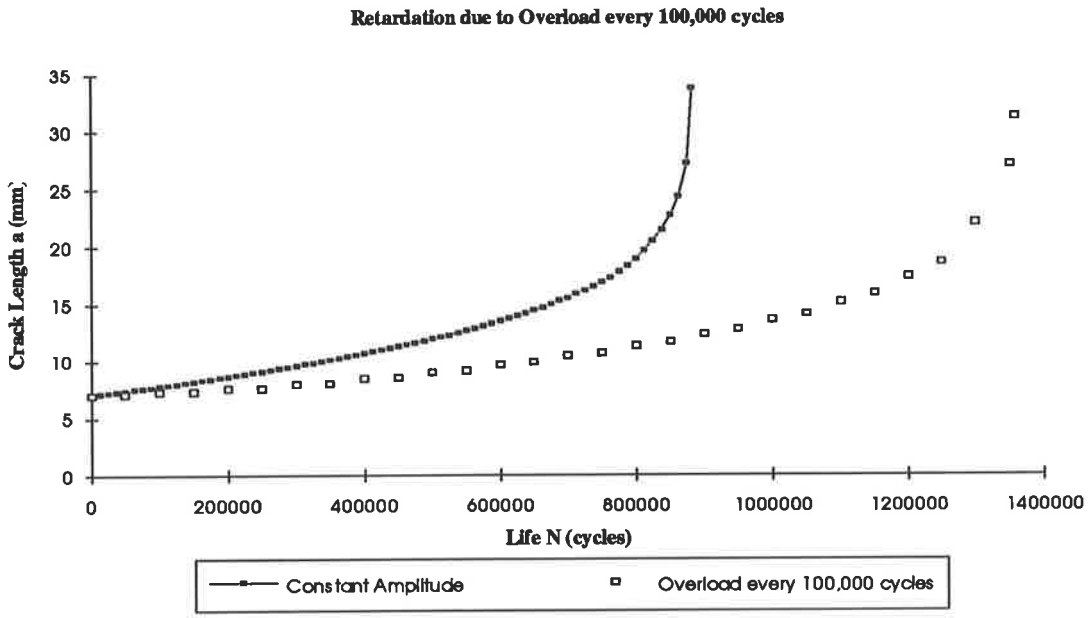

Figure 4.7 CG90ARL - Multiple Overload Retardation

4.2. Program based on Wheeler Retardation Model

Estimates of fatigue crack propagation using linear integration of constant amplitude data as described in equation (3.7) are bound to be conservative due to their neglect of the interaction effects which cause retarded crack growth. Sections 4.1.5 and 4.1.6 clearly indicate that it is incorrect to assume that the application of a higher than normal load in a constant amplitude fatigue test will necessarily produce increased crack growth. Simple linear integration techniques would calculate an increased ΔK value due to the increased

load resulting in a higher value for da/dN. Therefore, during the single overload cycle the technique would predict a larger crack increment "da" followed by normal crack growth rates resulting in an overall increase in crack growth rate caused by the overload. Wheeler proposed a modification to the concept of linear integration which involved a retardation parameter, Φ to overcome this shortfall:

$$\left(\frac{da}{dN}\right)_{retarded} = \Phi\left(\frac{da}{dN}\right)_{linear} = \Phi f(\Delta K) \tag{4.4}$$

The retardation parameter Φ was expressed in terms of the current plastic zone and the size of the plastic enclave formed at a previous overload [Meguid (1989)] as described in figure 4.8

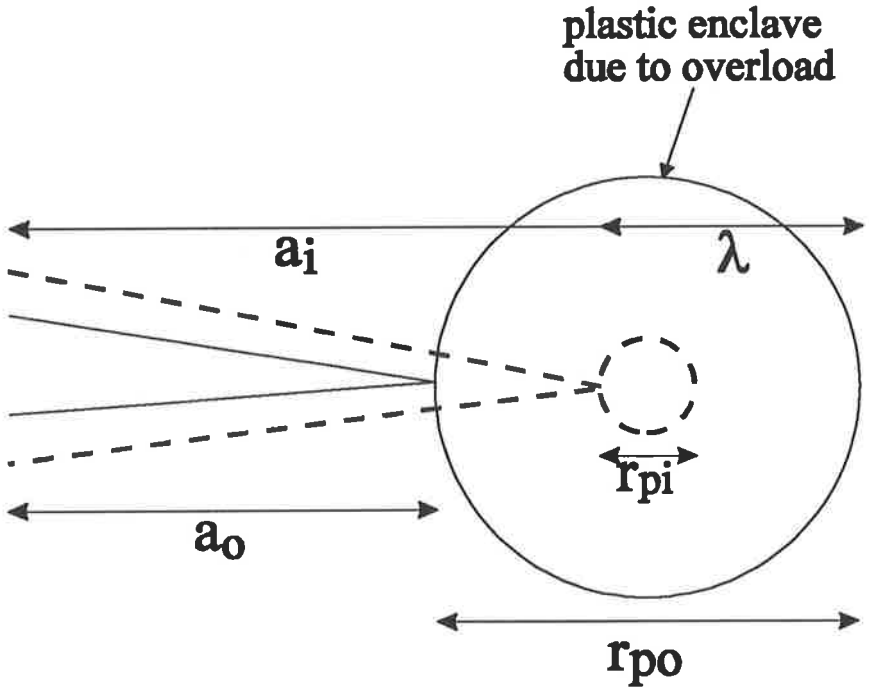

Figure 4.8 Wheeler's plastic zone model

An overload occurring at a crack of size a_0 will cause a crack tip plastic zone of diameter:

$$r_{p0} = C_1 \frac{S_0^2 a_0}{\sigma_{ys}^2} = C \frac{K_0^2}{\sigma_{ys}^2} \tag{4.5}$$

where S_0 is the overload stress and σ_{ys} the yield stress. When the crack has propagated further to some length a_i, the current plastic zone size will be:

$$r_{pi} = C_1 \frac{S_i^2 a_i}{\sigma_{ys}^2} = C \frac{K_i^2}{\sigma_{ys}^2} \tag{4.6}$$

where S_i is the stress in the *i*th cycle. As figure 4.8 indicates, the plastic zone r_{pi} is still within the plastic enclave of the overload and the current crack tip is a distance λ from the edge of the overload plastic zone. Wheeler assumed that the retardation factor Φ was a power function of r_{pi}/λ ranging in value from 0, indicating crack arrest, to 1, implying no retardation:

$$\Phi = \left(\frac{r_{pi}}{a_0 + r_{p0} - a_i} \right)^m \tag{4.7}$$

where m = material specific constant

while ai + rpi < a0 + rp0. Otherwise the plastic zone at the end of the current crack tip has grown through the overload plastic zone and therefore the retardation factor Φ becomes 1 and linear crack growth rates are again assumed. This therefore suggests that retardation only occurs over the distance r_{po}, the length of the plastic zone, which is consistent with the assumption made by the CG90ARL program.

A Pascal program was developed using the theory of Wheeler discussed above. Values for ΔK were calculated at each crack length using equation (3.9) and the linear crack growth

rates (da/dN) calculated using equation (3.6). The constants C and n in Paris' equation (equation 3.2) were obtained by fitting a straight line to the log/log data shown at Figure 4.1. The resulting straight line fit is plotted with the source data at figure 4.9.

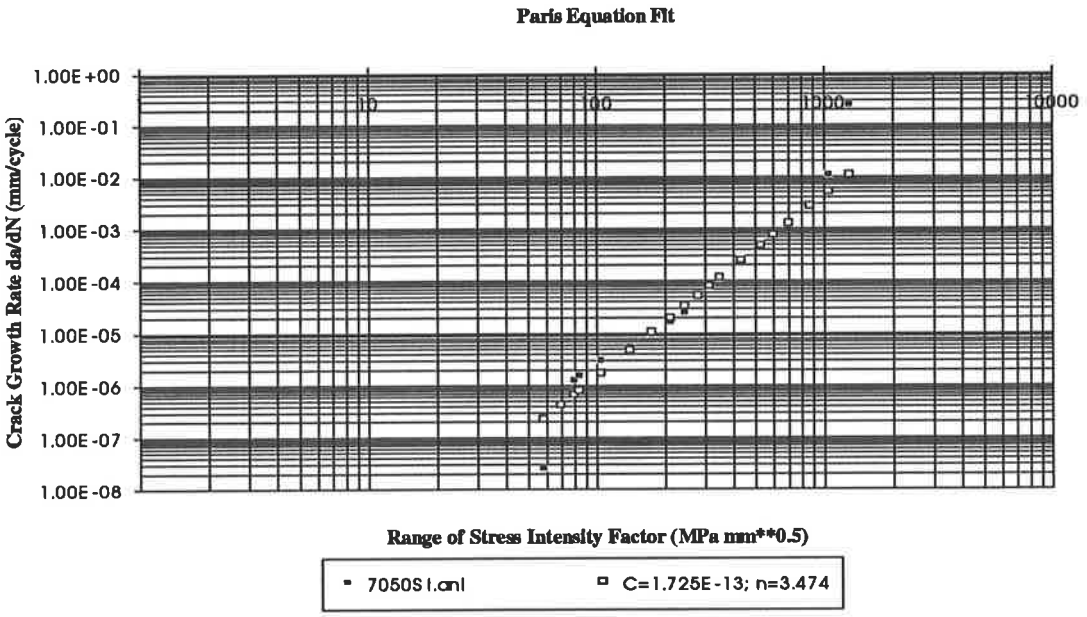

Figure 4.9 Paris' equation coefficients

The limitation of the Paris equation is evident in figure 4.9 in that it fails to map the curved growth rates at low ΔK values nor the steep increase in da/dN experienced at high ΔK values. However, in all the simulations performed using the Wheeler algorithm the minimum ΔK value experienced was greater than 100 MPa$\sqrt{mm}$ which meant that the required growth rates were in the straight line section of the graph. At values of ΔK greater than 1000 MPa$\sqrt{mm}$ though the Paris equation fails to increase the predicted crack growth rate as fast as is observed in practice. It would be expected therefore that the Paris equation would be non conservative as it would predict too many cycles to failure.

The Wheeler program was run with the Wheeler exponent 'm' set to zero which ensured that equation (4.6) was equal to one at every computation. With the value of the overload set the same as the peak load in the fatigue cycle the program therefore simulated simple linear

integration using Paris' equation. Figure 4.10 is the results of this investigation and as expected the life predicted (1268678 cycles) was considerably higher than that predicted by CG90ARL at figure 4.4.

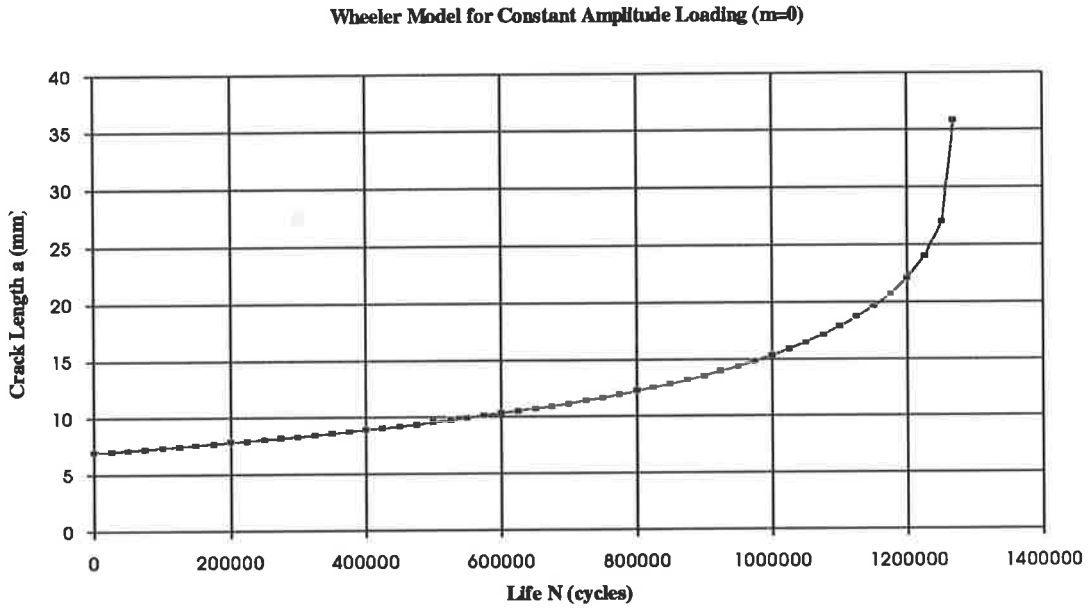

Figure 4.10 Crack growth prediction using Paris' equation

To use the Wheeler program for predicting retarded crack growth following overloads it was necessary to determine the power coefficient m in equation (4.7). This was done empirically and is discussed in chapter 6. Appendix D is a listing of the pascal code used to simulate Wheeler's model.

CHAPTER 5

EXPERIMENTAL TECHNIQUE

5.1. Introduction

5.1.1. Specimens

AMRL provided four standard centre-cracked tension specimens as shown in figure 3.2. The specimens were cut from a large piece of aluminium 7050-T7451 which AMRL acquired to conduct fatigue experiments for the RAAF. The specimens provided were 96 mm wide which was too wide for the testing machine grips at the University of Adelaide. The specimens were therefore cut down to 74 mm in width. An additional three specimens were manufactured by the Department of Mechanical Engineering Workshops. They were made from commercially available aluminium 6063-T5 and were used to verify the test machine and the planned test procedures.

Each specimen was etched with an AMRL code number identifying their location in the large slab from which they were cut. These were re-numbered ARL1 to ARL4 for simplicity as shown in Table 5.1:

AMRL code number	Assigned number
KD1A - 007	ARL1
KD1A - 119	ARL2
KD1A - 128	ARL3
KD1A - 129	ARL4

Table 5.1 Specimen numbering

The Adelaide University workshops cut a further three specimens, made from commercially available aluminium 6063-T5, to be used to validate proposed testing procedures and methodology. The specimens were assigned the names UNI1, UNI2, and UNI3.
ARL1 was used to obtain a da/dN versus ΔK curve for aluminium 7050-T7451 and to compare with results obtained at AMRL. Specimens ARL2 and ARL3 were used to investigate the effect of an overload on crack propagation. ARL4 was used to demonstrate how the life of the specimen could be extended using periodically applied overloads.

5.1.2. Application of Residual Stresses

The overload method of inducing compressive residual stresses at the crack tip was chosen for its simplicity of application. The specimens did not need to be removed from the testing machine and the desired loading sequence could be programmed into the machine's load input controller. The hole in the specimens shown in figure 3.2 was placed there so that the starter notches could be cut to control crack initiation.

5.2. Testing Machine

The testing machine used was a 250 kN Instron 1342 capable of testing specimens with maximum width 75 mm and thickness between 2 mm and 12.5 mm. A HP controller provided load control and an oscilloscope was used to confirm the requested input signal. All load inputs were sine wave in shape for a load ratio of practically zero with the minimum load set to 0.1 kN to avoid compressive loading.

5.3. Methods of Recording Crack Growth

This work was concerned with measuring crack growth rates and not simply the number of cycles to failure for a specimen experiencing fatigue loading. Three methods were developed to provide accurate measurement of crack length and crack growth in specimens tested in the Instron:

(i) A travelling microscope was mounted on a purpose built frame which attached to the Instron;

(ii) Crack propagation gauges were placed on the specimens and crack growth recorded using LABTECH Notebook software; and

(iii) A video camera with a graticuled lens was attached to the microscope.

5.3.1. Travelling Microscope

Figure 5.1 shows the general layout of the mounting frame and travelling microscope arrangement, designed by the author and built in the Mechanical Engineering Department Workshops. The structure was designed to provide motion in the X, Y, and Z directions so that it could be utilised for different specimen dimensions. Drawings of the individual items designed and constructed for the arrangement are shown at Appendix E. The rack and pinion attachment (component 2) for the existing Olympus type microscope, which provided travel in the Z direction, was mounted across another rack and pinion arrangement (component 1) to provide travel in the X direction. These were attached to the microscope platform (item B) which in turn was fitted to a shaft (item C) placed in a collar, providing adjustment in the Z direction. The attachment was fixed to the Instron machine using a manufactured mounting frame (item D). Y direction travel provided focal point adjustment, while X direction travel enabled the moving crack tip to be viewed. By attaching a digital display micrometer to Item A and component 1, and fitting a graticuled lens to the

microscope, provided a means of measuring crack length. The cross hairs were aligned with the start of the crack and the micrometer scale zeroed. The microscope was moved in the X direction until the cross hairs aligned with the crack tip (either side) and the resulting crack length read from the digital micrometer display.

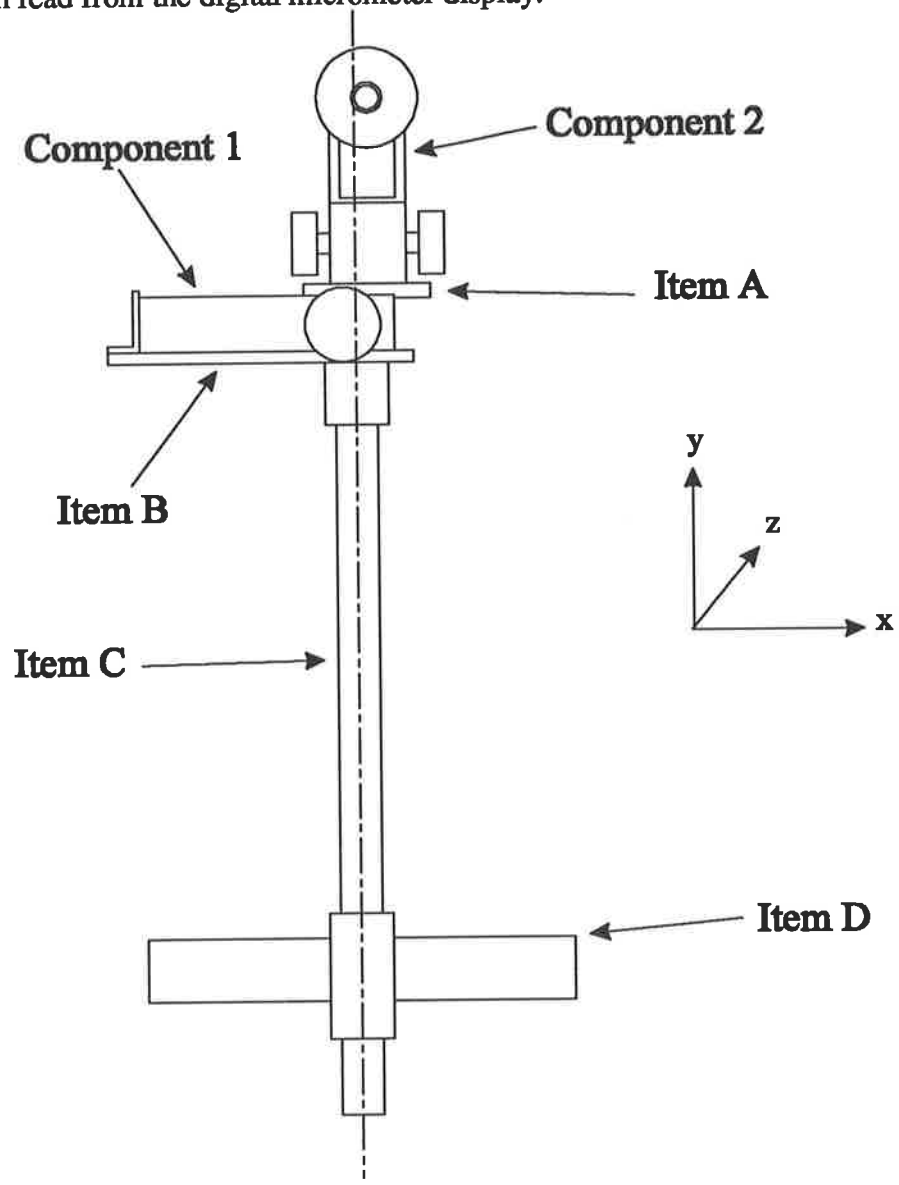

Figure 5.1 Travelling microscope arrangement

Unless the microscope was mounted square to the specimen surface then crack length measurements taken using the above mechanism would be in error. The adjusting slots placed on the mounting arms of item D of figure 5.1 (see Appendix E for item drawing)

were used to ensure correct alignment using the known distance between strands of the crack propagation gauges discussed in the next section.

5.3.2. Crack Propagation Gauges

Two different sized crack propagation gauges were purchased from the Measurements Group, Inc. They consisted of a number of resistor strands connected in parallel and when bonded to the specimens, provided a convenient method for indicating crack propagation. Figure 5.2 shows a schematic of the gauges and the dimensions of the two different gauges used.

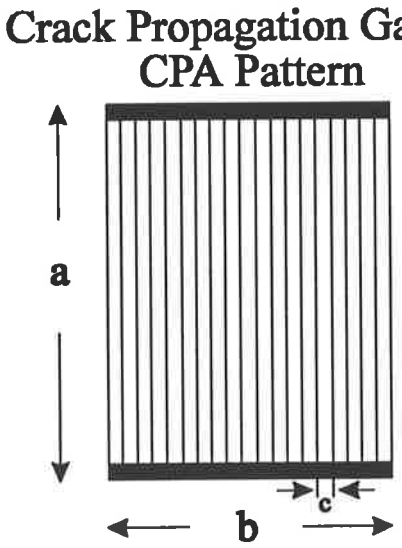

	Dimensions (mm)		
Gauge Designation	A	B	C
TK-09-CPA01-005/DP	25.4	5.1	0.25
TK-09-CPA02-005/DP	50.8	10.2	0.51

Figure 5.2 Crack propagation gauge dimensions

Progression of a crack through the gauge pattern caused successive open-circuiting of the strands, resulting in a stepped increase in total resistance[Measurements Group (1993)]. The output voltage from the crack propagation gauges (0.6mV-7mV) was passed through a DC amplifier (gain = 2000) to enable the RTI-800 card to better distinguish each voltage change corresponding to each broken strand. The RTI-800 card has an internal amplifier with software adjustable gain settings of 1, 10, 100, and 500. However, the version of LABTECH software used to control the RTI-800 card did not provide an option to change the gain setting for the RTI-800 analog-to-digital converter. A Pascal program was therefore written to interrogate the card and set the gain to 500. Unfortunately LABTECH reset the gain to 1 during initialisation thus the requirement to amplify the input signal using a DC amplifier. Figure 5.3 shows the circuitry used for the crack propagation gauges while Appendix F tabulates the results of a resistance and voltage output calibration performed on a type CPA02 gauge (also valid for type CPA01 gauges).

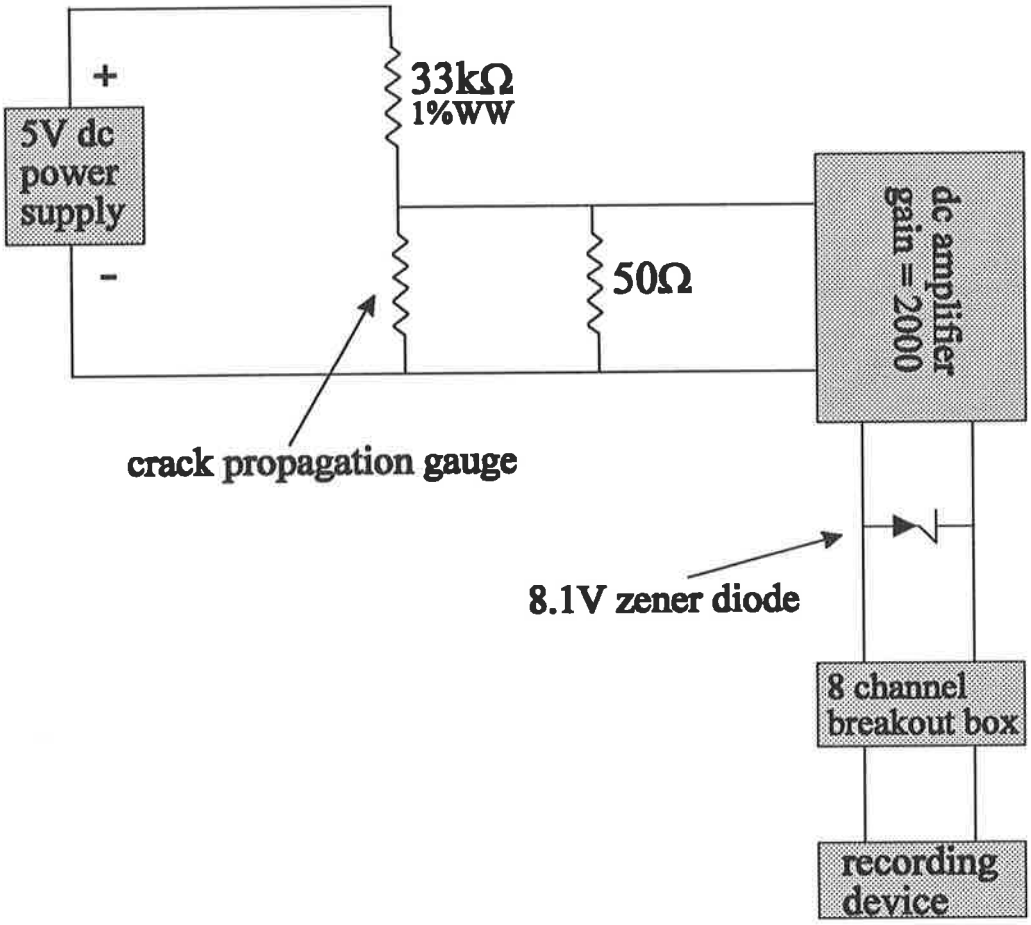

Figure 5.3 Crack propagation gauge circuitry

The 50 ohm resistor was used to prevent an open circuit situation when all of the strands in the gauge had been broken. The 33 kohm resistor was used to control the current through the gauges (15 micro Amps) to prevent over heating. The zener diode was placed in the circuit to prevent the output voltage exceeding the 10V maximum of the RTI-800 card when all of the strands in the gauge were broken.

LABTECH notebook software was used to record data from each experiment. It was an icon controlled package which was relatively easy to use. The output from each gauge (volts) and the time were recorded for each run. Results were displayed on screen and written to disk. The number of cycles applied was then calculated by multiplying the number of seconds of testing at each voltage jump by the frequency of load application.

Input load frequency was restricted to 12 Hz due to noise complaints from surrounding offices. The LABTECH sampling frequency was required to be at least twice that of the input signal to avoid aliasing. The amount of data recorded over a 30 hour period sampled at over 20 Hz would be prohibitively large. The only data required when using these gauges is the time and voltage at which a voltage jump occurs indicating a crack length increment. To accurately achieve this and cut down the amount of data recorded, data was sampled at 50 Hz for 0.25 seconds every 10 seconds. At typical load input frequencies of 10 Hz this represents a maximum error of 100 cycles for each crack length recorded. Figure 5.4 describes the layout of the crack propagation recording mechanism used in this work.

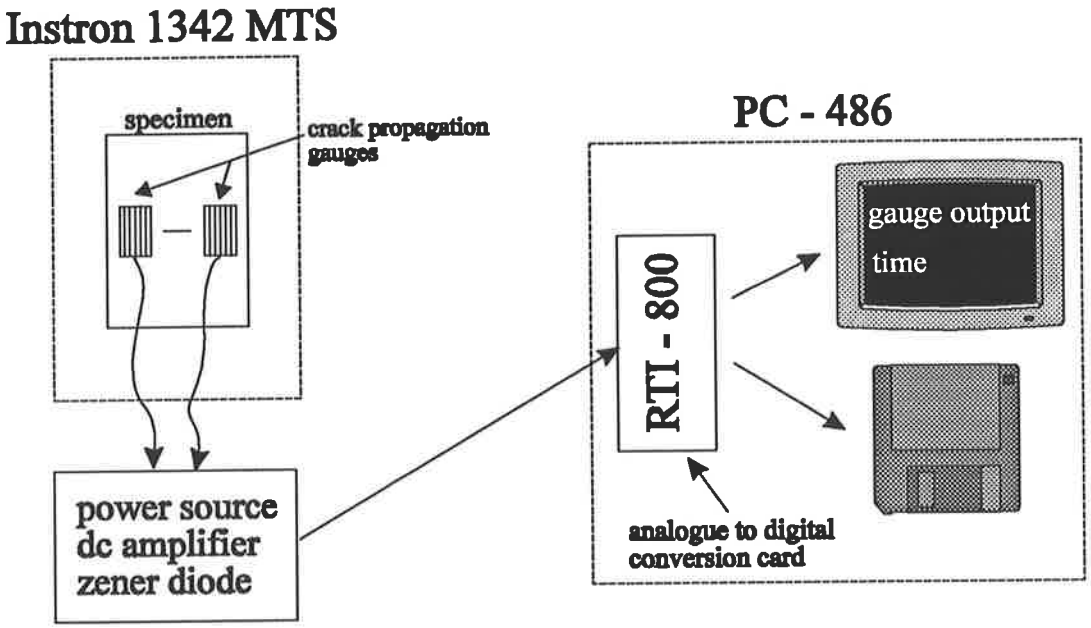

Figure 5.4 Crack propagation recording layout

The usefulness and accuracy of the crack propagation gauges was tested using specimens UNI2 and UNI3. Early tests revealed inaccuracies due to the crack growing under the gauges without causing the strands to fail. The gauges were found to lift from the material surface due to adhesive debonding. Three different adhesives were investigated together

with various surface treatment solutions. M-Bond 200 is a special cyanoacrylate recommended by the manufacturer of the gauges being used [Measurements Group (1994)] which in conjunction with the prescribed M-Prep surface cleaning supplies provided the desired gauge performance.

The type of gauges used for each experiment and their location on the specimens are shown at Appendix G and discussed in sections 5.4 to 5.6. A Nikon Profile Projector was used to measure the crack length corresponding to each gauge strand on the four AMRL specimens prior to placing them in the Instron for testing.

5.3.3. Video Camera with Graticuled Lens

A Panasonic video camera was fitted to the microscope described in section 5.3.1. This was connected through a video recorder to a high resolution TV monitor. Two lenses with an arbitrary scale etched on them were placed in one of the eye pieces of the microscope and between the microscope and the video camera connection respectively. Again the known distance between strands on the crack propagation gauges provided a means of "calibrating" the arbitrary scale seen through the eyepiece of the microscope or on the TV monitor and hence provided another means of measuring crack length. The monitor provided a means for more than one person to witness the experiments at the microscope magnification and negated the need to be continuously checking the specimens through the microscope itself.

This third method of crack length and crack growth measurement also provided a means of recording the experiments on video tape. Sections of the experiments described in sections 5.4 to 5.6 were recorded on video providing an ideal visual aid in the oral presentation of this work.

5.4. da/dN vs ΔK Curve

Specimen ARL1 was used to measure the crack growth rate of the material to compare it with published data to validate the experimental procedures and the measuring methods described in the above section. All testing and reporting was conducted in accordance with ASTM-E647-88a "Standard Test Method for Measurement of Fatigue Crack Growth Rates". Crack growth was recorded using crack propagation gauges as shown at Appendix G. Test frequency was 10 Hz and the load ratio R was 0.0 with a maximum load of 25 kN. Chapter 6 details the results of this experiment.

5.5. Retarded Crack Growth Testing

Experiments were carried out using specimens ARL2 and ARL3 to attempt to quantify the crack growth retardation resulting from the application of a single overload. Three different overload ratios were used at a different ΔK value for each of the two specimens. The value of ΔK was kept constant throughout the testing by reducing the load when crack lengths reached certain gauge strands. Three gauges were fixed to each of the specimens as shown in Appendix G. Figure 5.5 is a schematic diagram showing the load input at certain gauge strand positions including the single overload at the start followed by load shedding to maintain constant ΔK throughout the test. The dashed horizontal lines represent the expected crack growth rate (da/dN) at the corresponding ΔK level while the full lines represent the expected da/dN due to the retardation effects caused by the overload. Chapter 6 contains the results of the tests carried out on specimens ARL2 and ARL3 with graphs indicating the expected and obtained da/dN curves for the two levels of ΔK investigated.

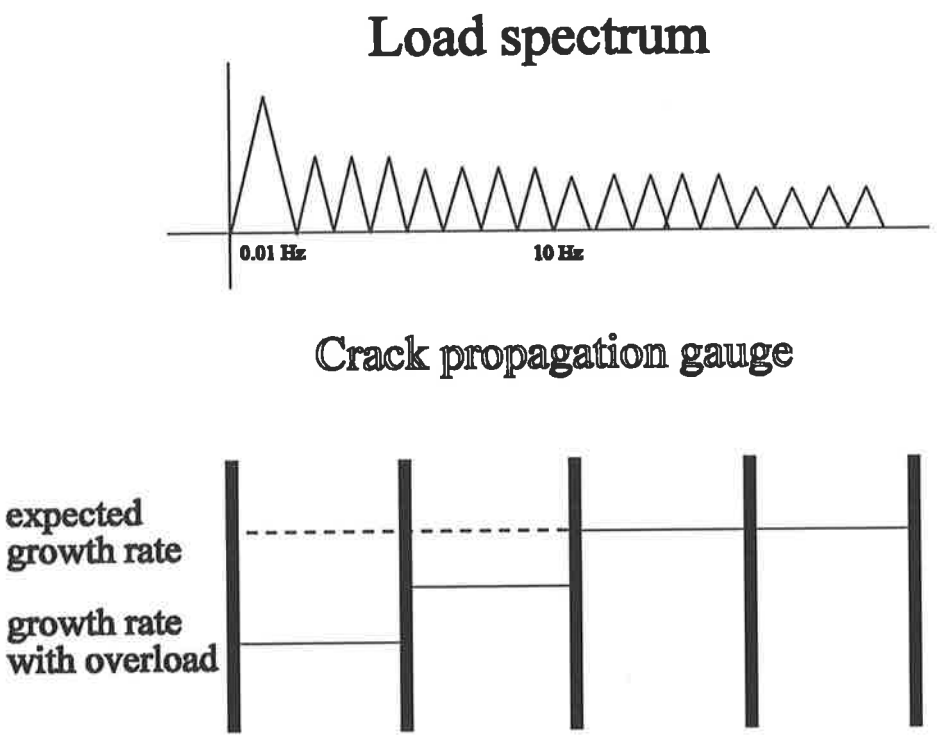

Figure 5.5 Load input for retarded crack growth testing

5.6. Increased Life Demonstration

Specimen ARL4 was used to show the effect on the fatigue life of a specimen when a series of overloads were applied periodically throughout the test. During a constant amplitude fatigue test with load conditions identical to those for ARL1 (see section 5.4) a single overload of ratio 1.8 was applied every 50,000 cycles. Figure 5.6 depicts the load input used in this experiment and the results and discussion of this test are in chapter 6. Appendix G shows the type and location of the crack propagation gauges used to record crack growth in specimen ARL4.

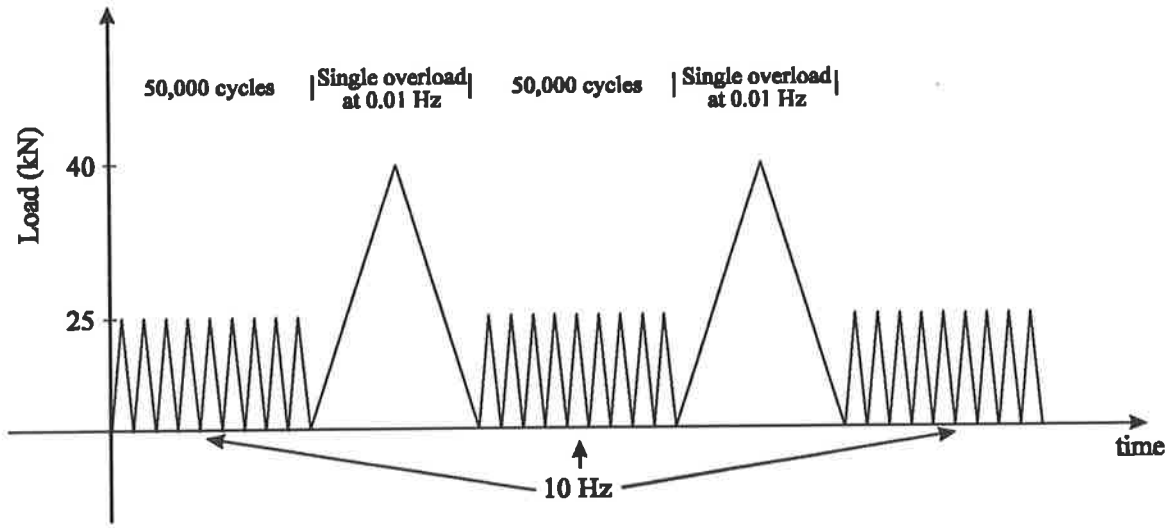

Figure 5.6 Load input for extended life demonstration

CHAPTER 6

EXPERIMENTAL RESULTS

6.1. Fatigue Precracking

Fatigue precracks of length 1 mm were introduced to the specimens (at both ends) to remove the effects of the machined starter notch and to provide a sharpened fatigue crack of adequate size, straightness and symmetry in accordance with ASTM E647-88a. Constant amplitude loading at load ratio R=0.0 was applied at a frequency of 2 Hz allowing the crack length to be measured using the travelling microscope and TV monitor without stopping the tests. Initial maximum loading was 60 kN which was gradually reduced so that at the required precrack length (1 mm) the loading was at the level required in the subsequent fatigue testing. The final load level varied for each specimen however figure 6.1 demonstrates the typical load shedding used during the precracking process. This ensured that any retardation effects induced by the initial higher load level was removed.

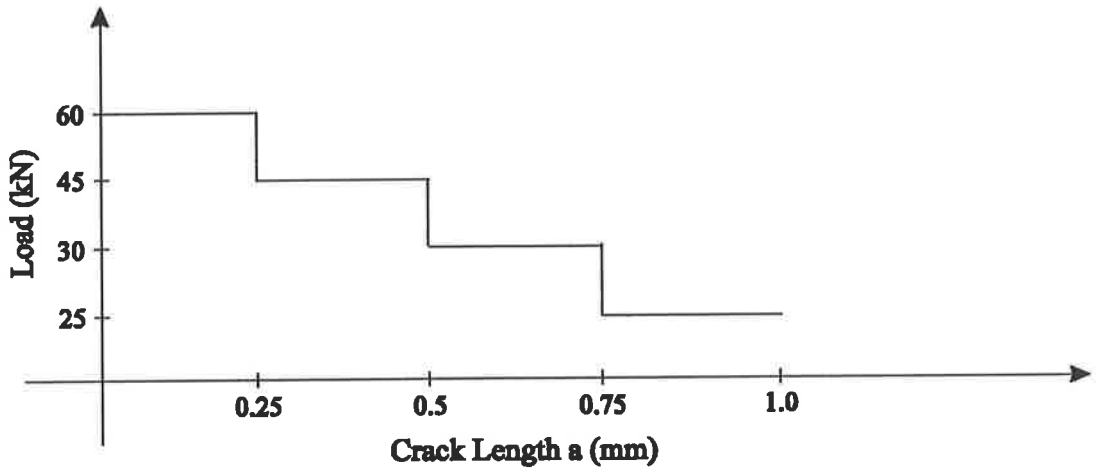

Figure 6.1 Typical load input during specimen precracking

6.2. Verification of Material Crack Growth Rates

Fatigue crack growth rate data for aluminium 7050-T7451 was obtained in accordance with ASTM E647 - 88a to verify with AMRL provided data and to obtain confidence in the testing procedures developed. This test method was used to determine the steady state fatigue crack growth rates for a centre-cracked-tension [M(T)] specimen. Results were expressed in terms of the crack-tip stress-intensity factor range (ΔK) using the equation recommended in the standard and shown at equation 3.9.

$$\Delta K = \frac{\Delta P}{B}\sqrt{\frac{\pi\alpha}{2W}\sec\frac{\pi\alpha}{2}} \qquad (3.9)$$

where alpha = 2a/W; expression valid for 2a/W < 0.95.

Constant amplitude cyclic loading from 0 kN to 25 kN was applied to specimen ARL1. The ΔK levels produced at load levels lower than 25 kN for this geometry were considered too low considering the accuracy of equipment used. Crack length was measured by crack propagation gauges as a function of elapsed fatigue cycles. Figure 6.3 is a picture of the specimen after testing showing the crack propagation gauges still intact.

The crack length corresponding to each gauge strand was measured before the test commenced. LABTECH notebook software was used to record the time at which each strand was broken and this time was converted to a number of elapsed cycles by multiplying by the test frequency of 10 Hz. Figure 6.4 shows an example of the data recorded by LABTECH, plotted in Excel. The signal appears quite noisy as it was sampled at only 0.1 Hz. As was discussed in chapter 5, a better sampling configuration was developed which sampled at 50 Hz for 0.25 seconds at 10 second intervals and produced a cleaner signal.

Figure 6.2 Photograph of gauge layout for overload experiments

Figure 6.3 Photograph of gauge layout for da/dN verification

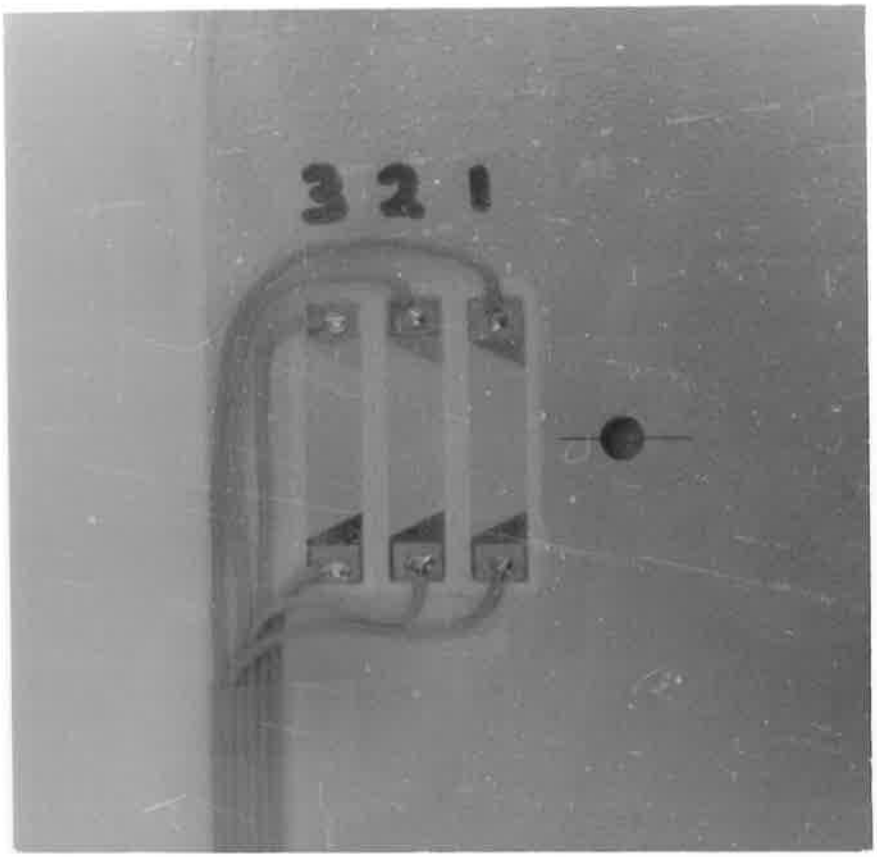
3 2 1

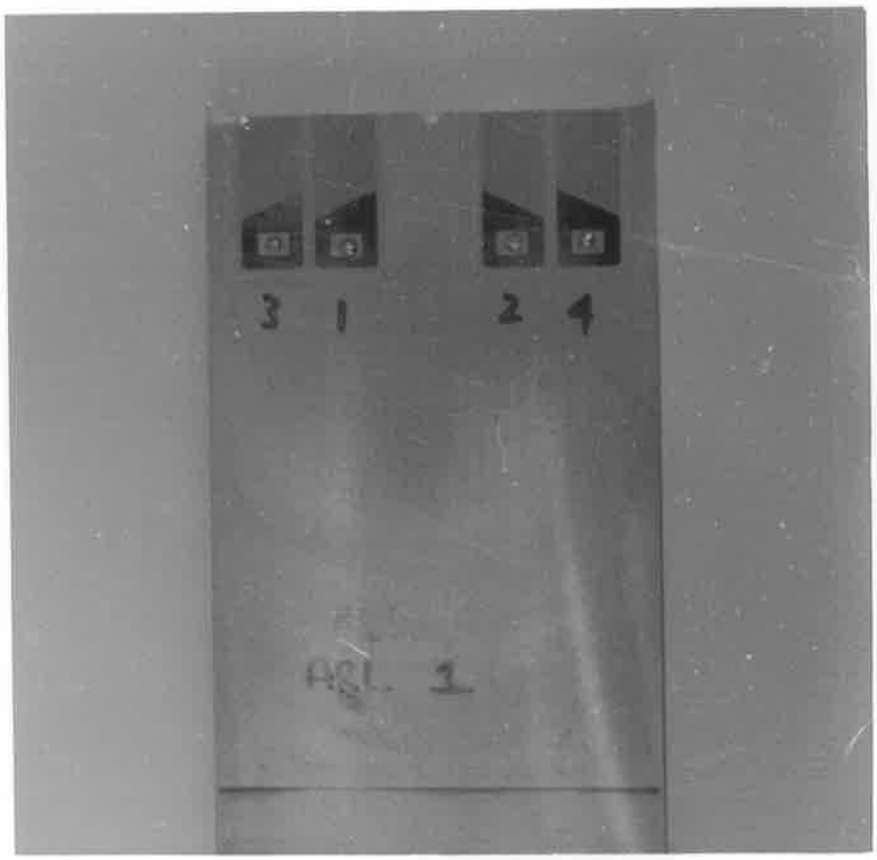
3 1
2 4
ASL 1

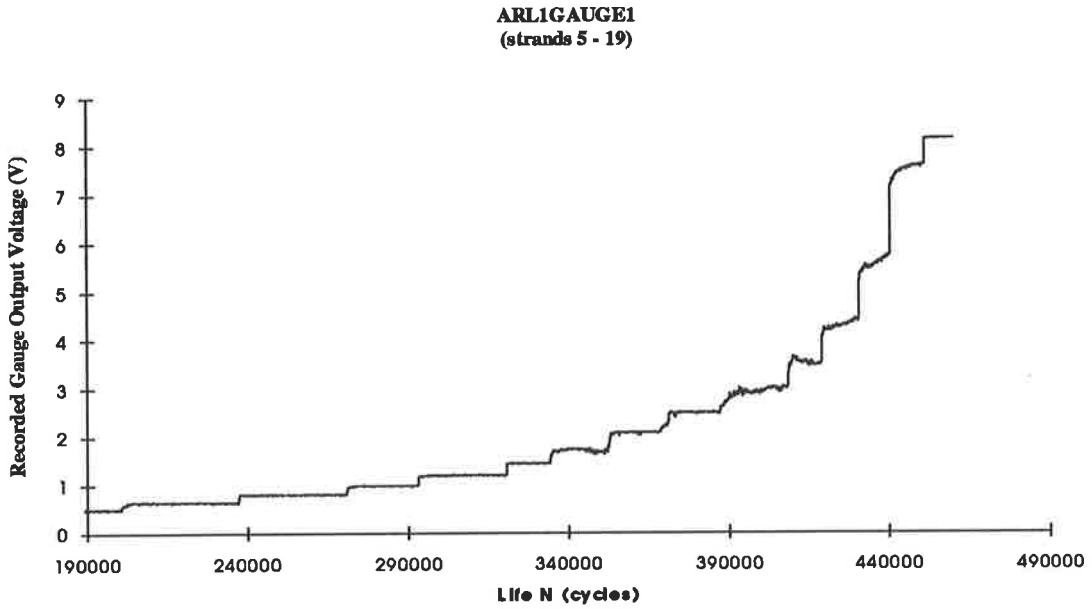

Figure 6.4 Data collected from gauge1 attached to ARL1

The strand number corresponding to each voltage jump shown in figure 6.4 was found using the calibration sheet shown at appendix F. The strand number was converted to a crack length using the measurements taken before the test (see section 5.3.2) and the results from all four gauges combined to form the crack length "a" versus life, N curve for this test as shown in figure 6.5. Data was only available from the first 19 strands of each gauge. The voltage jump associated with the 20th strand was above the 10 volt limit of the RTI-800 card with a gain setting of 2000. A gain of at least 2000 was deemed necessary to obtain clear indication of each voltage jump. This was particularly critical at the lower strand numbers where the voltage jump between strands was small.

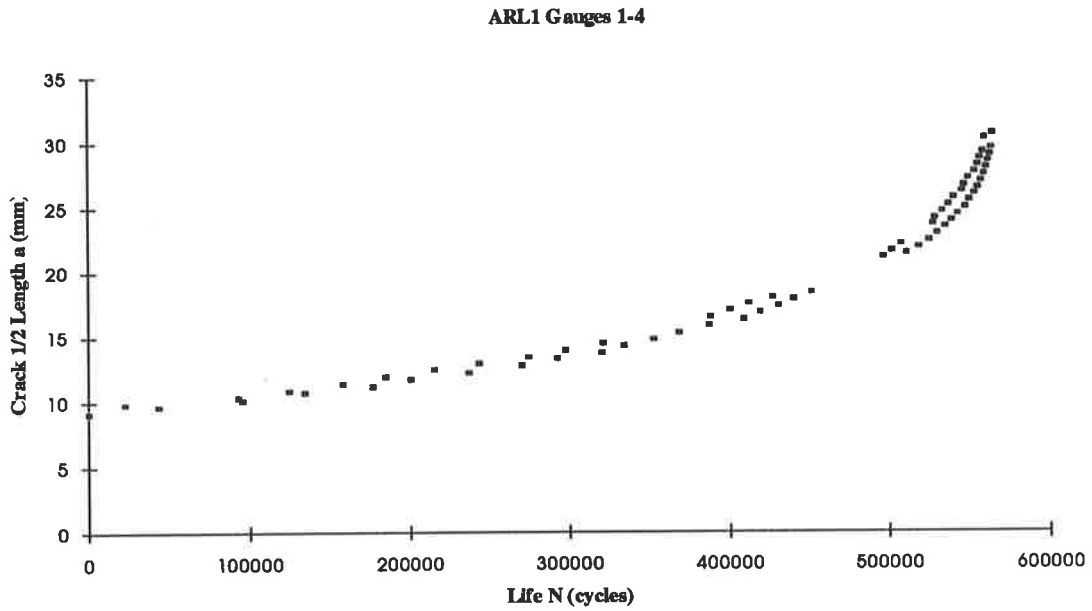

Figure 6.5 Crack length vs life diagram for ARL1

These data points were then used to determine the rate of crack growth using the numerical analysis techniques recommended in the ASTM standard E647: the Secant Method and the Incremental Polynomial Method. The standard provides a program listing for the incremental polynomial method which fits a second-order polynomial to sets of 7 successive data points to compute one ΔK, da/dN pair. This method does not therefore compute ΔK, da/dN pairs for the first three or the last three a vs N data points. The secant or point-to-point technique was used to compute ΔK, da/dN pairs for these points. The pascal program used to compute the crack growth rates from the crack length vs life data is shown at Appendix H and the output for the ARL1 gauges is shown at an appendix I.

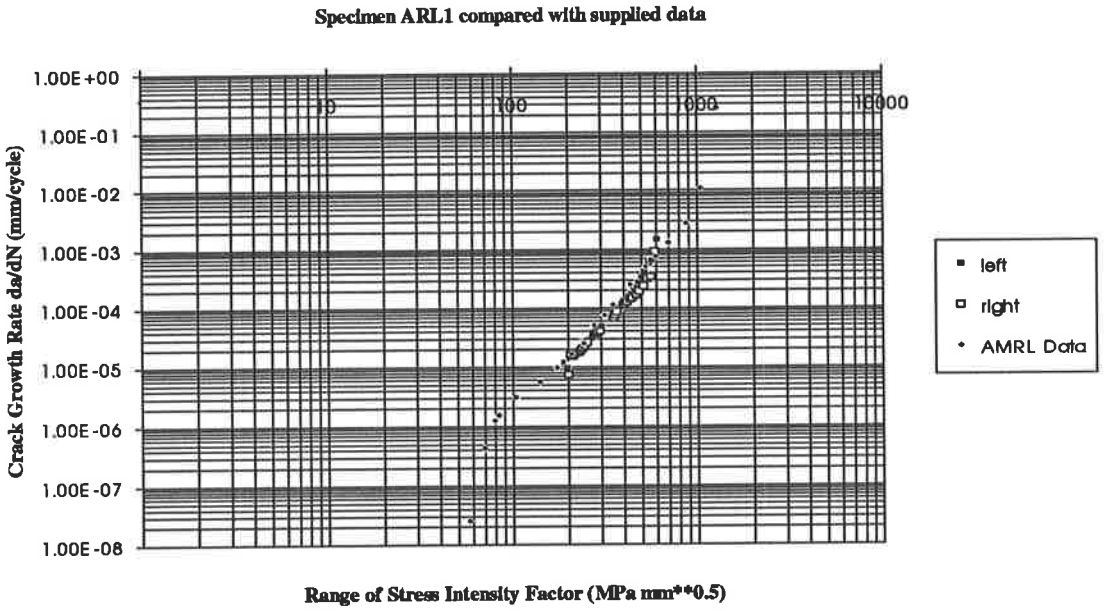

Figure 6.6 ARL1 processed data compared to supplied data

Figure 6.6 revealed a good correlation between the AMRL provided data and the data obtained using the techniques and procedures developed in this work. Using the secant method at the beginning and end of the data provided extra ΔK, da/dN pairs but their accuracy was questionable.

6.3. Retarded Crack Growth due to Overload

Specimens ARL2 and ARL3 were used to quantify the effect of an overload during a constant amplitude fatigue test. The stress intensity factor range ΔK was kept constant so that the results of multiple tests could be compared. Specimen ARL2 was tested at a ΔK value of 400 MPa $\sqrt{mm}$ while ARL3 was tested at a ΔK value of 300 MPa $\sqrt{mm}$. Three crack propagation gauges were fitted to each specimen (see appendix G) and each gauge was used to investigate a different overload ratio. The first experienced an overload ratio of 1.8, the second 1.6, and the third an overload ratio of 1.4. The CPA01 gauges used were 5

mm wide allowing 3 or 4 tests to be carried out at each overload ratio and ΔK level. Figure 6.2 is a photograph of the typical gauge layout used in these overload experiments.

LABTECH was used to display gauge voltages on the screen in real time. Fatigue cracks, at the relevant ΔK level, were grown until the first strand of the first gauge was broken (indicated by the first voltage jump seen on LABTECH screen). The Instron was manually stopped, the cycle counter was reset to zero, and a single overload applied at 0.01 Hz. The value of the overload was determined by multiplying the overload ratio by the maximum fatigue load being applied at that time to reach the relevant ΔK level. After the overload was applied constant amplitude loading resumed. The frequency of the constant amplitude loading was varied depending on the ΔK level and overload ratio. As each strand broke indicating crack growth of 0.25 mm the cycling ceased and the number of cycles recorded enabling an average da/dN to be calculated for that interval. The maximum load was adjusted (not necessary at every strand due to small ΔLoad) and fatigue loading continued until the expected growth rate (using data obtained in section 6.2) at the relevant ΔK level was achieved. This varied for the different loading combinations but usually involved three or four strands (0.75 - 1.0 mm) per test. Once satisfied that constant crack growth rates had been achieved the process was repeated. At the next strand fracture the Instron was stopped and an overload applied. This continued for the width of the gauge and was repeated in the remaining two gauges using the two smaller overload ratios.

The average crack growth rates for each 0.25 mm interval were used to calculate an effective ΔK value from the crack growth curve, for each interval. A straight line fit of the data shown at figure 6.6 (section 6.2) was used to obtain an equation relating ΔK and da/dN near each of the two ΔK values investigated. The following two sections will outline the results obtained.

6.3.1. Results at $\Delta K = 400$ MPa $\sqrt{mm}$

The data recorded and calculated for the three different overload ratios are shown at Appendix K. Bar graphs are included for the da/dN and ΔK values recorded during these experiments. Each vertical bar represents the average value of ΔK or da/dN between two strands of the crack propagation gauges. Table 6.1 and Figure 6.7 summarise the effective ΔK values calculated from the recorded da/dN values in the overload affected area. It shows that at a ΔK value of 400 MPa $\sqrt{mm}$ an overload level of 1.8 had a marked effect on crack growth producing effective ΔK values roughly 25% below the baseline level. As the overload decreased so too did the effect on da/dN. In all three cases ΔK_{eff} was found to decrease following the application of the overload.

	Overload Ratio			
test #	1.8	1.6	1.4	baseline
1	299.92	337.2	357.81	400
2	311.31	331.79	348.42	400
3	279.12	317.49	347.17	400
4	266.3	325.52	364.82	400
5	280.57			400
Average	287.44	328.00	354.56	

Table 6.1 ΔK effective results at $\Delta K = 400$ MPa$\sqrt{mm}$

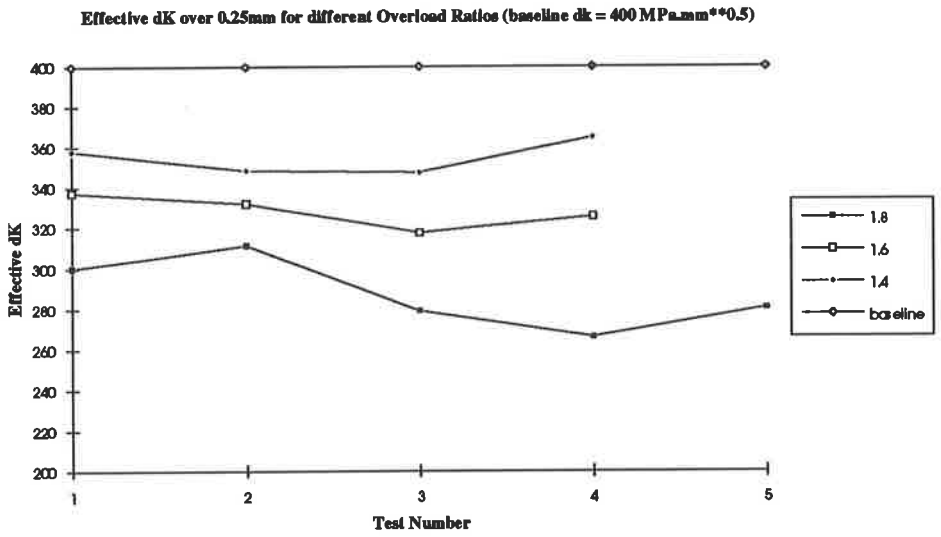

Figure 6.7 ΔK effective results at $\Delta K = 400$ MPa$\sqrt{mm}$

6.3.2. Results at $\Delta K = 300$ MPa $\sqrt{mm}$

The data recorded and calculated for the three different overload ratios are shown at Appendix L. Bar graphs are included for the da/dN and ΔK values recorded during these experiments. Each vertical bar represents the average value of ΔK or da/dN between two strands of the crack propagation gauges. Table 6.2 and Figure 6.8 summarise the effective ΔK values calculated from the recorded da/dN values in the overload affected area. The results at this level of ΔK were not as well defined as the ones shown at section 6.3.1. Figure 6.8 shows that at a ΔK value of 300 MPa $\sqrt{mm}$ an overload level of 1.8 had a smaller effect on crack growth producing effective ΔK values roughly 20% below the baseline level. At an overload ratio of 1.6 the tests still revealed decreases in ΔK_{eff} (16%) but again smaller than those recorded at the higher overload level of 1.8. At an overload ratio of 1.4 the crack growth rate was found to increase with a corresponding increase in ΔK_{eff} of nearly 12%. The retardation effect of the overload had apparently disappeared.

	Overload Ratio			
test #	1.8	1.6	1.4	baseline
1	262.03	264.96	334.4	300
2	243.52	240.4	336.62	300
3	227.81			300
4	243.02			300
5	234.07			300
Average	242.09	252.68	335.51	

Table 6.2 ΔK effective results at $\Delta K = 300\ MPa\sqrt{mm}$

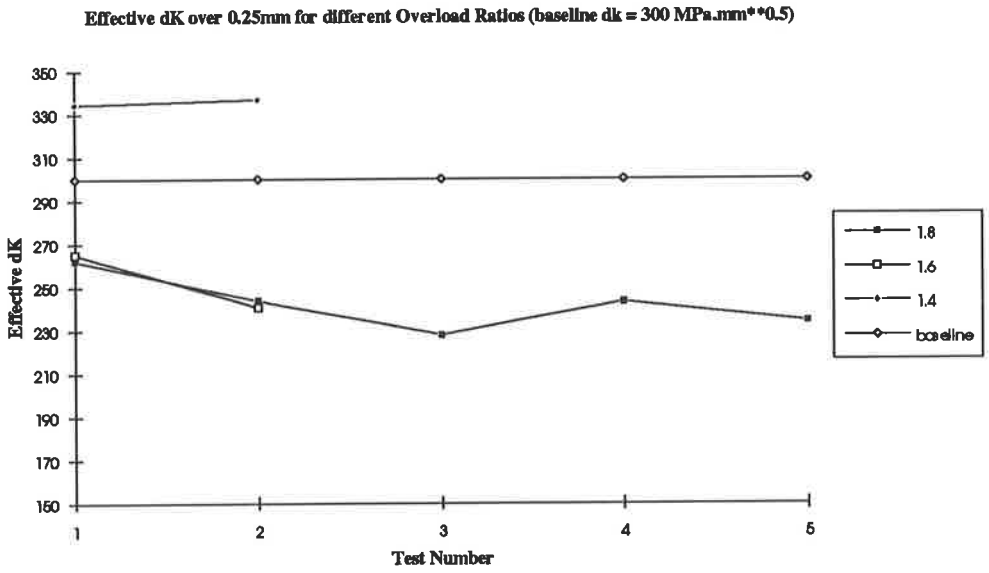

Figure 6.8 ΔK effective results at $\Delta K = 300\ MPa\sqrt{mm}$

The author cites two sources of error which may have caused this out of trend behaviour. The first involves the method by which step wise load shedding was used to maintain a constant value of ΔK and the second lies in the analysis technique used to determine the effective ΔK value from the average recorded crack growth rate for an interval of crack growth.

The value of ΔK is directly proportional the range in load applied to the specimen and was kept at a constant value by periodically reducing the load applied. Load reduction was carried out when the crack reached certain strands of the crack propagation gauges

corresponding to known crack lengths. The mode I stress intensity factor is also proportional to the crack half length and increases non-linearly with an increase in crack length. Experiments at the overload level of 1.4 were measured using the gauges placed closest to the edge of the specimens and were therefore the most sensitive to changes in ΔK due to increasing crack length. Figure 6.9 indicates how quickly ΔK increased above the required level of 300 MPa $\sqrt{mm}$ before load shedding was able to restore it.

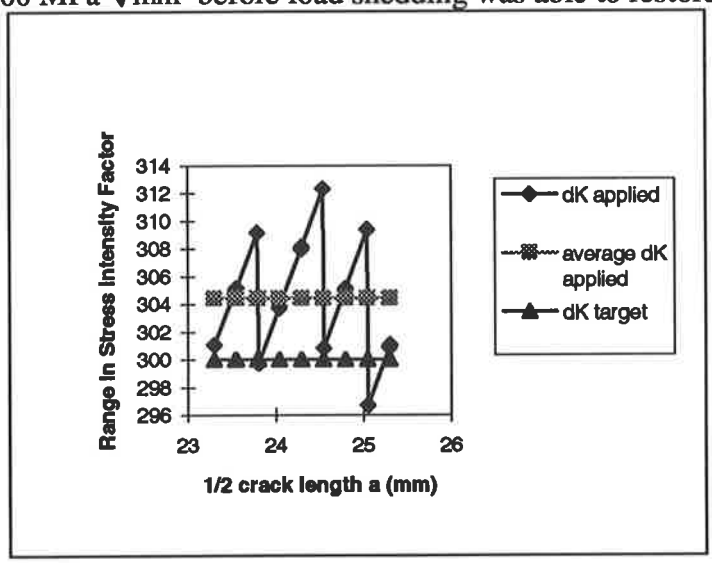

Figure 6.9 Actual vs Target ΔK for OL=1.4 at ΔK=300 MPa $\sqrt{mm}$

Figure 6.9 shows that load shedding should have been performed after each gauge strand fracture and not after two or three failures as in this experiment. The resulting average ΔK for this experiment (ΔK=300, OL=1.4) was consequently above the desired level of ΔK=300 MPa $\sqrt{mm}$ but not enough to explain the observed increase in effective ΔK at this overload level.

The average crack growth rates for each 0.25 mm interval were used to calculate an effective ΔK value from the experimentally obtained crack growth curve for aluminium 7050-T7451. A straight line fit of the log-log data at figure 6.6 (section 6.2) was used to calculate the ΔK value corresponding to the recorded crack growth rate between each two strands of the crack propagation gauges. A straight line fit of any log-log plot is

convenient but also has the potential to introduce very large errors. This was highlighted by the large differences in crack growth rates predicted using only slightly different values of C and n in the Paris equation used to describe the straight line fit of da/dN vs ΔK data. The author again refers to Finney and Deirmendjian (1992) who cited that the known variability in crack growth rate data may be of the order of two.

This suggests that the method of calculating an effective range in stress intensity factor value from a straight line fit of log-log data which could vary by as much as a factor of two has the potential to introduce significant error and may explain the observed increase in effective ΔK at this overload level.

6.4. Results of Extended Life Demonstration

The final specimen ARL4 was used to demonstrate how the application of overloads could be used to enhance the fatigue life of a component. The results above show that by applying overloads during a constant amplitude fatigue test the fatigue life can be extended. If an overload was applied periodically at a point when the retardation effects of the last overload had subsided then the increase in fatigue life could be significant. The results of sections 6.2 and 6.3 provided some insight into the number of cycles affected by overloads of different ratios. To be able to determine the ideal overload ratio to apply at every ΔK value and the number of cycles between each overload application, would require far more testing. An arbitrary value of 50000 cycles was used between overloads in this demonstration.

The crack propagation gauges were placed on specimen ARL4 asymmetrically as shown in Appendix G. The inner gauges (2,4,6) recorded the lower crack growth rates while the remaining three gauges were placed near the edge of the plate to record the higher crack

growth rates. During a constant amplitude fatigue test with loading from 0 to 25 kN at 10 Hz an overload of 40 kN (overload ratio of 1.8) was applied every 50000 cycles. Figure 6.10 shows the results recorded automatically by LABTECH notebook:

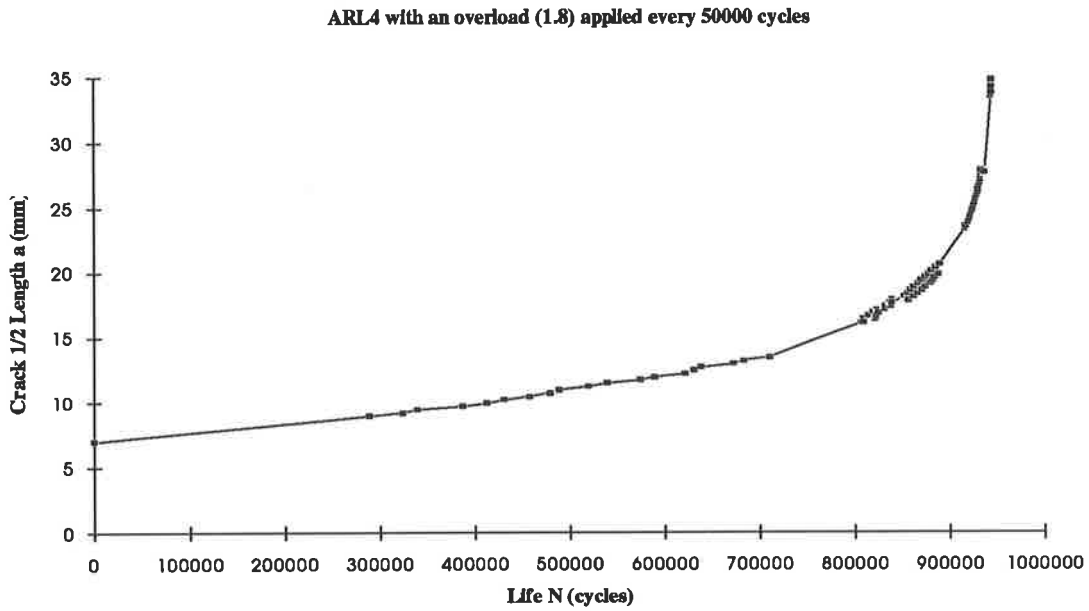

Figure 6.10 Results of fatigue life enhancement experiment

The results of this experiment were then compared to the experimentally obtained constant amplitude data shown at figure 6.5 (using a life shift to align starting crack lengths). Figure 6.11 shows an increase in fatigue life for the M(T) specimen of over 35 %.

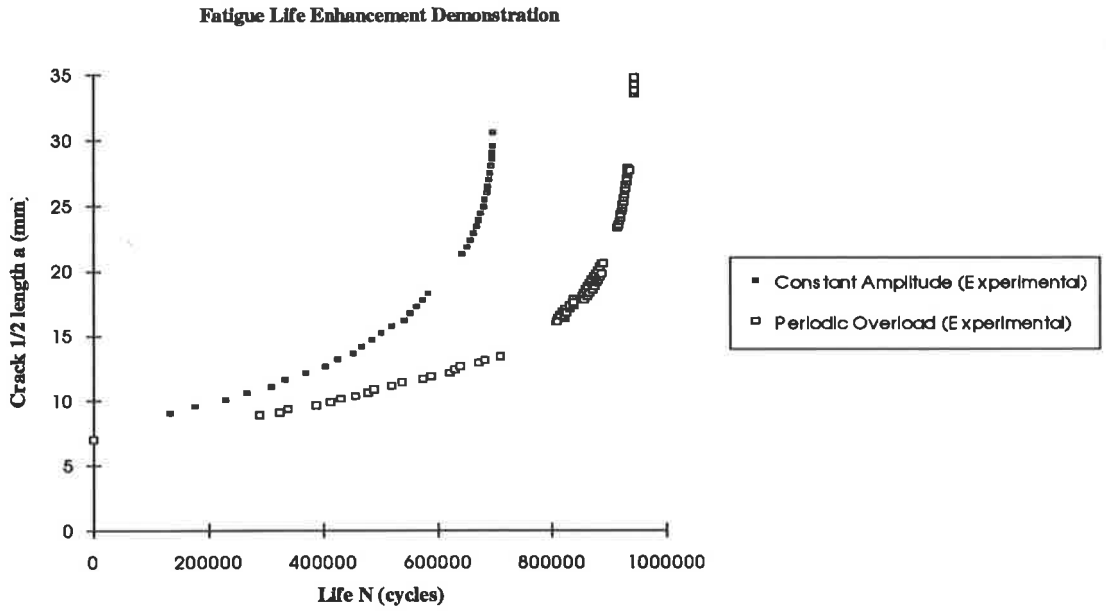

Figure 6.11 Comparison of periodic overload and constant amplitude experimental results

6.5. Shape of crack front measured

The shape of the crack front on specimen ARL4 was measured after testing to validate the use of surface crack growth measurement techniques. The specimen failure surface shown at figure 6.12 was viewed under a Zeiss type microscope in the Defects and Fracture Analysis Section at AMRL. A number of the visible striations induced by overload application were traced and their shape measured using a Apple Macintosh 7100/66 connected to a digital Mitutoyo micrometer. One of the striations traced is photographed under high magnification at figure 6.13. The results of five overload induced striations measured on the fracture surface of specimen ARL4 are shown in figure 6.14.

Figure 6.12 Photograph of specimen ARL4 crack face

10 mm

Figure 6.13 Photograph of measured striation induced by overload in specimen ARL4

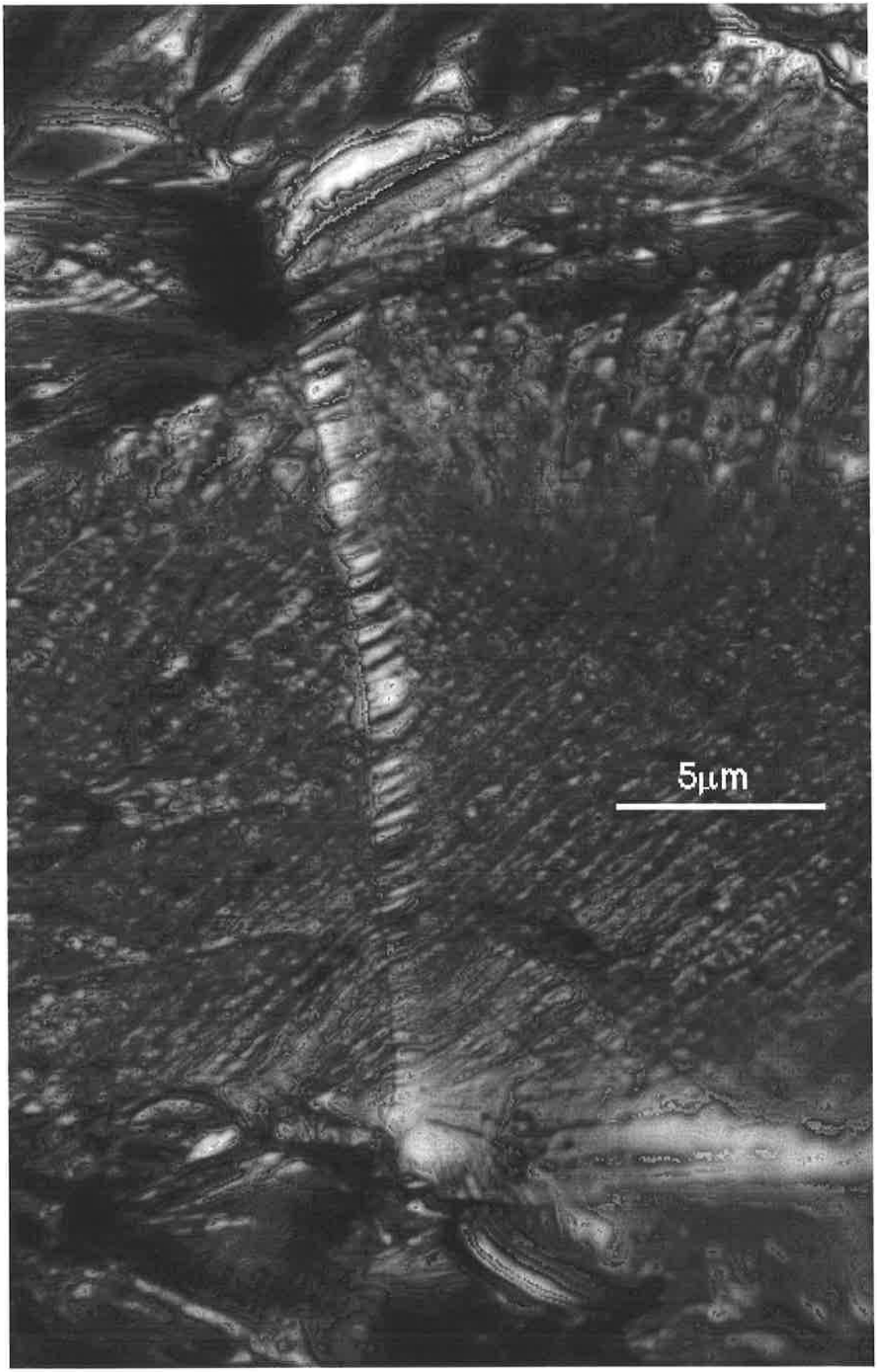
5μm

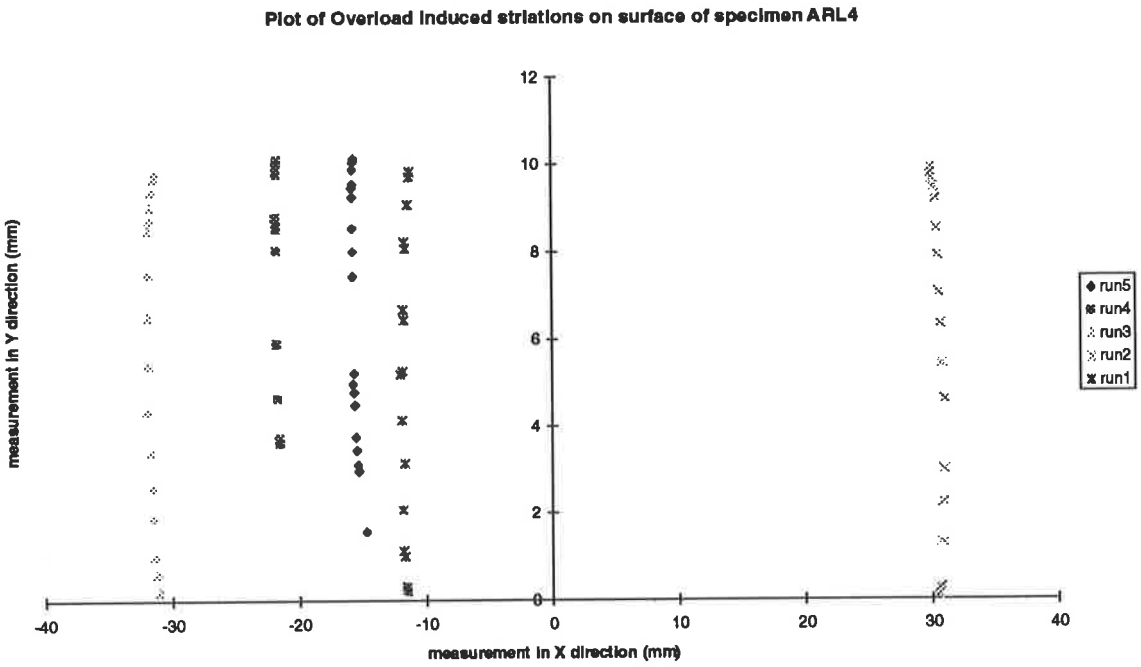

Figure 6.14 Summary of striations measured on specimen ARL4

The results of figures 6.12 to 6.14 indicate quite clearly that the crack front was straight and remained perpendicular to the surface of the specimen and hence justifies in this instance the use of surface-mounted crack propagation gauges to measure crack growth.

6.6. Results using CG90ARL

The CG90ARL model was used to predict crack growth in M(T) specimens under loading conditions identical to those described in sections 6.2 and 6.4. The results predicted for constant amplitude loading were found to be conservative. Figure 6.15 indicates that the fatigue life predicted by CG90ARL was roughly 48 % of the life which the constant amplitude fatigue loading experiments revealed. The CG90ARL model was also found to give conservative results for the case of periodically applied overloads. Figure 6.16 shows that the CG90ARL life prediction was nearly 21% less than the experiments at section 6.4 revealed. Appendix J describes how the CG90ARL processing was achieved.

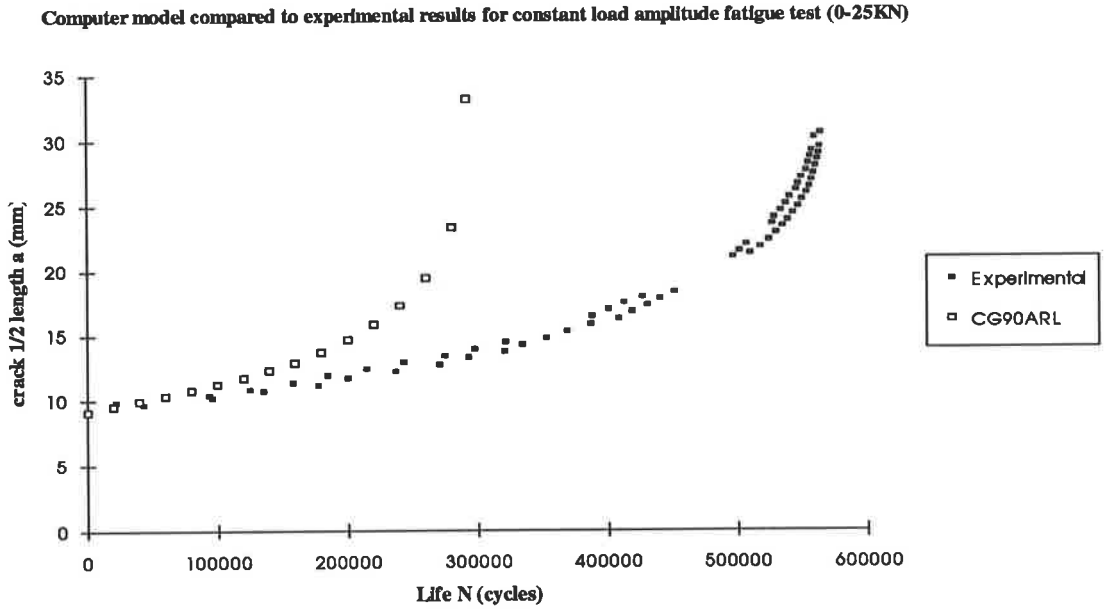

Figure 6.15 CG90ARL constant amplitude prediction compared to experimental results

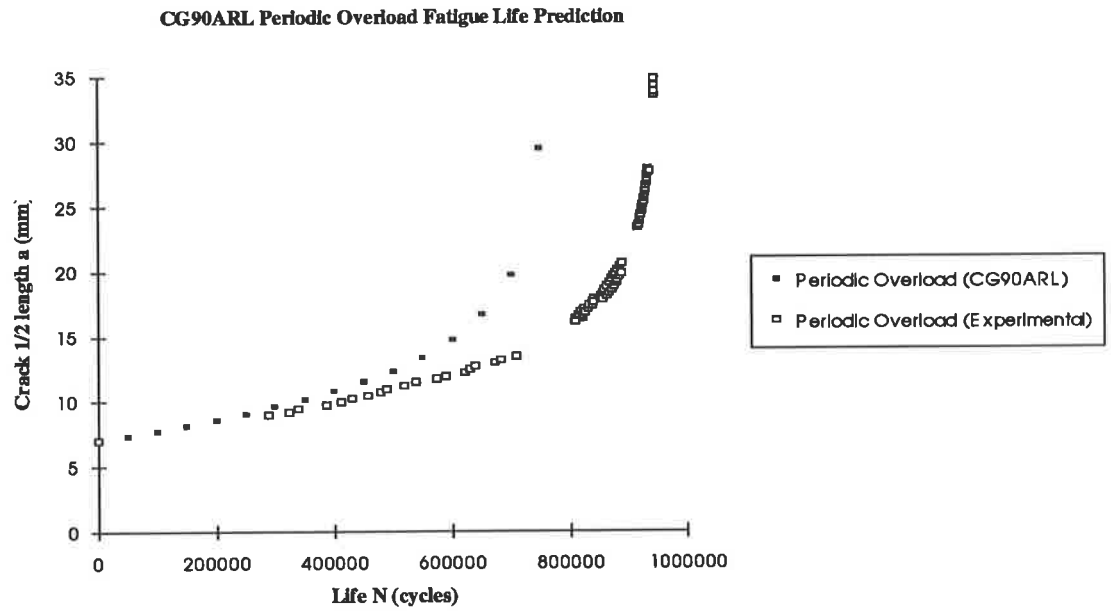

Figure 6.16 CG90ARL periodic overload prediction compared to experimental results

The CG90ARL program provides the user with the option to set a retardation parameter alpha between -1 and 1 (see section 2.6 and Appendix J). A series of alpha values within

this range were investigated using the periodic overload loading case and the results shown at Figure 6.17. The graph shows that as the value of alpha is increased from -1 the CG90ARL predictions become less conservative until at an alpha value of 0.25 the results align with the experimental results. CG90ARL predicted almost no crack growth at an alpha value of 1.0.

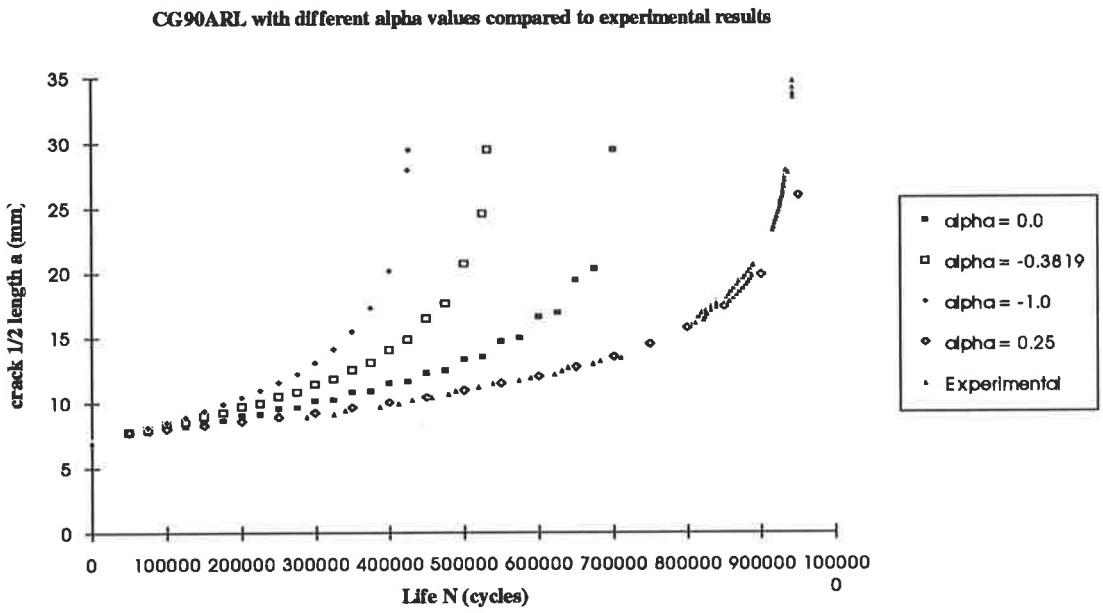

Figure 6.17 CG90ARL predictions for different retardation parameter (alpha) values

6.7. Results using Wheeler model

A program was developed to predict crack growth using the Wheeler algorithm described in section 4.2. A program listing of the Pascal program used is listed at Appendix D. The program was used to predict crack growth rates during a constant amplitude fatigue test by setting the material constant "m" in equation (4.7) to zero. This ensured that a linear value for crack growth rate da/dN was calculated at each crack length. Figure 6.18 indicates that this Wheeler model was less conservative than the CG90ARL model but still nearly 28% more conservative than the experimental results for a constant load amplitude fatigue test.

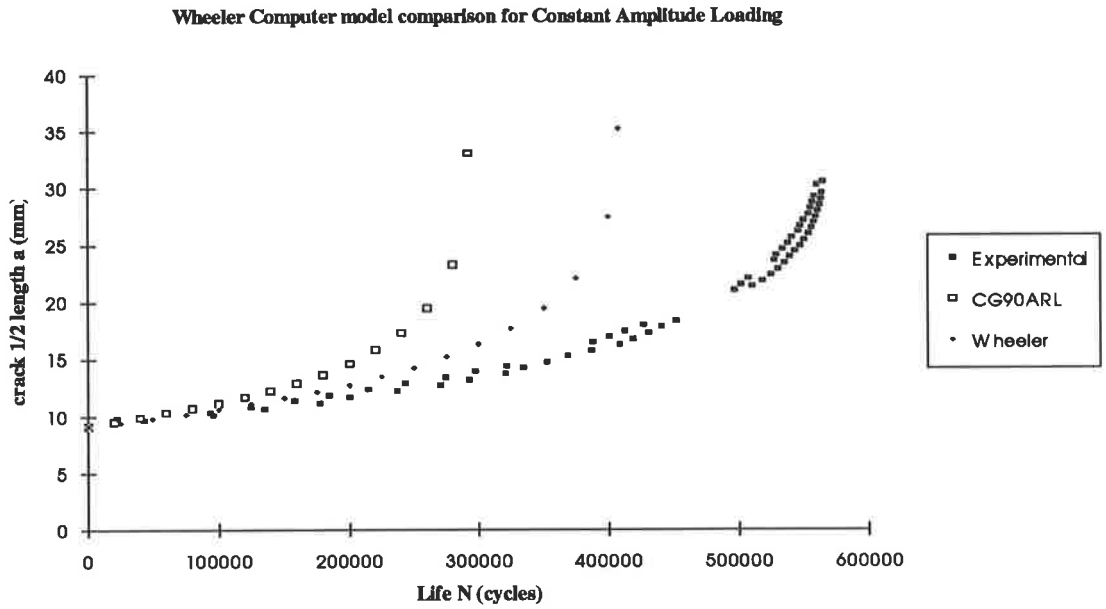

Figure 6.18 Wheeler model prediction for constant amplitude loading

The Wheeler program was then used to find the value for the material constant *m* which would describe the crack growth rates produced in the periodic overload experiment of section 6.4. The program prompted for a value of *m* and the resulting data produced by the program was compared to the experimental data obtained. This "tuning" continued until an acceptable value of *m* was obtained. Figure 6.19 shows that a value of m=1.55 matched the experimental results to within 3%. It is important to note that this result is only valid for the material used and for the loading condition applied.

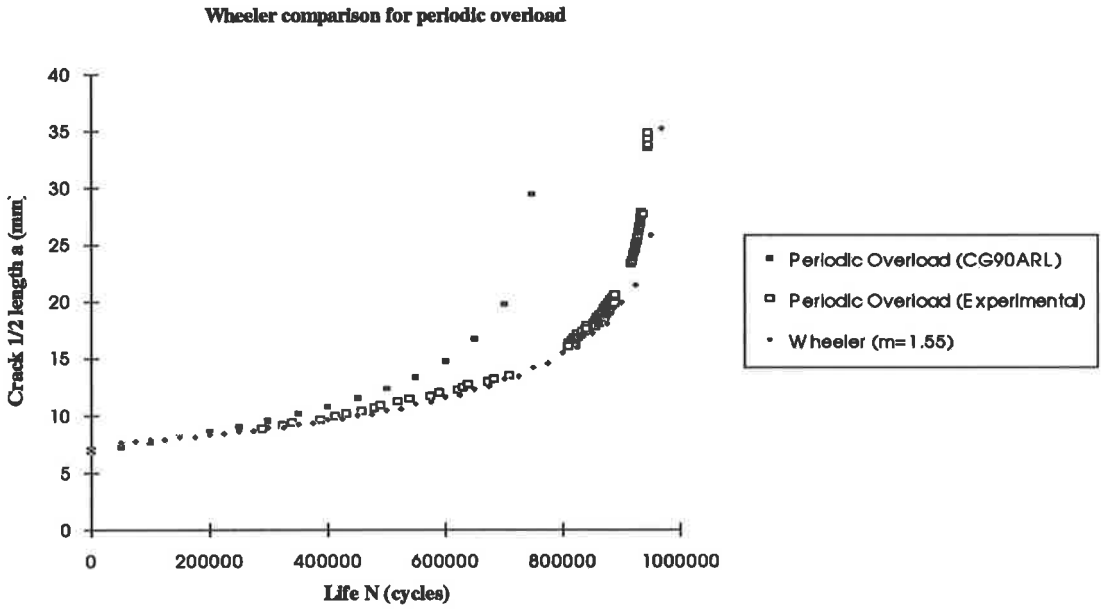

Figure 6.19 Wheeler model "tuned" to periodic overload experimental results

CHAPTER 7

DISCUSSION, CONCLUSIONS AND RECOMMENDATIONS

7.1. Discussion

The main objective of determining the effective stress intensity arising from residual stress distribution at a fatigue crack tip was achieved in this work. The theory of the stress intensity factor was studied and the various methods of determining its value were investigated. Using FEM packages would appear to be the most appropriate method for calculating stress intensity factors in practical situation because they allow modelling of structures of any shape and dimension. Tables of ΔK values and equations developed for calculating ΔK values are only suitable for experimental work in which the specimens used are of a standard geometry.

Three satisfactory methods of measuring crack growth were developed in this work. The use of a video camera connected to a microscope provided an excellent media from which to observe crack growth experiments in real time and by attaching a video recorder also provided an excellent means of reviewing and demonstrating the work to others. The most effective and manpower efficient method of crack growth measurement was achieved using crack propagation gauges recorded by an IBM PC. The travelling microscope arrangement was used to verify that the gauges were accurately recording crack growth on dummy specimens before the testing for this research commenced.

The crack propagation gauges were used to record crack growth during a constant amplitude fatigue test. The resulting da/dN versus ΔK compared well with AMRL provided data instilling confidence in the system developed. The gauges were also used to record the retarded crack growth rates experienced following application of a tensile overload during a constant ΔK fatigue test. The data recorded by the gauges was used to

quantify the effective stress intensity factor in the overload affected area. Resources and time limited the study to two levels of ΔK and three overload ratios and it is recommended that this procedure be repeated for a greater range of ΔK levels and overload ratios. If computer models based on ΔK_{eff} are to be used to predict crack growth in components subjected to variable amplitude loading then it is imperative that tests are carried out for a full range of ΔK levels expected in practice and at numerous overload ratios.

The final phase of this work demonstrated the increase in specimen fatigue life attainable using periodically applied overloads. The test revealed the potential to vastly increase the fatigue life of components experiencing constant amplitude loading by periodically applying single tensile overloads. In practice this may well mean applying a tensile overload at some predefined time in the life of the component such as an overhaul or major servicing.

7.2. Conclusions

The research conducted investigated current methods in linear elastic fracture mechanics for their suitability to predict crack growth in aluminium 7050-T7451 when a compressive residual stress field was introduced by an overload. As a result of this work the following results and general conclusions can be drawn:

1. The Mode-I Stress intensity factor ΔK for a plate with a centre crack was investigated using a range of available techniques: an FEM package, a Weight Function technique, K_I data tables, and an established formula. The results were compared revealing differences in the K_I values predicted of up to 27% at the longest crack length value.

2. Three methods of measuring crack growth during fatigue testing on an Instron were developed:

   (i) a travelling microscope with a digital micrometer attached;

(ii) a video camera with a graticuled lens attached to the microscope;

(iii) crack propagation gauges connected to PC based data recording software.

The video camera connected to the microscope arrangement provided a means to view and videotape the crack growth experiments conducted while the crack propagation gauges were used to record crack growth measurements. An investigation of the shape of the crack front justified the use of specimen surface-mounted crack propagation gauges to measure crack growth in these experiments.

3. Crack growth rates recorded during a constant amplitude fatigue test were consistent with published data for aluminium alloy 7050-T7451.

4. Experiments demonstrated definite crack growth retardation following the application of an overload during constant amplitude fatigue loading. The number of cycles found to be retarded by the overload effect was found to increase with an increase in overload ratio and to decrease with increased ΔK level.

5. Values for the effective ΔK value over 0.25 mm intervals beyond the point of application of an overload were successfully determined using the crack propagation gauges. The effective ΔK values were below the baseline ΔK values for all of the three overload ratios investigated at the highest ΔK level as well as at the two highest overload ratios investigated at the lower ΔK level. An increase in overload produced a decrease in effective ΔK. The effective ΔK was found to *increase* in value for an overload level of 1.4 at the lower baseline ΔK value of 300 $MPa\sqrt{mm}$, with a corresponding increase in crack growth rate. The author recommends further experimental investigations be carried out at

this combination of ΔK and overload ratio before any conclusions should be drawn from this result (see section 6.3).

6. A computer program was developed using the Wheeler model for predicting crack growth. The empirical model required only one material specific constant which was calculated for a specific loading condition applied to the aluminium alloy investigated.

7. The computer program CG90ARL provided by the Aeronautical and Maritime Research Laboratory was used to predict crack growth rates and then compare them with experimental data. The program contained a retardation parameter which when used with the default value of zero produced conservative crack growth predictions for both constant amplitude fatigue loading and overload induced retarded crack ground. The full range of allowable retardation parameter values was investigated revealing a considerable difference in life prediction. With a retardation parameter of -1 the program predicted a life 39% less than at the default value of zero and a retardation parameter of 1 predicted virtual crack arrest.

8. The ability of compressive residual stresses to extend the fatigue life of a specimen was demonstrated. During a constant amplitude fatigue test a single overload ratio of 1.8 was applied every 50,000 cycles resulting in a 35% increase in specimen fatigue life.

7.3. Recommendations

1. If a testing machine which accepts feedback could be utilised then a large combination of ΔK/overload ratios could be tested with little effort. Overload application and load shedding could be automated using the voltage output provided by the crack propagation gauges representing predefined crack lengths.

2. The applicability of these crack propagation gauges in aircraft fatigue monitoring should be investigated. The full scale fatigue test of a RAAF F/A-18 aircraft being conducted by AMRL could be used to trial the gauges. Fatigue cracks which will eventually appear during the AMRL tests could be monitored using these crack propagation gauges providing invaluable crack growth data from a variable amplitude fatigue test on actual aircraft structures.

LIST OF REFERENCES

Aliabadi, M.H., and Rooke, D.P., "Numerical Fracture Mechanics", Kluwer Academic Publishers, Dordrecht, 1991.

ANSYS User's Manual, Revision 5.0, Swanson Analysis Systems Inc., 1992.

ASTM E647-88a, Annual Book of ASTM Standards, Vol 03.01, pp648-668, 1990.

Averbach, B.L., and Bingzhe Lou., "Fatigue Crack Propagation Through Residual Stress Fields", Advances in Fracture Research (Fracture 84), 3, 1631-1640.

Bos, M.J., "Critical Appraisal of the McDonnell Douglas Closure Model for Predicting Fatigue Crack Growth", DSTO ARL Aircraft Structures Report 444, Commonwealth of Australia, 1991.

Broek, D., "Elementary Engineering Fracture Mechanics", Kluwer Academic Publishers, Netherlands, 1986.

Buch, A., "Fatigue Strength Calculation", Trans Tech Publications, Switzerland, 1988.

Bueckner, H.F., "Weight Functions for the notched bar", Mathematic. Mechan. 51, pp. 97-109, 1971, edited by Z. Angewandte.

de Konig, A.U. and Richmond, M.J., Task Report 2.1, National Aerospace Laboratory NLR, The Netherlands, 1992.

Elber, W. "The significance of fatigue crack closure", ASTM STP 486, American Society for Testing Materials, 1971.

Ewalds, H.L., and Wanhill, R.J.H., "Fracture Mechanics", Edward Arnold Publications, London, 1991.

Finney, J.M. and Deirmendjian, G., "Delta-K-Effective: Which Formula?", Fatigue Fract. Engng Mater. Struct. Vol. 15, No. 2, 151-158, 1992.

Fleck, N.A., and Smith, R.A., "A Discussion of Mechanisms of Accelerated and Retarded Fatigue Crack Growth", Advances in Fracture Research (Fracture 84), 3, 1823-1829.

Fuchs, H.O., and Daly, J.J., "Advances in Surface Treatments Volume 4 - International Guidebook on Residual Stresses", pp. 73-86, edited by Niku-Lari, A., Pergamon Press, Sydney, 1987.

Hauk, V., "Advances in Surface Treatments Volume 4 - International Guidebook on Residual Stresses", pp. 251-25, edited by Niku-Lari, A., Pergamon Press, Sydney, 1987.

Heller, M., Jones, R., and Williams, J.F., "Analysis of Cold-Expansion for Cracked and Uncracked Fastener Holes", Engineering Fracture mechanics, Vol. 39, No. 2, pp. 195-212, 1991.

Herman, R., "Fatigue crack growth in ductile materials under cyclic compressive loading", Fatigue Fract. Engng Mater. Struct., Vol. 17, pp. 93-103, 1994.

Jones, R., and Miller, N.J., Preface to International Conference on Aircraft Damage Assessment and Repair, Melbourne, 1991.

Lai, M.O., Nee, A.Y.C. and Oh, J.T., "Effect of residual stress on the fatigue performance of the structure of a ballised hole", Journal of Materials Processing Technology, 29, pp. 301-309, 1992.

Lam, Y.C., "A Fatigue Crack Growth Model based on the Contact Stress Intensity Factor Approach", Theoret. Appl. Fracture Mech., 12, 149-154, 1989.

Lam, Y.C. and Lian, K.S., "The effect of residual stress and its redistribution on fatigue crack growth", Theoret. Appl. Fracture Mech., 12, 59-66, 1989.

Lam, Y.C., "A comparative study on the effects of interference fit and cold expansion on the fatigue life of cracked holes", Scripta Metallurgica et Materialia, Vol 28, 191-195, 1993.

Lam, Y.C., "Fatigue life enhancement of cracked holes", International Conf. on Aircraft Damage Assessment and Repair", pp. 105 -108, 1991.

Lees, W.A., "Adhesives and the Engineer", Mechanical Engineering Publications Limited, London, 1989.

McDonnell Douglas Aircraft Company, "CG90 User's Manual for the prediction of crack growth", 1991.

Measurements Group Inc, "Catalog 500 - Precision Strain Gages", Micro-Measurements Division, 1993.

Measurements Group Inc, "Catalog A-110-7 - Strain Gauge Accessories", Micro-Measurements Division, 1994.

Meguid, S.A., "Engineering Fracture Mechanics", Elsevier Applied Science, New York 1989.

Nelson, D.V., "Effects of Residual Stress on Fatigue Crack Propagation", ASTM STP 776, pp 172-194, 1982.

Press, W.H., Flannery, B.P., Teukolsky, S.A., and Vetterling, W.T., "Numerical Recipes - The Art of Scientific Computing", Cambridge University Press, New York, 1986.

Parker, A.P., "The Mechanics of Fracture and Fatigue - An Introduction", E. & F.N. SPON LTD, New York, 1981.

Polakovics, D., "Aging Aircraft, The United States Navy Experience", International Conference on Aircraft Damage Assessment and Repair, 1991.

Pook, L.P.,"The Role of Crack Growth in Metal Fatigue", The Metals Society, London, 1983.

Potts, E.M., "Crack Growth Predictions at Open Fastener Holes Using Crack Closure Models CG90 and CG90ARL", DSTO ARL Aircraft Structures Technical Memorandum 588, Commonwealth of Australia, 1992.

Ranganathan, N., Petit, J., and de Fouquet, J., "On the Influence of the Initial ΔK level on the post overload crack propagation behaviour", Advances in Fracture Research (Fracture 84), 3, p 1767-1774.

Reid, L.F., "Airframe life extension through cold expansion techniques", International Conf. on Aircraft Damage Assessment and Repair", pp. 109 -114, 1991.

Robin, C., Chehimi, C., Louah, M., Pluvinage, G., Schneider, M.L., Bignonnet, A., Truchon, M., and Lieurade, H.P., "Influence of multiple overloads on fatigue crack growth", Advances in Fracture Research (Fracture 84), 3, 2007-2014.

Rooke, D.P. and Cartwright D.J., "Compendium of Stress intensity factors", Her Majesty's Stationary Office, London, 1976.

Saunder, T.J., "Fatigue crack growth from coldworked eccentrically located holes in 7075-T651 Aluminium", a Masters Thesis submitted at Purdue University, USA, 1991.

Skalli, N. and Flavenot, J.F., "Fatigue Strength Estimation Incorporating Residual Stresses: Comparison of Different Fatigue Criteria", Advances in Fracture Research (Fracture 84), 3, pp. 1959-1965.

Taira, S., and Tanaka, K., "Local Residual Stress near Fatigue Crack Tip", Transactions of The Iron and Steel Institute of Japan, 1978.

Taylor, D., and Knott, J.F., "The Effect of Frequency on Fatigue Crack Propagation Rate", Advances in Fracture Research (Fracture 84), 3, 1759-1766.

Ward-Close, C.M., and Ritchie, R.O., "On the Role of Crack Closure Mechanisms in Influencing Fatigue Crack Growth Following Tensile Overloads in a Titanium Alloy: Near Threshold Versus Higher ΔK Behaviour", Mechanics of Fatigue Crack Closure, ASTM STP 982, 1988, pp. 93-111.

Willenborg, J., "A Crack Growth Retardation Model Using an Effective Stress Concept", AFFDL-TM-71-1-FBR (1971).

APPENDIX A - EXAMPLE KI OUTPUT FROM ANSYS

(a=15mm)

**** CALCULATE MIXED-MODE STRESS INTENSITY FACTORS ****

ASSUME PLANE STRAIN CONDITIONS

ASSUME A HALF-CRACK MODEL WITH SYMMETRY BOUNDARY CONDITIONS
(USE 3 NODES)

EXTRAPOLATION PATH IS DEFINED BY NODES: 81158 81246 81245
WITH NODE 81158 AS THE CRACK-TIP NODE

USE MATERIAL PROPERTIES FOR MATERIAL NUMBER 1
EX = 68900. NUXY = 0.33000 AT TEMP = 0.00000E+00

PRINT THE LOCAL CRACK-TIP DISPLACEMENTS

CRACK-TIP DISPLACEMENTS:
UXC =-0.70357E-02 UYC= 0.00000E+00 UZC= 0.78886E-30

NODE	CRACK FACE	RADIUS	UX-UXC	UY-UYC	UZ-UZC
81158	TIP	0.00000E+00	0.00000E+00	0.00000E+00	0.00000E+00
81246	TOP	0.12500	0.56372E-04	0.16940E-02	0.00000E+00
81245	TOP	0.50000	0.21629E-03	0.33657E-02	0.00000E+00

LIMITS AS RADIUS (R) APPROACHES 0.0 (TOP FACE) ARE:
(UX-UXC)/SQRT(R) = 0.11063E-03 (UY-UYC)/SQRT(R) = 0.48020E-02
(UZ-UZC)/SQRT(R) = 0.00000E+00

**** KI = 232.67 , KII = 0.00000E+00, KIII = 0.00000E+00 ****

APPENDIX B - PROGRAM FOR KANAZAWA'S WEIGHT FUNCTION

FORTRAN PROGRAM FOR CALCULATING KANAZAWA'S K_1 SOLUTIONS

```
      PROGRAM INTEGRATION_KANAZAWA
C
      IMPLICIT UNDEFINED (A-Z)

C     USE INTEGRATION ROUTINES WRITTEN USING CODE FROM "NUMERICAL
C     RECIPES"
      INCLUDE 'INTEG.DEF'
      LOGICAL OK, INTEG_SET
      REAL A,  ANSWER, ANSWER1, ANSWER2, INTEG_GET, INTEGRATE,
     KANAZAWA
      REAL PI,W,B,LOAD,Q,MAX_X
      COMMON A,MAX_X

C     USE SUBROUTINE TO CALCULATE P(X) AND M(X,A) AND THEIR PRODUCT
C     AT EACH VALUE OF X REQUIRED
C     BY THE INTEGRATION ROUTINE
      EXTERNAL KANAZAWA

      PI = 3.14159
      W = 74.0
      B = 10.0
      LOAD = 20000.0
C
      DO 100 A  = 7.5,35.0,2.5

C     INITIALISE VARIABLE FOR REPORTING MAXIMUM X VALUE REACHED IN
C     THE OPEN INTEGRATION
      MAX_X = 0.0
C       A  = 6.0

C     SET THE PARAMETERS FOR CALCULATING THE CLOSED INTEGRATION
C     FROM -A TO +A-0.1
      OK = INTEG_SET( INTEG_MAX_EVAL, 1.0E4 )
      OK = OK .AND. INTEG_SET( INTEG_METHOD,
     1                  REAL( INTEG_TRAPEZ + INTEG_CLOSED ) )
      OK = OK .AND. INTEG_SET( INTEG_PRECIS, 1.0E-4 )
      OK = OK .AND. INTEG_SET( INTEG_ZER_TOL, 1.0E-6 )
      ANSWER1 = INTEGRATE( KANAZAWA, (-A), (A-0.1) )
      WRITE( 6, 1 ) OK, INT( INTEG_GET( INTEG_EVALNS ) + 0.1 ),
     1    INT( INTEG_GET( INTEG_CONVERG ) + 0.5 ), -A, A-0.1,ANSWER1
```

```
1    FORMAT( ' INTEGRATION PARAMETERS SET ?', 9X, L1 /
     1       ' NUMBER OF FUNCTION EVALUATIONS   ', I6 /
     2       ' CONVERGED TO REQUIRED ACCURACY ? ', I2 /
     3       ' LOWER LIMIT OF INTEGRATION       ', F9.4 /
     4       ' UPPER LIMIT OF INTEGRATION       ', F9.4 /
     5       ' RESULT                           ', G15.7 )

C    SET THE PARAMETERS FOR CALCULATING THE OPEN INTEGRATION
FROM
C    +A-0.1 TO +A
     OK = INTEG_SET( INTEG_MAX_EVAL, 1.0E4 )
     OK = OK .AND. INTEG_SET( INTEG_METHOD,
     1                  REAL( INTEG_RHOMBERG + INTEG_OPEN ) )
     OK = OK .AND. INTEG_SET( INTEG_PRECIS, 1.0E-4 )
     OK = OK .AND. INTEG_SET( INTEG_ZER_TOL, 1.0E-6 )
     ANSWER2 = INTEGRATE( KANAZAWA, (A-0.1),A )
     WRITE( 6, 2 ) OK, INT( INTEG_GET( INTEG_EVALNS ) + 0.1 ),
     1   INT( INTEG_GET( INTEG_CONVERG ) + 0.5 ), A-0.1, A, ANSWER2
2    FORMAT( ' INTEGRATION PARAMETERS SET ?', 9X, L1 /
     1       ' NUMBER OF FUNCTION EVALUATIONS   ', I6 /
     2       ' CONVERGED TO REQUIRED ACCURACY ? ', I2 /
     3       ' LOWER LIMIT OF INTEGRATION       ', F9.4 /
     4       ' UPPER LIMIT OF INTEGRATION       ', F9.4 /
     5       ' RESULT                           ', G15.7 )

C    ADD THE TWO INTEGRATION RESULTS TOGETHER
     ANSWER = ANSWER1 + ANSWER2

C    CALCULATE K1/K0 FACTOR AT EACH CRACK LENGTH
     Q = ANSWER/((LOAD/(W*B))*SQRT(PI*A))

C    PRINT THE CRACK LENGTH, K1, K1/K0, AND THE MAXIMUM X VALUE
C    REACHED
     WRITE(6,10) A,ANSWER,Q,MAX_X
10   FORMAT(  F9.4,G15.7,F9.4,F9.4 )

100  CONTINUE
     STOP
     END

C    SUBROUTINE
     REAL FUNCTION KANAZAWA( X )
     REAL ABS_X, A, X, MX, PX, W, PI, B, LOAD, MAX_X
     COMMON A,MAX_X
     ABS_X = ABS(X)
     PI = 3.14159
     W = 74.0
```

```
      B = 10.0
      LOAD = 20000.0

C     INCREASE MAX_X IF A HIGHER VALUE OF X REACHED
      IF (X.GT.MAX_X)MAX_X = X

C     CALCULATE M(X)
      MX=SQRT(2*SIN(PI*(A+X)/W)/(W*SIN(2*PI*A/W)*SIN(PI*(A-X)/W)))

C     CALCULATE P(X)

      IF ( ABS_X .LT. 0.25 ) THEN
        PX=-3.8964
      ELSE IF ( ABS_X .LE. 2.0 ) THEN
        PX=-14.2559+49.0957*ABS_X-66.9986*ABS_X**2+32.9991*ABS_X**3
      ELSE IF ( ABS_X .LT. 2.72917 ) THEN
        PX=-45.1664 * ( ABS_X - 2 ) + 79.906
      ELSE
        PX=26.791006+7.450222/(ABS_X-2)+20.169341*EXP(-(ABS_X-2))
      ENDIF

C     MULTIPLY P(X) AND M(X)
      KANAZAWA=PX*MX

C       WRITE(6,10) X, KANAZAWA
C 10    FORMAT(  2G13.5 )

C     PASS RESULT BACK TO MAIN PROGRAM
      RETURN
      END
```

APPENDIX C - CG90ARL MATERIAL FILE

```
" X7050T74LP.ANL:  7050-T7451 PLATE L-T, PROTECTED ENVIRONMENT, S.I.
Units"
 68900.00   0.33
 275.6   406.5  427.2
 496.1   0.08
 1288.28   19
57.643          2.54E-08
69.449          4.32E-07
78.825          1.27E-06
83.339          1.52E-06
104.174         3.05E-06
138.898         5.59E-06
173.623         9.65E-06
208.347         1.65E-05
243.072         2.54E-05
277.796         5.08E-05
300.0           6.6E-05
312.521         7.62E-05
347.245         1.14E-04
400.0           0.00019
430.584         2.54E-04
524.34          5.08E-04
597.262         7.62E-04
694.49          1.27E-03
868.113         2.79E-03
1041.735        1.09E-02
1284.807        2.54E-01
0
C     FILE = 7050SI.ANL
C     FOR 7050-T7451 PLATE
C     ORIENTATION:  L-T
C     ENVIRONMENTS:  DATA USED IN DEVELOPING THIS CURVE WAS LAB
AIR.
C     THIS CURVE IS TO BE USED FOR LAB AIR, LHA, AND HHA.
C     THICKNESS:  USE FOR PLATE WITH ORIGINAL THICKNESS LESS THAN
C               150 mm.
C
C     Converted to SI units by M.J. Richmond, ARL, May 1993
C
C     NOTES:
C     1.  DATA USED WAS AT 0 < R <= 0.10 FROM:
C           A.  F-15 DATABASE
C           B.  A-12 DATA GENERATED BY UNIV. OF DAYTON RESEARCH INST.
C
C      X7050T74LP.ANL: 7050-T7451 PLATE L-T, PROTECTED ENVIRONMENT,
91
```

APPENDIX D - PROGRAM WHEELER

The following program uses the Wheeler plastic zone model for predicting retarded crack growth due to overloads. The Paris equation is used to compute da/dN for a given ΔK value. The program prompts the user to enter a value for the Wheeler exponent m. If the value of m is set to zero then the program can be used for constant amplitude fatigue crack growth prediction.

```
program wheeler(input,output);

{  In a constant amplitude fatigue test for N cycles with maximum load dP and load ratio R,
apply an overload of value dPo every Nol cycles.  If purely constant amplitude is required
enter dPo = dP and Nol is no longer relevant.  The material yield stress ys , Kmax, and
dimensions B and W are constants in the program.}

const
   pi = 3.141592654;
   ys = 480;
   R  = 0.0;
   W  = 74;
   B  = 10;
   dP = 25000; {N}
   dPo = 45000;

   KIc =17.5;
   ParisC = 1.255589427E-13;
   ParisN = 3.521010054;
   N =2000000;

var
   phi,a,ao,alpha,ΔKi,ΔKo: real; K1,rpo,rpi,dadn,dA:real;
   running_dA,running_dadn,running_phi:real; i,report_cycles,counter:real;
   m,Nol,Nol_counter:real;
   OutFile  : text;
   Filename : string[15];

function deltaK (load,a:real):real;

{  This function takes a crack length a and computes the Mode I stress intensity factor KI.
The formula used is the one shown at equation 3.9. }

   var alpha : real;
   begin
        alpha:=2*a/W;
        deltaK:=load/B*sqrt( (pi*alpha/(2*W))/(cos((pi*alpha)/2)) );

   end;

procedure Report;
```

```
{ This procedure is used to control the output to the screen and to file Outfile. The name
of Outfile is entered at run time. It keeps running totals for reporting every report_cycles
number of applied cycles. The value for report_cycles is entered at run time. }


   begin

      IF (i=1) THEN dadN:=running_dadn
         ELSE
         begin
            dadN:=running_dadn/report_cycles;  phi:=running_phi/report_cycles;
            counter:=0;
         end;
      writeln(i:7:0,' ',rpi:7:5,' ',(a+rpi):7:5,' ',phi:7:5, ' ',K1:7:2,' ',dadN:7,'
',running_dA:7:3,' ',a:7:5);

{  where K1 is the value of K_I at the end of the report_cycles, dadn is the average da/dN
for the period, da is the total change in crack length a for the period, a is the crack length at
the end of the period. }

      writeln(Outfile,i:7:0,',',a:8:5);
      running_dA:=0;
      running_dadn:=0;
      running_phi:=0;
   end;

begin  {main program}

   ao := 7.7086;        {set the value for the initial crack length}
   write('enter m for wheeler: ');
   readln(m);
   write('enter output file name ');
   readln(Filename);
   assign(OutFile,Filename);
   rewrite(OutFile);

{  this section commented out so user not prompted for variables already set in CONST}
{  write('enter the number of constant load amplitude cycles after the overload ');
   readln(Nol);
   write('enter the interval between data reporting ');
   readln(report_cycles);
}

   Nol:=50000;
   report_cycles:=25000;
   writeln;
   writeln('An overload =',dPo/1000:6:0,'KN was applied at start.');
```

```
writeln('This produces plastic zone size, rpo = ',rpo:7:5,'mm');
writeln('Max cyclic load was then =',dP/1000:6:0,'KN for remainder of test.');
writeln('The load ratio, R = ',R:2:1);
writeln('The Paris constants were C = ',ParisC:10,' N = ',ParisN:7:5); writeln('The exponent
m used was = ',m:4:2);
writeln;
writeln('  N    rpi   a+rpi   phi    ΔK    da/dN    dA     a');

a:=ao;
dadN:=0.0;
dA:=0.0;
running_dA:=0.0;
running_dadn:=0.0;
running_phi:=0.0;
Nol_counter:=0.0;

i:=0;
counter:=0;


{loop here}

Repeat

{ If on this loop an overload is being applied then use dPo to calculate K_I and the plastic
zone.  Nol_counter is set to 0.0 at the start and then every Nol cycles after that.}

        IF (Nol_counter=0.0) THEN
        begin
                K1:=deltaK(dPo,a);
                rpo:=0.393*sqr(deltaK(dPo,a)/ys);
                ao:=a;
        end
        ELSE

{ otherwise this loop is a normal fatigue cycle and therefore dP is used to calculate K_I and
the plastic zone.}

        K1:=deltaK(dP,a);
        rpi:=0.393*sqr(K1/ys);

{ Wheeler retardation is calculated here using the formula discussed in section 4.2. and
listed at equation (4.7).  If the crack has grown out of the effect of the overload (ie ao+rpo)
then phi is set to 1 resulting in no reduction in the calculated da/dN.  If not then equation
(4.7) is used to calculate phi and hence the retarded da/dN.}

        IF ((a+rpi) > (ao+rpo)) THEN phi:=1
```

```
        ELSE phi := exp(m*ln((rpi/(ao+rpo-a))));

        running_phi:=running_phi+phi;


{Linear da/dN is calculated using equation (3.6) }

        dadN:=ParisC* exp(ParisN*ln(K1)); {Paris Equation}

          running_dadn:=running_dadn+dadn;
          dA:=phi*dadN*1;
          running_dA:=running_dA+dA;

        a:= a + da;
        i:= i + 1;
        Nol_counter:=Nol_counter+1;
        counter := counter + 1.0;

IF( (counter>=report_cycles)OR(i=1.0) ) THEN Report; IF(Nol_counter>=Nol) THEN
Nol_counter:=0.0;

until ( (i >= N)OR(K1>=1288.28) );

{ This is the end of the Repeat Loop. The program jumps out of the loop if the maximum
fatigue cycles N is exceeded or the material KIc is exceeded.}

report_cycles:=counter;
Report;

close(Outfile);

end.
```

APPENDIX E - TRAVELLING MICROSCOPE COMPONENT DRAWINGS

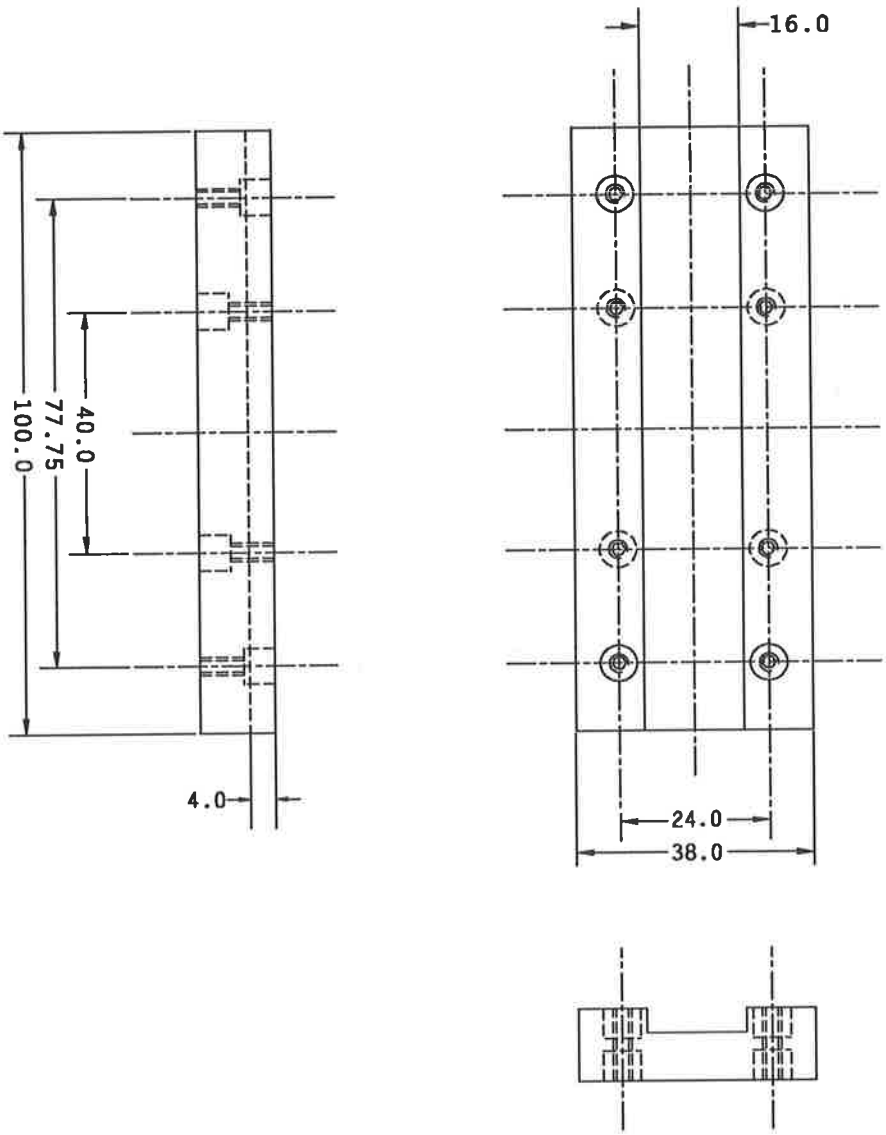

Item A: Aluminium Spacer

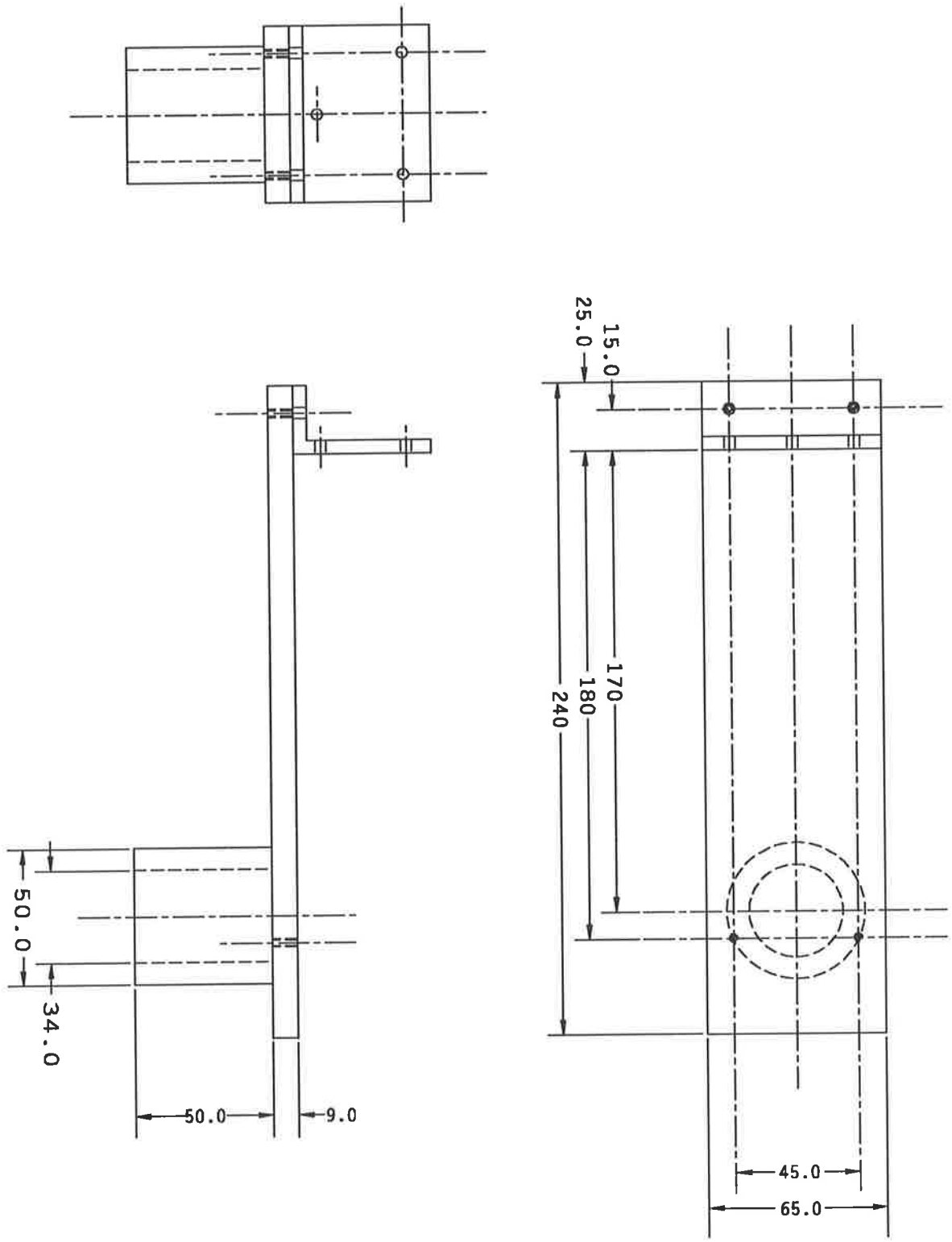

Item B: Microscope Platform

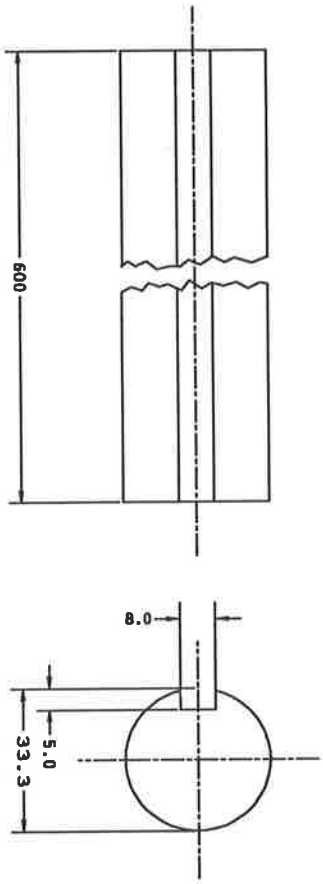

Item C: Column with key way

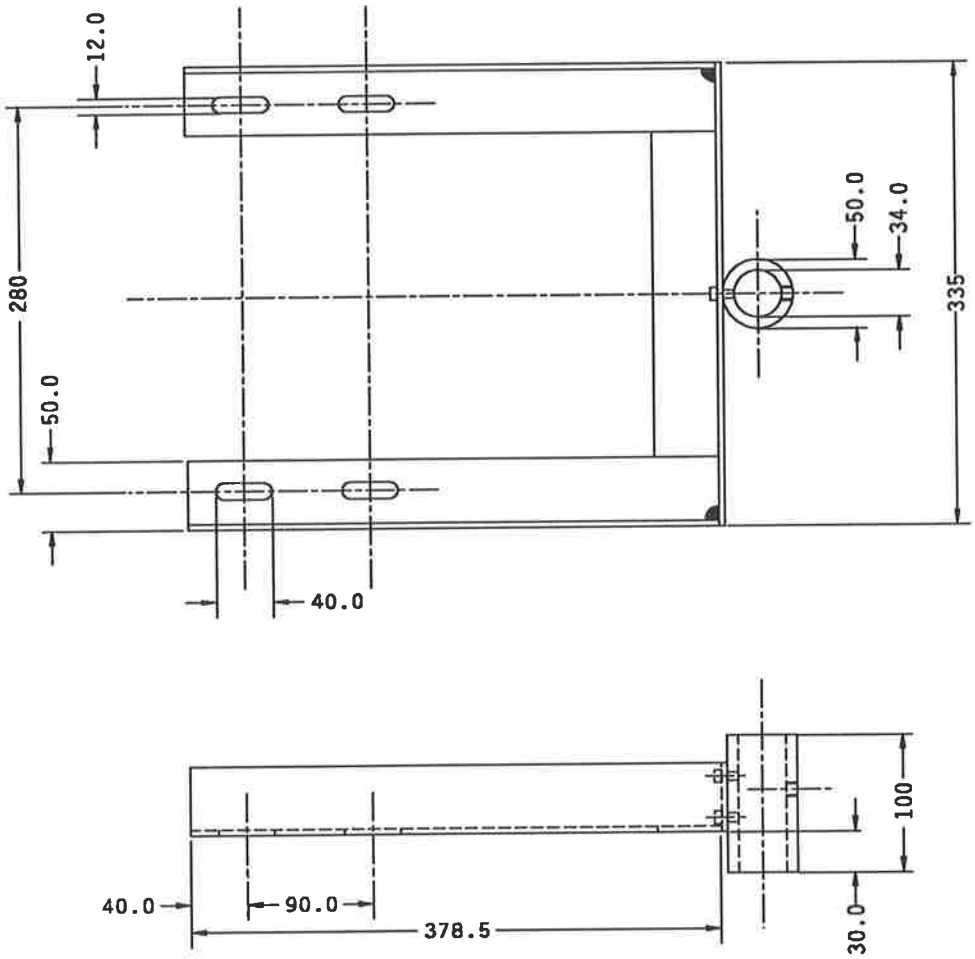

Item D: Mounting Frame

APPENDIX F - CRACK PROPAGATION GAUGE CALIBRATION

Crack Propagation Gauge Circuitry Calibration								
CPA02 Type Gauges								
		Voltage recorded						
Strands Broken	Resistance	Channel 1	Channel 2	Channel 3	Channel 4	Channel 5	Channel 6	Ave
0	5.26	0	0	0	0	0	0	0
1	5.51	0.063	0.068	0.078	0.049	0.068	0.049	0.0625
2	5.85	0.156	0.165	0.176	0.161	0.171	0.146	0.1626667
3	6.2	0.254	0.254	0.273	0.254	0.269	0.249	0.2588333
4	6.59	0.365	0.365	0.391	0.371	0.381	0.361	0.3726667
5	7.04	0.493	0.493	0.508	0.493	0.503	0.488	0.4963333
6	7.55	0.63	0.63	0.6544	0.635	0.645	0.63	0.6374
7	8.15	0.801	0.801	0.82	0.801	0.805	0.796	0.8041667
8	8.87	0.986	0.981	1.006	0.981	0.985	0.977	0.9861667
9	9.67	1.187	1.191	1.216	1.191	1.196	1.187	1.1946667
10	10.66	1.44	1.436	1.46	1.436	1.436	1.436	1.4406667
11	11.9	1.729	1.724	1.753	1.729	1.729	1.724	1.7313333
12	13.42	2.08	2.075	2.104	2.08	2.075	2.07	2.0806667
13	15.38	2.51	2.5	2.534	2.505	2.495	2.495	2.5065
14	18	3.037	3.027	3.065	3.037	3.018	3.027	3.0353333
15	21.66	3.711	3.695	3.745	3.716	3.691	3.701	3.71
16	27.15	4.619	4.595	4.644	4.609	4.58	4.595	4.607
17	36.4	5.869	5.84	5.903	5.869	5.825	5.845	5.8585
18	54.4	7.686	7.642	7.729	7.681	7.617	7.646	7.6668333
19	108.02	8.164	7.9	7.896	7.91	8.271	8.345	8.081
20	open circuit							

CPA02 Resistance

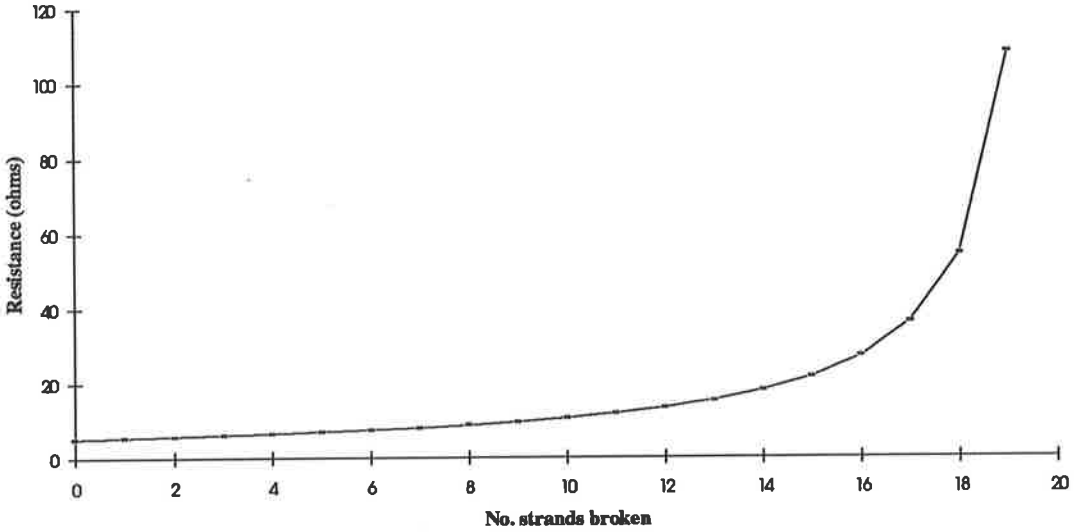

CPA02 Voltage Outputs

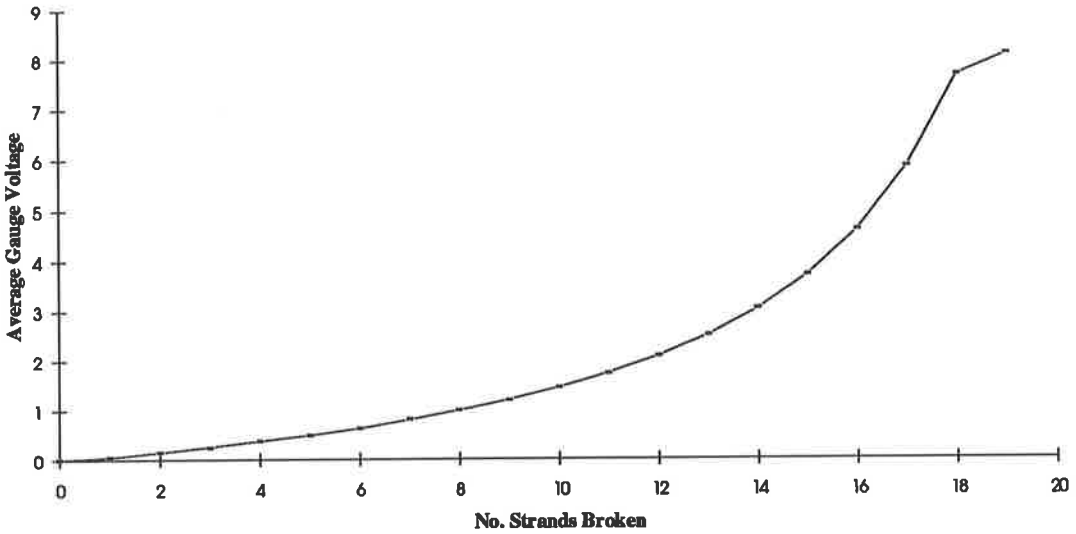

APPENDIX G - LAYOUT OF CRACK PROPAGATION GAUGES

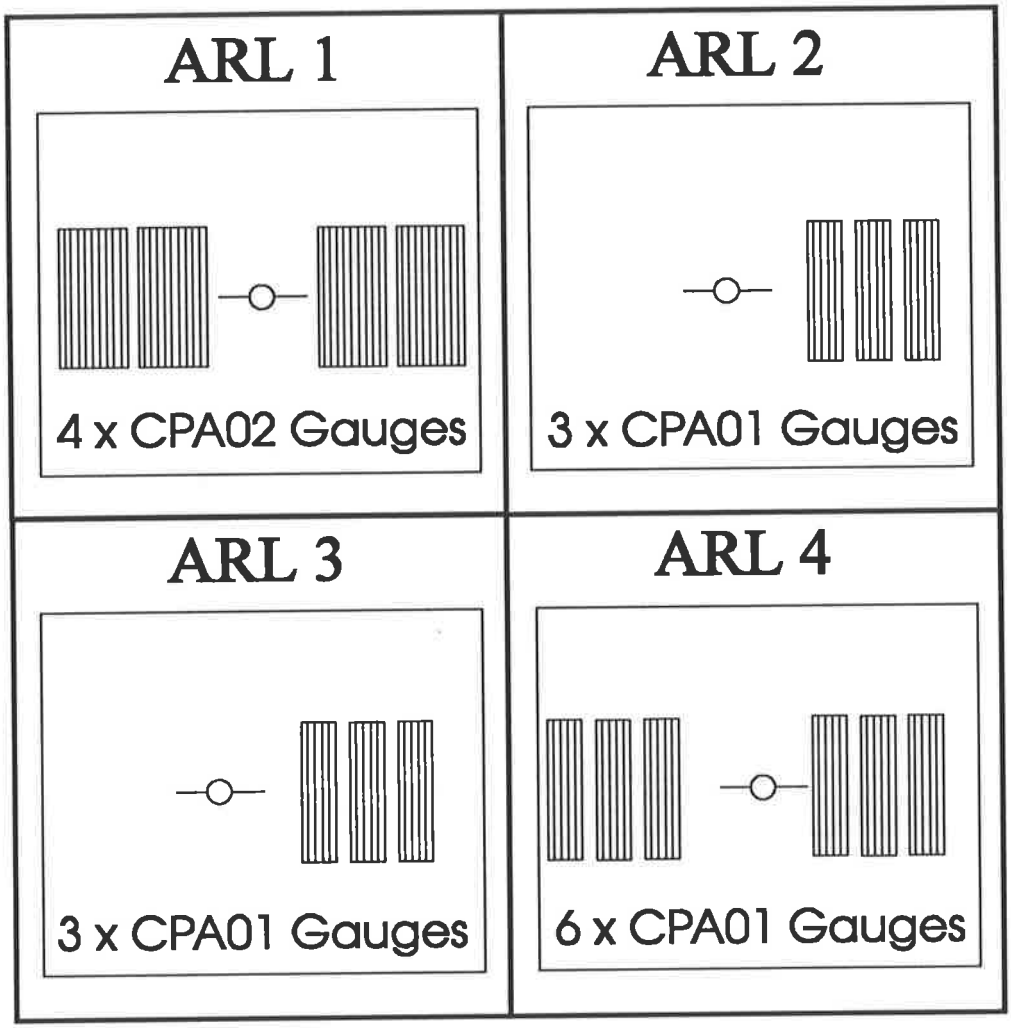

APPENDIX H - PROGRAM FOR DATA REDUCTION

```
program ASTM_V2;
{  This program uses the Incremental Polynomial Method and the  Secant or point-to-point
method for computing da/dN vs delta K from experimentally obtained a vs N data.  The
method involves fitting a second-order polynomial (parabola) to sets of 7 (in this case) sets
of successive data points.  ASTM-E647 provides a Fortran program listing which utilizes
the 7 point incremental polynomial technique.  This program is a Pascal translation of that
code written by G.R. Rohrsheim. The program is capable of reducing data for C(T) and
M(T) type specimens. The delta K formulas used are the ones listed in ASTM-E647.}

const   PI = 3.141592654;

type        mat200=array [1..200] of real;

{  This mat200 array limits the program to 200 a,N pairs.
                    increase this if required, remembering that you will be
   using more RAM. }

            mat10=array [1..10] of real;
            mat7 =array [1..7] of real;
            mat3 =array [1..3] of real;
            astrixtype =string[2];
            envirtype  =string[10];

var         a,n,dadn,delk                                       : mat200;
            aa,nn                                               : mat10;
            id                                                  : mat7;
            bb                                                  : mat3;
            astrix     : astrixtype;
            envir,spec_name,spec_type                           : envirtype;
            outfile,outans                                      : text;
            gq,qq,npts,nptcount,ctype,l,k,k1,i,j: integer;
            sec_loop: integer;
            b,w,an,pmin,pmax,testfreq,t2,t3,t4  : real; x,yy,den,temp,r,pp,c1,c2      : real;
            ax,sx,sx2,sx3,sx4,sy,syx,syx2                       : real;
            yb,rss,tss,yhat,r2,ar,s,snet,t,ft                   : real;
            ftch1,ftch2,ftch3,sx3ch,sx4ch,ys,sec: real;
            flag                                                : boolean;

procedure TYPE1;
{  If Type 1 [C(T)] specimen selected, calculate variables required
                    for delta K calculations and for yield criteria checking.}

begin
   T:=ar/w;
   IF t<0 THEN BEGIN
   ftch1:=-exp(3*ln(-t));
   ftch3:=exp(4*ln(-t));
```

```
    end
    ELSE BEGIN
    ftch1:=exp(3*ln(t));
    ftch3:=exp(4*ln(t));
    end;

    IF (1-t)<0 THEN ftch2:=-exp(1.5*ln(-(1-t)))
    ELSE                ftch2:=exp(1.5*ln(1-t));

                        ft:=( (2+t)*(0.886+4.64*t-13.32*sqr(t)+14.72*ftch1
                                    -5.6*ftch3 ) )/(ftch2);

    s:=ys*sqrt(pi*w*(1-t))/2;

end;

procedure TYPE2;
{   If Type 2 [M(T)] specimen selected, calculate variables required
    for delta K calculations and for yield criteria checking.}

begin
    t:=2*ar/w;
    IF (cos(pi*t/2)= 0) then writeln('divide by zero error'); sec:=1.0/(cos(pi*t/2));
                IF (sec < 0) then writeln('sqrt of a negative number error!!!!!');
    ft:=sqrt( (pi*t*sec)/2.0);
    snet:=pmax/(b*w*(1-t));
end;


procedure OUTPUTOPEN(var out:text);
{   Opens a file for output. The user is prompted to enter the file name.}

 var filename:string[15];

begin
    write('enter the output file name:-');
    readln(filename);
    assign(out,filename);
    rewrite(out)
{   clears the file if it already exists }

end;

procedure PRINTOUT;
{   writes each line of computed data to the .ans file }

begin
```

```
    writeln(OUTANS,qq:4,'  ',n[qq]:9:1,'  ',a[qq]:5:3,'  ',ar:8:3,'  ', r2:10:6,'
    ',delk[nptcount]:5:2,'    ',dadn[nptcount]:10,astrix);
    writeln(outfile,delk[nptcount],',',dadn[nptcount]);
end;

procedure KEYBOARD;
{   this procedure prompts the user for all the information required to
    perform the data reduction.  The author recommends producing a text file (batch file)
    containing all the required input data.  The a vs N
data can then be cut from the file which recorded it and pasted directly into this input text
file.  All the data can then be entered into the program by redirecting standard input from
the keyboard to the
    text file using the "<" symbol. (e.g astm < astm.in).
}

begin
    k:=0;
write('enter no. of points:-');
readln(npts);
write('enter type of crack [C(T)=1 or M(T)=2]:-');
readln(ctype);
writeln;
writeln('enter dimensions[mm]:-');
write('B= ');
read(b);
write('W= ');
read(w);
write('An= ');
readln(an);
writeln;
writeln('enter test conditions:- ');
write('Pmin [Newtons] = ');
readln(pmin);
write('Pmax [Newtons] = ');
readln(pmax);
write('YS= ');
readln(ys);
write('test frequency= '); readln(testfreq);
write('temp [ C ] = ');
readln(temp);
write('environment cond. = '); readln(envir);
writeln('enter cycles and A meas'); FOR i:= 1 TO npts DO
BEGIN
    write('A',i:2,' N',i:2,' =  '); read(a[i]);
    readln(n[i]);
END;
```

```
end;

procedure Secant_start(sec_loop:integer);
var sec_end:integer;
begin
sec_end:=sec_loop+2;
FOR i:=sec_loop TO (sec_end) DO
BEGIN
ar:=(a[i]+a[i+1])/2;
r2:=0.0;
{  Perform specimen type specific calculations }

   CASE ctype OF
      1: TYPE1;
      2: TYPE2
   END;
delk[i]:=(ft*pp)/(b*sqrt(w));
dadn[i]:=(a[i+1]-a[i])/(n[i+1]-n[i]);
                  writeln(OUTANS,i:4,'  ',n[i]:9:1,'  ',a[i]:5:3,'  ',ar:8:3,'  ',
   r2:10:6,'  ',delk[i]:5:2,'    ',dadn[i]:10); writeln(outfile,delk[i],',',dadn[i]);

   end;
   end;
   procedure Secant_end(sec_loop:integer);
   var sec_end:integer;
   begin
   sec_end:=sec_loop+2;
   FOR i:=sec_loop TO (sec_end) DO
   BEGIN
   ar:=(a[i]+a[i-1])/2;
   r2:=0.0;
   {  Perform specimen type specific calculations }

      CASE ctype OF
        1: TYPE1;
        2: TYPE2
      END;
   delk[i]:=(ft*pp)/(b*sqrt(w));
   dadn[i]:=(a[i]-a[i-1])/(n[i]-n[i-1]);
                    writeln(OUTANS,i:4,'  ',n[i]:9:1,'  ',a[i]:5:3,'  ',ar:8:3,'  ',
   r2:10:6,'  ',delk[i]:5:2,'    ',dadn[i]:10); writeln(outfile,delk[i],',',dadn[i]);

   end;
   end;

   begin  { main }
   flag:=false;
```

```
   write('Enter the specimen name: ');
readln(spec_name);

{  Two output files are created:

1. a file with extension .dat contains only the computed deltaK
     and da/dN values ready for plotting.
2. a file with extension .ans contains the table showing all input data
     and computed results as shown at Table X1.2 of ASTM-E647
}

writeln('For the data to be used in pc-graph (.dat),');
OUTPUTOPEN(Outfile);
writeln('For the table to be printed and handed in (.ans),'); OUTPUTOPEN(Outans);

{  receive the input data either from the keyboard or from a file
   redirected as explained in procedure KEYBOARD above:
}
KEYBOARD;
{  Calculate the load ratio: }
r:=pmin/pmax;
{  assign C(T) or M(T) according to sepecimen type (1 or 2) }
IF ctype = 1 THEN spec_type := 'C(T)'
ELSE spec_type :='M(T)';

{  output the header to the .ans file }

writeln(OUTANS,'SEVEN POINT INCREMENTAL POLYNOMIAL METHOD FOR
DETERMINING DA/DN'); writeln(OUTANS);
writeln(OUTANS,'Specimen name: ',spec_name);
writeln(OUTANS);
writeln(OUTANS,spec_type:4,' specimen   B = ',b:5:3,' mm     W = ',
            w:5:3,' mm   AN = ',an:5:3,' mm');
writeln(OUTANS,'Pmin = ',pmin:5:2,' N   Pmax = ',pmax:5:2,' N  R = ' ,r:5:2,'     TEST
FREQ = ',testfreq:5:1,' Hz'); writeln(OUTANS,'temp.= ',temp:4:1,' C   ENVIRONMENT =
',envir); writeln(OUTANS);
writeln(OUTANS,'OBS.NO. CYCLES   A(meas.)  a(reg.)   M.C.C.   DELK
DA/DN'); writeln(OUTANS,'                [mm]    [mm]        [MPa sqrt(mm)]
[mm/cycle]'); writeln;

IF (r > 0) then pp:=pmax-pmin
ELSE pp:=pmax;

{  Add the notch length to the input crack lengths.  If the crack lengths
   include the notch length then the user should enter an=0.0.
}
```

```
FOR i := 1 TO npts DO
a[i]:=a[i] + an;

{  As the polynomial method incorporated is a seven point polynomial
   routine, the first three and last three points remain unchanged
   and do not get corresponding deltaK and da/dN values computed.  The
            first three data points are therefore computed using the secant method
   and also printed to the required files using procedure Secant.
}

Secant_start(1);

{  (npts-6) computations are performed using all (npts) points }
npts:=npts-6;

FOR nptcount:= 1 TO npts DO
BEGIN
   l:=0;
   k:=k+1;
   k1:=k+6;
   FOR j:= k TO k1 DO BEGIN
   l:=l+1;
   aa[l]:=a[j];
   nn[l]:=n[j];
   end;
   c1:=0.5*(nn[1]+nn[7]); c2:=0.5*(nn[7]-nn[1]);
   sx:=0;
   sx2:=0;
   sx3:=0;
   sx4:=0;
   sy:=0;
   syx:=0;
   syx2:=0;
   FOR j:= 1 TO 7 DO
   BEGIN
      x:=( nn[j]-c1)/c2;
      yy:=aa[j];
      sx:=sx+x;
      sx2:=sx2+sqr(x);
                              IF (x<0) THEN sx3ch:=-exp(3*ln(-x))
      ELSE  IF x=0 THEN sx3ch:=0
      ELSE  sx3ch:=exp(3*ln(x)); sx3:=sx3+sx3ch;
      IF (x<0) THEN
      sx4ch:=exp(4*ln(-x))
      ELSE  IF x=0 THEN sx4ch:=0
      ELSE  sx4ch:=exp(4*ln(x));
```

```
    sx4:=sx4+sx4ch;
    sy:=sy+yy;
    syx:=syx+x*yy; syx2:=syx2+yy*sqr(x);

  END;
            den:=7.0*(sx2*sx4-sqr(sx3))-sx*(sx*sx4-sx2*sx3) +sx2*(sx*sx3-sqr(sx2) );
  t2:=sy*(sx2*sx4-sqr(sx3))-syx*(sx*sx4-sx2*sx3) +syx2*(sx*sx3-sqr(sx2) );
  bb[1]:=t2/den; t3:=7.0*(syx*sx4-syx2*sx3)-sx*(sy*sx4-syx2*sx2)
            +sx2*(sy*sx3-syx*sx2);
  bb[2]:=t3/den; t4:=7.0*(sx2*syx2-sx3*syx)-sx*(sx*syx2-sx3*sy)
            +sx2*(sx*syx-sx2*sy);
  bb[3]:=t4/den;
  yb:=sy/7.0;
  rss:=0;
  tss:=0;
  FOR j:= 1 TO 7 DO
  BEGIN
    x:=(nn[j]-c1)/c2; yhat:=bb[1]+bb[2]*x+bb[3]*sqr(x); rss:=rss+sqr(aa[j]-yhat);
    tss:=tss+sqr(aa[j]-yb);
  END;
  r2:=1.0-rss/tss; dadn[nptcount]:=bb[2]/c2+2.0*bb[3]*(nn[4]-c1)/sqr(c2); x:=(nn[4]-
  c1)/c2;
  ar:=bb[1]+bb[2]*x+bb[3]*sqr(x);
  s:=1E+10;
  snet:=0;
  qq:=nptcount+3;

{ Perform specimen type specific calculations }

  CASE ctype OF
    1: TYPE1;
    2: TYPE2
  END;

{ Calculate deltaK using the data obtained in procedure TYPE1 or TYPE2 }

  delk[nptcount]:=(ft*pp)/(b*sqrt(w));

{ Check that failure criteria have not been met - if they have
            print an asterix next to the data as shown at Table X1.2 in
  ASTM-E647. }

  ax:=delk[nptcount]/(1-r);
  IF (ax>=s) OR (snet>=ys) THEN begin
                                    astrix:='*';
                                    flag:=true
                                end
```

```
    ELSE astrix:='';

{   Having completed the calculations for this data point, write the
    associated line of data to the .ans file }

    PRINTOUT;

END;        { nptcount loop }

{   Write the final three a and N values to the .ans file }
j:=npts+4;
Secant_end(j);

{   If any asterix were written to file, display the following explanation }

If flag THEN writeln(OUTANS,'* - DATA VIOLATE SPECIMEN SIZE
REQUIREMENTS');


close(outfile);
close(outans);
end.
```

APPENDIX I - OUTPUT FROM DA/DN PROGRAM

SEVEN POINT INCREMENTAL POLYNOMIAL METHOD AND SECANT METHOD FOR DETERMINING DA/DN

Specimen name: ARL1LEFT (GAUGES 1 AND 3)

M(T) specimen B = 10.000 mm W = 74.000 mm AN = 0.000 mm
Pmin = 0.00 N Pmax = 25000.00 N R = 0.00 TEST FREQ = 10.0 Hz
temp.= 21.0 C ENVIRONMENT = AIR

OBS.NO.	CYCLES	a(meas.) [mm]	a(reg.) [mm]	M.C.C.	DELK [MPa sqrt(mm)]	DA/DN [mm/cycle]	
1	0.0	9.120	9.375	0.000000	190.96	1.167E-05	]
2	43700.0	9.630	9.885	0.000000	197.01	9.751E-06	]
3	96000.0	10.140	10.395	0.000000	203.03	1.304E-05	]
4	135100.0	10.650	10.651	0.997733	206.05	1.336E-05	
5	176900.0	11.160	11.227	0.997717	212.85	1.441E-05	
6	200500.0	11.670	11.586	0.997577	217.10	1.554E-05	
7	237100.0	12.180	12.175	0.997563	224.08	1.683E-05	
8	270600.0	12.690	12.752	0.994279	230.98	1.938E-05	
9	292900.0	13.200	13.160	0.997594	235.90	2.190E-05	
10	320600.0	13.710	13.803	0.998028	243.72	2.606E-05	
11	334200.0	14.220	14.180	0.997198	248.37	2.720E-05	
12	353000.0	14.730	14.730	0.994936	255.23	2.767E-05	
13	368600.0	15.240	15.206	0.996151	261.26	2.981E-05	
14	387200.0	15.750	15.715	0.994807	267.83	3.125E-05	
15	408500.0	16.260	16.385	0.994463	276.65	3.728E-05	
16	418900.0	16.770	16.754	0.997758	281.60	4.129E-05	
17	430700.0	17.280	17.304	0.997781	289.16	4.264E-05	
18	440400.0	17.790	17.771	0.999849	295.72	4.851E-05	
19	451100.0	18.300	18.262	0.999460	302.79	4.852E-05	
20	510600.0	21.370	21.440	0.998695	353.97	6.489E-05	
21	518400.0	21.880	21.935	0.998933	363.02	7.756E-05	
22	524900.0	22.390	22.460	0.998980	373.01	8.859E-05	
23	530300.0	22.900	22.898	0.999908	381.69	1.011E-04	
24	535200.0	23.410	23.419	0.999829	392.48	1.117E-04	
25	539500.0	23.920	23.921	0.999714	403.38	1.233E-04	
26	543300.0	24.430	24.403	0.999580	414.34	1.352E-04	
27	547400.0	24.940	24.971	0.998322	428.01	1.556E-04	
28	550500.0	25.450	25.450	0.997564	440.20	1.828E-04	
29	553500.0	25.960	26.010	0.999192	455.34	2.176E-04	
30	555600.0	26.470	26.481	0.999481	468.90	2.473E-04	
31	557400.0	26.980	26.939	0.999211	482.87	2.825E-04	
32	559300.0	27.490	27.506	0.996928	501.45	3.379E-04	
33	560900.0	28.000	28.052	0.996441	520.82	4.162E-04	
34	562100.0	28.510	28.552	0.984363	540.05	5.953E-04	
35	563000.0	29.020	28.765	0.000000	548.74	5.667E-04	]

36	563800.0	29.530	29.275	0.000000	570.86	6.375E-04	]
37	564500.0	30.550	30.040	0.000000	608.19	1.457E-03	]

SEVEN POINT INCREMENTAL POLYNOMIAL METHOD AND SECANT FOR DETERMINING DA/DN

Specimen name: ARL1RITE (GAUGES 2 AND 4)

M(T) specimen B = 10.000 mm W = 74.000 mm AN = 0.000 mm
Pmin = 0.00 N Pmax = 25000.00 N R = 0.00 TEST FREQ = 10.0 Hz
temp.= 21.0 C ENVIRONMENT = AIR

OBS.NO.	CYCLES	A(meas.) [mm]	a(reg.) [mm]	M.C.C.	DELK [MPa sqrt(mm)]	DA/DN mm/cycle]	
1	22900.0	9.810	10.065	0.000000	199.14	7.244E-06	]
2	93300.0	10.320	10.575	0.000000	205.16	1.609E-05	]
3	125000.0	10.830	11.085	0.000000	211.17	1.555E-05	]
4	157800.0	11.340	11.317	0.996718	213.92	1.592E-05	
5	184800.0	11.850	11.834	0.999652	220.04	1.702E-05	
6	215000.0	12.360	12.350	0.999302	226.17	1.763E-05	
7	243700.0	12.870	12.856	0.998960	232.23	1.846E-05	
8	274800.0	13.380	13.392	0.998558	238.71	2.101E-05	
9	297700.0	13.890	13.869	0.999449	244.53	2.306E-05	
10	321400.0	14.400	14.414	0.999717	251.28	2.590E-05	
11	387700.0	16.440	16.472	0.999616	277.80	3.609E-05	
12	400400.0	16.950	16.950	0.999653	284.27	3.673E-05	
13	412100.0	17.460	17.395	0.999068	290.42	3.918E-05	
14	426900.0	17.970	17.953	0.997159	298.32	4.080E-05	
15	496600.0	21.060	21.259	0.997299	350.74	6.612E-05	
16	501800.0	21.570	21.567	0.997152	356.26	7.694E-05	
17	507500.0	22.080	21.998	0.996475	364.18	8.547E-05	
18	527500.0	23.610	23.878	0.992375	402.41	1.137E-04	
19	529100.0	24.120	24.014	0.994470	405.45	1.244E-04	
20	533300.0	24.630	24.545	0.990704	417.68	1.249E-04	
21	537400.0	25.140	25.175	0.985518	433.12	1.419E-04	
22	540800.0	25.650	25.593	0.990397	443.97	1.484E-04	
23	545800.0	26.160	26.374	0.989995	465.75	1.639E-04	
24	546900.0	26.670	26.548	0.989679	470.88	1.716E-04	
25	549900.0	27.180	27.070	0.988136	487.04	1.953E-04	
26	553400.0	27.690	27.806	0.986050	511.90	2.384E-04	
27	555300.0	28.200	28.229	0.979431	527.47	3.356E-04	
28	556900.0	28.710	28.455	0.000000	536.21	3.187E-04	]
29	558400.0	29.220	28.965	0.000000	557.18	3.400E-04	]
30	559500.0	30.240	29.730	0.000000	592.40	9.273E-04	]

] - Secant method used

APPENDIX J - RUNNING PROGRAM CG90ARL

A text file (or batch file) was created to automate the CG90ARL processing. Each line of the file contained the input normally prompted for by the program during run time. The CG90ARL program could therefore be run for different by simply editing this text file and executing the .COM file by typing *@filename* (where the text file was saved as *filename*.com). This also provided a means of running multiple tests one after another automatically. Shown below is a typical .com file with a descriptor shown beside each row of input (not included in the .com file). Blank lines indicate that the default was accepted.

run cg	VAX command to run Fortran program cg
ALPHANEG	job name
GRR	operator's name
45kN Overload every 50000 cycles	title for the problerm
1	type of part for this analysis (plate with hole)
10.0000	specimen thickness
2.0000	hole radius
37.0000	distance from hole centre to edge of plate
6	type of crack (double thru crack)
7.0	initial crack length
1	type of loading (thru stress only)
33.78	fatigue reference thru stress
C	no residual stress intensities desired
0.0	retardation parameter phi
25000.	number of cycles between output
3000000.	maximum number of cycles to run
7050SI	material file
ML50K.SEQ	loading sequence file
50000.0	life shift
D	end run

APPENDIX K - RESULTS OF OVERLOAD STUDIES AT ΔK = 400 MPA$\sqrt{mm}$

Specimen	ARL2	Overload ratio =	1.8								
Gauge	1	delta K =	400								
W =	74 mm										
B =	10 mm										
i	a	a ave	delta a	P (N)	N actual	dK	da/dN (7050)	da/dN ave	dK eff	N (7050)	N retarded
1	8.69	8.815	0.25	55000	3768	405.4	0.000203097	6.635E-05	299.916889	1230.941671	2537.05833
2	8.94	9.065	0.25	54000	2088	404.5	0.000201408	0.0001197	351.615357	1241.262764	846.737236
3	9.19	9.315	0.25	53000	1141	403.3	0.000199246	0.0002191	413.779017	1254.730744	-113.730744
4	9.44	9.565	0.25	52000	3281	401.9	0.000196632	7.62E-05	311.309704	1271.409816	2009.59018
5	9.69	9.815	0.25	51000	2414	400.2	0.000193589	0.0001036	338.138245	1291.398105	1122.60189
6	9.94	10.065	0.25	51000	1250	406.2	0.000204642	0.0002	403.732734	1221.644543	28.3554567
7	10.19	10.315	0.25	51000	908	412.3	0.000216134	0.0002753	440.03997	1156.691118	-248.691118
8	10.44	10.565	0.25	49000	4920	401.9	0.000196605	5.081E-05	279.119828	1271.588281	3648.41172
9	10.69	10.815	0.25	49000	1248	407.7	0.000207309	0.0002003	403.906931	1205.928662	42.0713378
10	10.94	11.065	0.25	48000	836	405.0	0.000202341	0.000299	449.943319	1235.536148	-399.536148
11	11.19	11.315	0.25	84600	1	723.8	0.001746385	0.25	2756.62537	143.152891	-142.152891
12	11.44	11.565	0.25	47000	5875	407.7	0.000207341	4.255E-05	266.094537	1205.743657	4669.25634
13	11.69	11.815	0.25	47000	1048	413.2	0.00021805	0.0002385	423.365635	1146.524753	-98.5247533
14	11.94	12.065	0.25	45000	1627	401.0	0.000195021	0.0001537	376.057792	1281.912111	345.087889
15	12.19	12.315	0.25	44000	4826	397.3	0.000188475	5.18E-05	280.574114	1326.43298	3499.56702
16	12.44	12.565	0.25	44000	1527	402.6	0.00019779	0.0001637	382.539205	1263.265336	263.734664
17	12.69	12.815	0.25	44000	860	407.9	0.000207701	0.0002907	446.525628	1203.650882	-343.650882
18	12.94	13.065	0.25	44000	730	413.2	0.000217897	0.0003425	466.68146	1147.332488	-417.332488
19	13.19	13.315	0.25	44000		418.5	0.000228503			1094.076233	
20	13.44										

Key:

i	gauge strand number (1-20)
a	crack length at each strand number (measured before testing)
a ave	average crack length used for all calculations (= $[a_i + a_{i+1}]/2$)
delta a	distance between strands (interval over which average calculations are valid)
P (N)	load applied (if **bold** indicates overload was applied at start of that interval)
N actual	number of cycles for crack to grow through that interval (indicated by LABTECH and recorded by Instron)
ΔK	ΔK calculated using equation 6.1 at crack length = a_{ave}
da/dN (7050)	calculated da/dN at that ΔK value using equation 3.2 fitted to the data shown in figure 6.6
da/dN ave	recorded da/dN = delta a / N_{actual}
ΔK eff	ΔK_{eff} calculated from da/dN_{ave} using equation 3.2 and figure 6.6
N (7050)	number of cycles expected at that ΔK level over delta a using data in figure 6.6
Nretarded	number of cycles crack growth was retarded = N actual - N (7050)

Recorded da/dN compared to da/dN calculated using ARL1 data (overload=1.8)

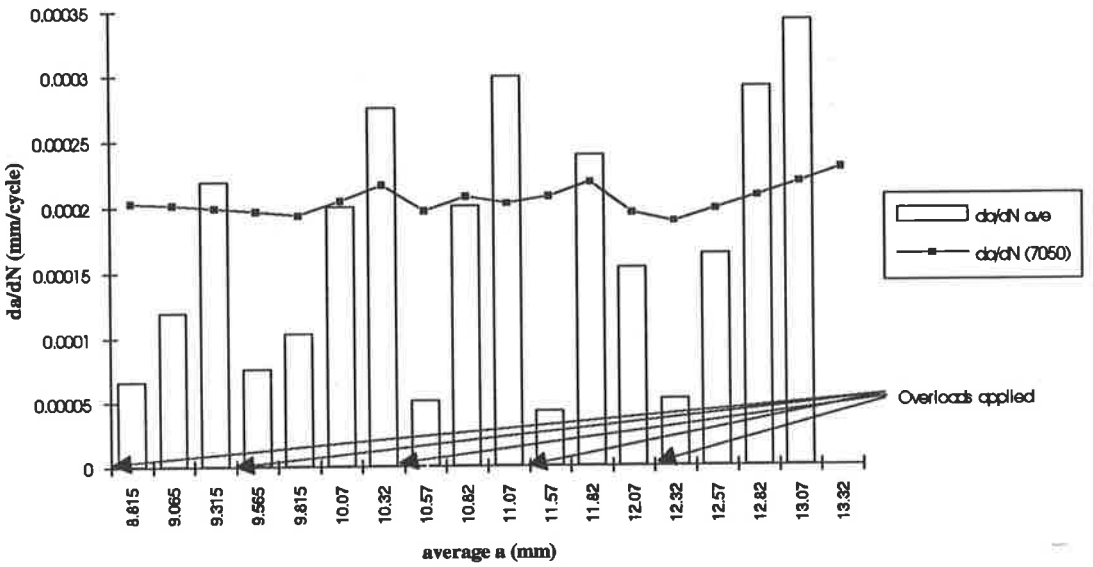

Effective delta K values Specimen ARL2 Gauge 1 (overload=1.8)

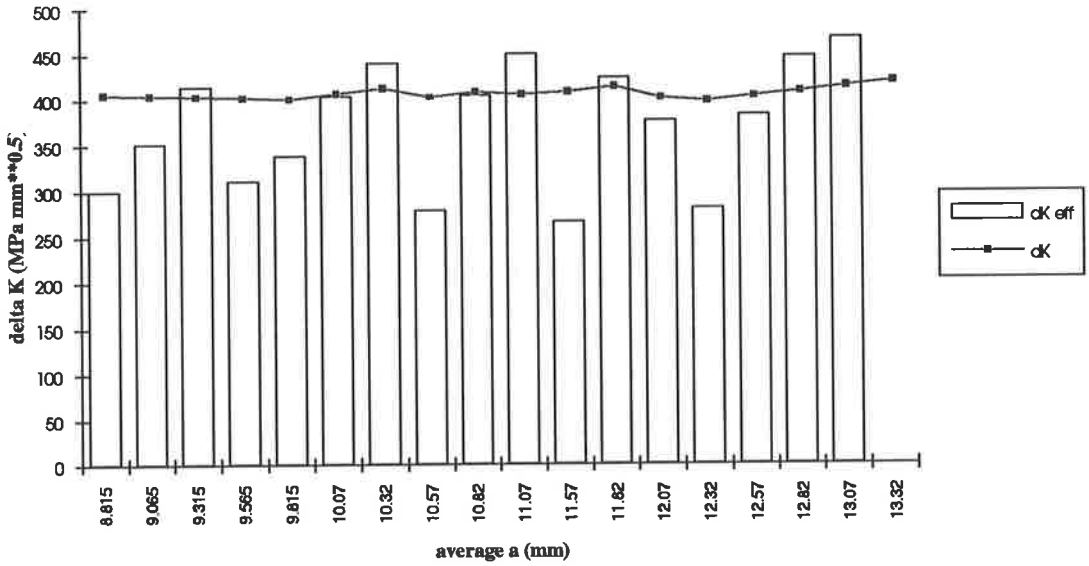

Specimen	ARL2 Overload ratio =	1.6								
Gauge	2									
W =	74 mm									
B =	10 mm									
i	a	a ave	delta a	P (N)	N actual	dK	da/dN (7050)	da/dN ave	dK eff	N (7050)	Nretarded
1	15.97	16.095	0.25	36800	2440	401.6	0.00019602 8	0.00010 25	337.16379	127.5.3305	116.4.6594 76
2	16.22	16.345	0.25	36800	1052	406.4	0.00020 501 3	0.00023 54	421.8.5484	121.9.4823	1.57.432 281
3	16.47	16.595	0.25	36000	1650	402.4	0.00019 759 7	0.00015 15	374.6.3838	125.5.2034	384.7.956 29 6
4	16.72	16.845	0.25	36000	1250	407.3	0.00020 662 5	0.00 02	403.7.3273	120.9.5203	400.7.97.334 2
5	16.97	17.095	0.25	35000	2590	400.8	0.00019 460 5	9.653E-05	331.7.8824	128.4.6548	130.5.34.520 5
6	17.22	17.345	0.25	35000	1530	405.6	0.00020 348 3	0.00016 34	382.3.3699	122.8.602	301.3.97.965 1
7	17.47	17.595	0.25	35000	930	410.5	0.00021 276 6	0.00026 88	437.2.1115	117.5.0006	-2.45.0.00.565
8	17.72	17.845	0.25	34000	1250	403.6	0.00019 977 9	0.00 02	403.7.3273	125.1.3839	-1.38.394.358
9	17.97	18.095	0.25	33000	3050	395.5	0.00018 698 9	8.197E-05	317.4.9297	133.6.9785	171.3.02.148 7
10	18.22	18.345	0.25	33000	1440	401.3	0.00019 553 8	0.00017 36	388.6.3252	127.8.5268	161.4.73.225 7
11	18.47	18.595	0.25	33000	970	406.2	0.00020 449 1	0.00025 77	432.2.7923	122.2.5473	-2.52.5.47.336
12	18.72	18.845	0.25	32000	1340	398.6	0.00019 078 7	0.00018 66	395.2.4128	131.0.364	296.359.617 3
13	18.97	19.095	0.25	32000	2780	403.5	0.00019 956 1	8.993E-05	325.5.2063	125.2.7523	152.7.24.766 3
14	19.22	19.345	0.25	31000	1200	395.7	0.00018 555 5	0.00020 83	408.1.9714	134.7.3124	-1.47.3.12.378
15	19.47	19.595	0.25	31000	930	400.5	0.00019 413 9	0.00026 88	437.2.1115	128.7.1378	-3.57.7.37.832
16	19.72	19.845	0.25	31000	513	405.4	0.00020 315 3	0.00048 73	513.2.0743	123.0.602	-7.17.6.02.025
17	19.97	20.095	0.25	30000	1557	397.2	0.00018 825 6	0.00016 06	380.5.3946	132.7.9817	229.0.18.285 4
18	20.22	20.345	0.25	30000	1380	402.1	0.00019 707	0.00018 12	393.1.1392	126.8.5863	111.4.13.664 2
19	20.47	20.595	0.25	30000		407.1	0.00020 634 1			121.1.5867	
20	20.72										

Key:

i	gauge strand number (1-20)
a	crack length at each strand number (measured before testing)
a ave	average crack length used for all calculations (= $[a_i + a_{i+1}]/2$)
delta a	distance between strands (interval over which average calculations are valid)
P (N)	load applied (if **bold** indicates overload was applied at start of that interval)
N actual	number of cycles for crack to grow through that interval (indicated by LABTECH and recorded by Instron)
ΔK	ΔK calculated using equation 6.1 at crack length = a_{ave}
da/dN (7050)	calculated da/dN at that ΔK value using equation 3.2 fitted to the data shown in figure 6.6
da/dN ave	recorded da/dN = delta a / N_{actual}
ΔK eff	ΔK_{eff} calculated from da/dN_{ave} using equation 3.2 and figure 6.6
N (7050)	number of cycles expected at that ΔK level over delta a using data in figure 6.6
Nretarded	number of cycles crack growth was retarded = N actual - N (7050)

Recorded da/dN compared to da/dN calculated using ARL7050 data (overload=1.6)

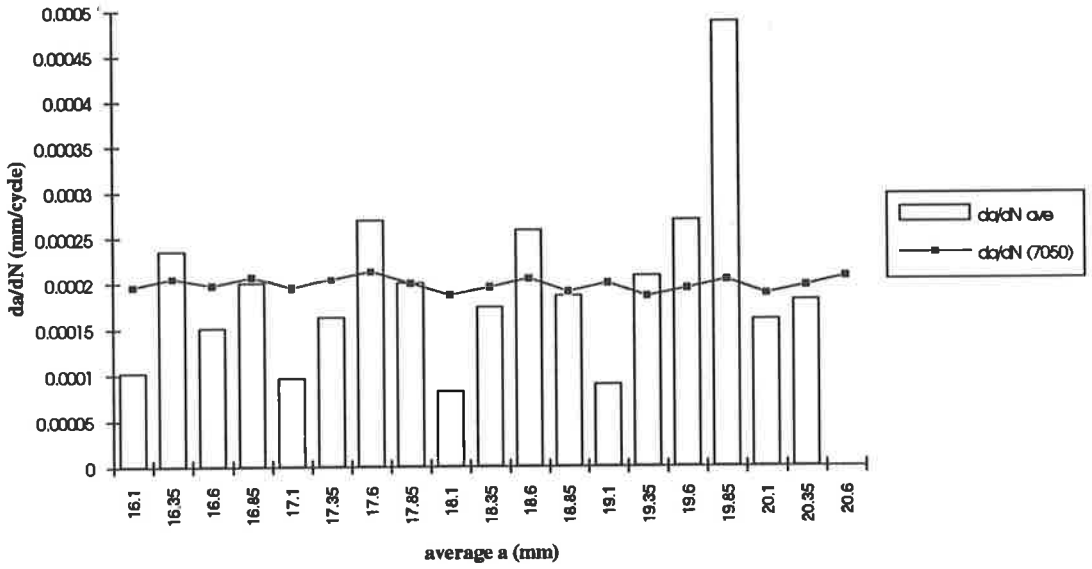

Effective delta K values Specimen ARL2 Gauge 2 (oload=1.6)

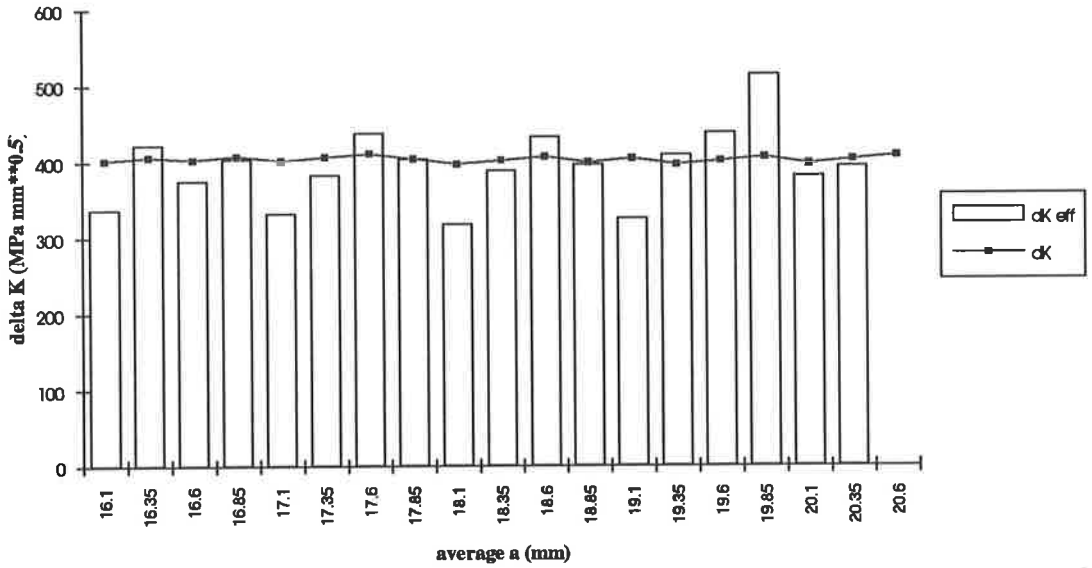

Specimen		ARL2	Overload ratio =		1.4						
Gauge		3									
W =	74	mm									
B =	10	mm									
i	a	a ave	delta a	P (N)	N actual	dK	da/dN (7050)	da/dN ave	dK eff	N (7050)	Nretarded
1	23.29	23.415	0.25	25700	1957	40.34	0.0001.9934	0.0001.277	35.780.668	12.54.1197	70.288.0299
2	23.54	23.665	0.25	25700	976	40.89	0.0002.0964	0.0002.561	43.1.56.172	11.92.5391	-216.5391
3	23.79	23.915	0.25	25000	1237	40.32	0.0001.9909	0.0002.021	40.4.87.139	12.55.7399	-18.739904
4	24.04	24.165	0.25	25000	1380	40.89	0.0002.0959	0.0001.812	39.3.11.392	11.92.8043	187.195716
5	24.29	24.415	0.25	24000	2160	39.80	0.0001.8973	0.0001.157	34.8.41.874	13.17.6412	842.358835
6	24.54	24.665	0.25	24000	1093	40.37	0.0001.9998	0.0002.287	41.8.59.766	12.50.1128	-157.11279
7	24.79	24.915	0.25	24000	992	40.96	0.0002.1092	0.0002.52	42.9.67.541	11.85.2798	-193.27979
8	25.04	25.165	0.25	23000	1526	39.82	0.0001.9008	0.0001.638	38.2.60.672	13.15.2498	210.750192
9	25.29	25.415	0.25	23000	2189	40.41	0.0002.0076	0.0001.142	34.7.16.919	12.45.2945	943.705479
10	25.54	25.665	0.25	23000	1175	41.02	0.0002.1219	0.0002.128	41.0.51.886	11.78.1665	-3.166479 1
11	25.79	25.915	0.25	23000	1175	41.65	0.0002.2446	0.0002.128	41.0.51.886	11.13.7656	61.234.3785
12	26.04	26.165	0.25	22000	1175	40.45	0.0002.0149	0.0002.128	41.0.51.886	12.40.7266	-65.72656
13	26.29	26.415	0.25	22000	1025	41.09	0.0002.1352	0.0002.439	42.5.90.413	11.70.8715	-145.87152
14	26.54	26.665	0.25	21000	1821	39.85	0.0001.9055	0.0001.373	36.4.81.717	13.11.9868	509.013222
15	26.79	26.915	0.25	21000	1269	40.50	0.0002.0231	0.0001.97	40.2.09.531	12.35.723	33.277.0274
16	27.04	27.165	0.25	21000	1620	41.17	0.0002.1502	0.0001.543	37.6.49.485	11.62.6672	457.332763
17	27.29	27.415	0.25	20000	1660	39.87	0.0001.9089	0.0001.506	37.4.02.906	13.09.6691	350.330907
18	27.54	27.665	0.25	20000	?	40.55	0.0002.0335			12.29.4164	
19	27.79	27.915	0.25	20000	NA	41.26	0.0002.1689			11.52.6373	
20	28.04										

Key:

i	gauge strand number (1-20)
a	crack length at each strand number (measured before testing)
a ave	average crack length used for all calculations (= $[a_i + a_{i+1}]/2$)
delta a	distance between strands (interval over which average calculations are valid)
P (N)	load applied (if **bold** indicates overload was applied at start of that interval)
N actual	number of cycles for crack to grow through that interval (indicated by LABTECH and recorded by Instron)
ΔK	ΔK calculated using equation 6.1 at crack length = a_{ave}
da/dN (7050)	calculated da/dN at that ΔK value using equation 3.2 fitted to the data shown in figure 6.6
da/dN ave	recorded da/dN = delta a / N_{actual}
ΔK eff	ΔK_{eff} calculated from da/dN_{ave} using equation 3.2 and figure 6.6
N (7050)	number of cycles expected at that ΔK level over delta a using data in figure 6.6
Nretarded	number of cycles crack growth was retarded = N actual - N (7050)

Recorded da/dN compared to da/dN calculated using ARL7050 data (overload = 1.4)

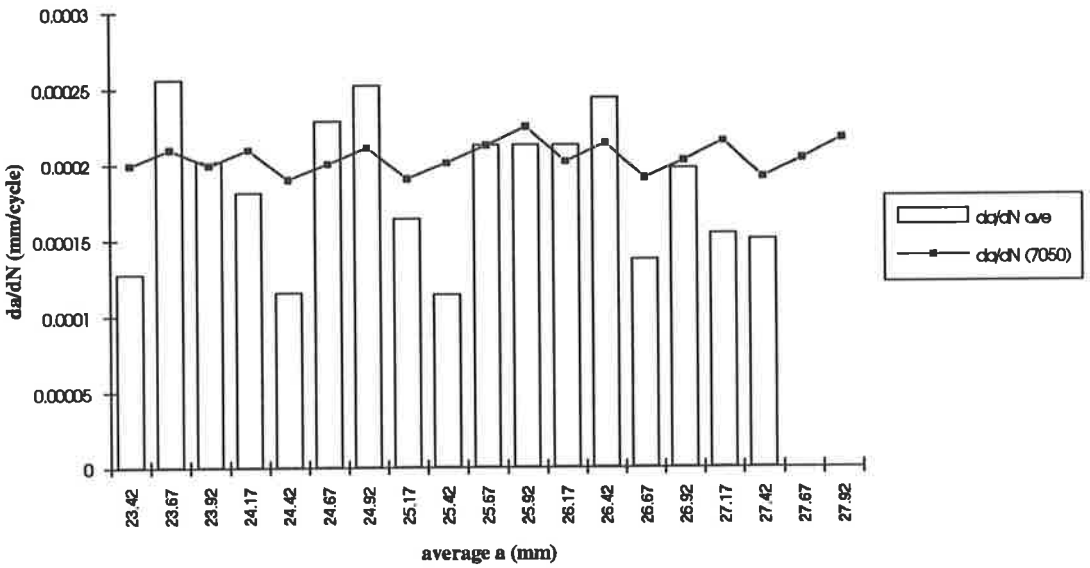

Effective delta K values Specimen ARL2 Gauge 3 (overload = 1.4)

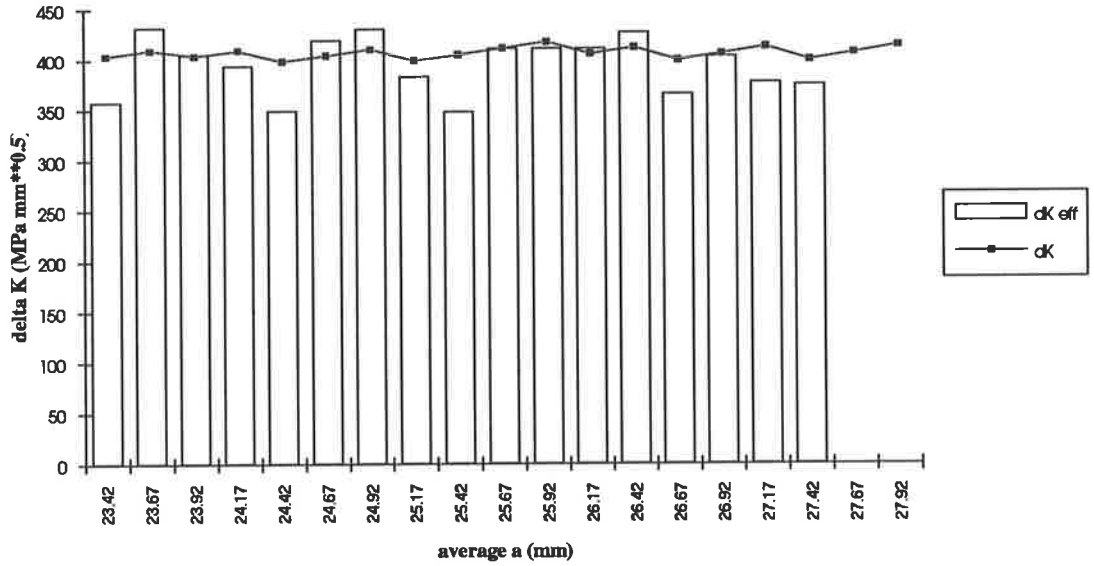

APPENDIX L - RESULTS OF OVERLOAD STUDIES AT ΔK = 300 MPA$\sqrt{mm}$

Specimen	ARL3	Overload ratio =	1.8							
Gauge	1	delta K =	300							
W =	74 mm									
B =	10 mm									
i	a	a ave	delta a	P (N)	N actual	dK	da/dN (ARL1)	da/dN ave	dKeff	N (ARL1)	N retarded
1	88	89.25	0.25	410.00	901.9	304.4	4.33175E-05	2.772E-05	262.034008	5771.3421	3247.65795
2	90.5	91.75	0.25	400.00	435.0	301.7	4.22044E-05	5.747E-05	334.659306.6	5923.5555	-1573.55553
3	93	94.25	0.25	400.00	516.5	306.5	4.42201E-05	4.84E-05	315.922319.7	5653.542	-488.541997
4	95.5	96.75	0.25	390.00	529.8	303.5	4.29279E-05	4.719E-05	313.238941.2	5823.7221	-525.722098
5	98	99.25	0.25	380.00	1122.0	300.2	4.15587E-05	2.228E-05	243.522935.5	6015.5804	520.441959
6	100.5	101.75	0.25	380.00	613.5	304.7	4.34396E-05	4.075E-05	298.196791.8	5755.1156	379.8841388
7	103	104.25	0.25	370.00	616.0	301.0	4.19078E-05	4.058E-05	297.790205.6	5965.5391	191.4410937
8	105.5	106.75	0.25	370.00	577.4	305.4	4.37446E-05	4.33E-05	304.326326.3	5714.9878	590.1224499
9	108	109.25	0.25	360.00	1368.8	301.4	4.20564E-05	1.826E-05	227.808358.1	5944.4045	774.3595465
10	110.5	111.75	0.25	360.00	734.7	305.6	4.38487E-05	3.403E-05	280.694662.6	5701.4202	164.557985
11	113	114.25	0.25	350.00	598.0	301.3	4.20131E-05	4.181E-05	300.767983	5950.521	29.47902
12	115.5	116.75	0.25	350.00	582.0	305.4	4.37584E-05	4.296E-05	303.517189.2	5713.8859	105.8141125
13	118	119.25	0.25	340.00	533.8	300.7	4.17849E-05	4.683E-05	312.449453.5	5983.1079	-645.107931
14	120.5	121.75	0.25	340.00	1128.9	304.8	4.34803E-05	2.215E-05	243.022530.9	5749.5579	553.9341206
15	123	124.25	0.25	330.00	766.8	299.7	4.13774E-05	3.26E-05	276.695177.6	6041.94	162.606
16	125.5	126.75	0.25	330.00	544.2	303.7	4.30237E-05	4.594E-05	310.433239.7	5810.754	-368.753951
17	128	129.25	0.25	330.00	679.8	307.6	4.47197E-05	3.678E-05	288.104795.4	5590.3824	120.7617577
18	130.5	131.75	0.25	320.00	713.2	302.2	4.23951E-05	3.505E-05	283.506691.8	5896.9102	123.5089777
19	133	134.25	0.25								
20	135.5										
1	16	161.25	0.25	276.00	1262.5	301.6	4.21536E-05	1.98E-05	234.071693.8	5930.4972	669.4302783
2	162.5	163.75	0.25	276.00	730.2	305.3	4.35978E-05	3.424E-05	281.273853.2	5721.1095	158.0490511
3	165	166.25	0.25	270.00	558.0	302.3	4.24236E-05	4.48E-05	307.835951.2	5892.9437	-312.943685
4	167.5	168.75	0.25	270.00	578.0	305.9	4.39729E-05	4.325E-05	304.220299.3	5685.3151	94.6848818
5	17	171.25	0.25	260.00	688.0	298.1	4.07284E-05	3.65E-05	287.651208.2	6138.2292	69.17708144
6	172.5	173.75	0.25	260.00	595.0	301.7	4.22137E-05	4.201E-05	301.275924.3	5922.2477	27.75234356
7	175	176.25	0.25	260.00	346.2	305.4	4.37531E-05	7.221E-05	361.303929.7	5713.8773	-2251.87773
8	177.5	178.75	0.25	254.00	510.0	302.0	4.23008E-05	4.902E-05	317.267552	5910.0534	-810.0534054
	18										

Key:

i	gauge strand number (1-20)
a	crack length at each strand number (measured before testing)
a ave	average crack length used for all calculations (= $[a_i + a_{i+1}]/2$)
delta a	distance between strands (interval over which average calculations are valid)
P (N)	load applied (if **bold** indicates overload was applied at start of that interval)
N actual	number of cycles for crack to grow through that interval (indicated by LABTECH and recorded by Instron)
ΔK	ΔK calculated using equation 6.1 at crack length = a_{ave}
da/dN (7050)	calculated da/dN at that ΔK value using equation 3.2 fitted to the data shown in figure 6.6
da/dN ave	recorded da/dN = delta a / N_{actual}

ΔK eff	ΔK_{eff} calculated from da/dN_{ave} using equation 3.2 and figure 6.6
N (7050)	number of cycles expected at that ΔK level over delta a using data in figure 6.6
Nretarded	number of cycles crack growth was retarded = N actual - N (7050)

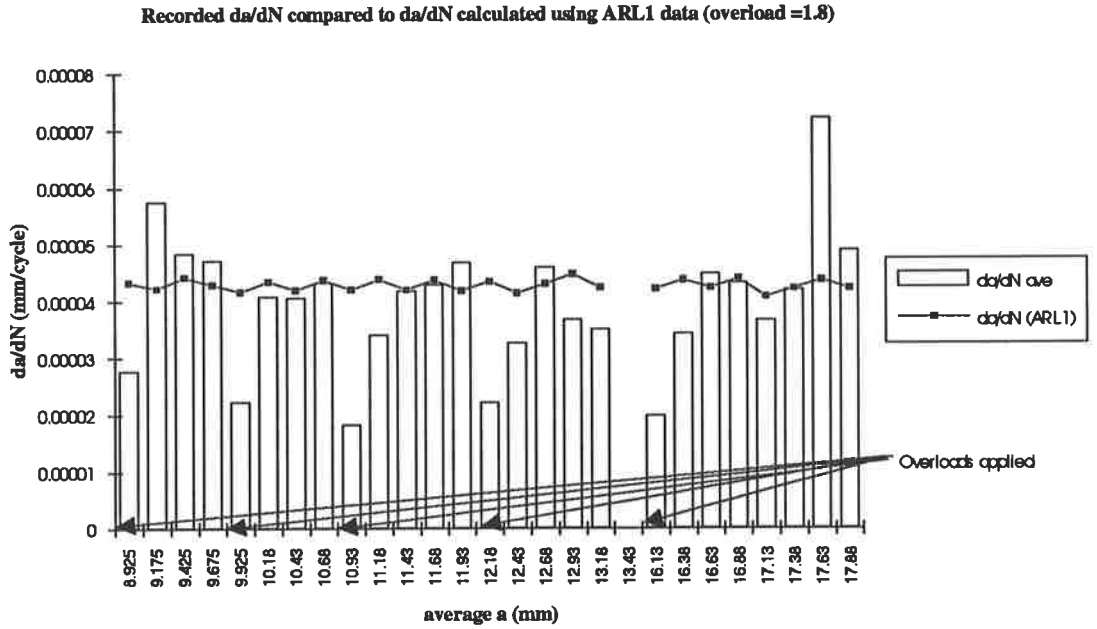

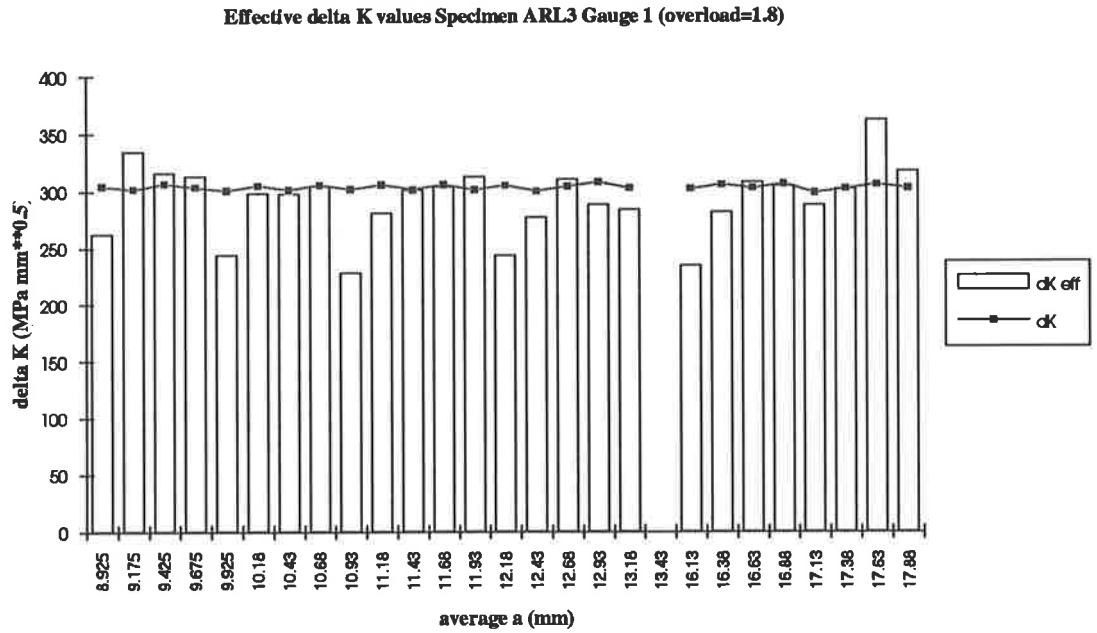

Specimen		ARL3 Overload ratio =		1.6						
Gauge		2 delta K =		300						
W =	74 mm									
B =	10 mm									
i	a	a ave	delta a	P (N)	N actual	dK	da/dN (ARL1)	da/dN ave	dK eff	N (ARL1)	N retarded
9	18	18.125	0.25	250.00	872.5	300.8	4.18191E-05	2.865E-05	264.9638	597.8307	274.6693
10	18.25	18.375	0.25	250.00	557.5	301.4	4.33477E-05	4.484E-05	307.9286	576.7219	-19.2781
11	18.5	18.625	0.25	245.00	540.1	302.0	4.23088E-05	4.629E-05	311.2219	590.8904	50.79037
12	18.75	18.875	0.25	245.00	556.5	305.6	4.38603E-05	4.492E-05	308.1141	569.9816	13.18454
13	19	19.125	0.25	245.00	479.5	309.4	4.54737E-05	5.214E-05	323.9001	549.7682	-70.2682
14	19.25	19.375	0.25	235.00	1166.0	301.7	4.21737E-05	2.144E-05	240.4003	592.7871	573.2128
15	19.5	19.625	0.25	235.00	531.6	305.4	4.37339E-05	4.703E-05	312.8827	571.6394	40.03935
16	19.75	19.875	0.25	227.50	803.0	298.0	4.06601E-05	3.113E-05	272.4468	614.8529	188.1471
17	20	20.125	0.25	227.50	603.5	301.7	4.21759E-05	4.143E-05	299.8455	592.7557	10.74428
18	20.25	20.375	0.25	227.50	535.5	305.4	4.37551E-05	4.669E-05	312.1163	571.3616	-35.8616
19	20.5	20.625	0.25	227.50		309.2	4.54014E-05			550.6436	
20	20.75										

Key:

i	gauge strand number (1-20)
a	crack length at each strand number (measured before testing)
a ave	average crack length used for all calculations (= $[a_i + a_{i+1}]/2$)
delta a	distance between strands (interval over which average calculations are valid)
P (N)	load applied (if **bold** indicates overload was applied at start of that interval)
N actual	number of cycles for crack to grow through that interval (indicated by LABTECH and recorded by Instron)
ΔK	ΔK calculated using equation 6.1 at crack length = a_{ave}
da/dN (7050)	calculated da/dN at that ΔK value using equation 3.2 fitted to the data in figure 6.6
da/dN ave	recorded da/dN = delta a / N_{actual}
ΔK eff	ΔK_{eff} calculated from da/dN_{ave} using equation 3.2 and figure 6.6
N (7050)	number of cycles expected at that ΔK level over delta a using data in figure 6.6
Nretarded	number of cycles crack growth was retarded = N actual - N (7050)

Recorded da/dN compared to da/dN calculated from ARL1(oload=1.6)

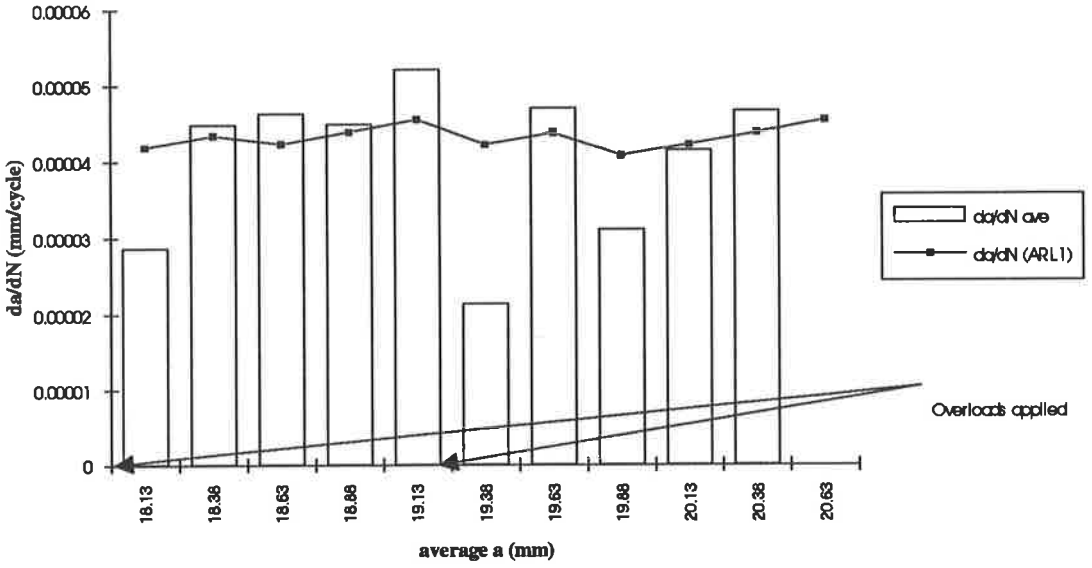

Effective delta K values Specimen ARL3 Gauge 2 (oload=1.6)

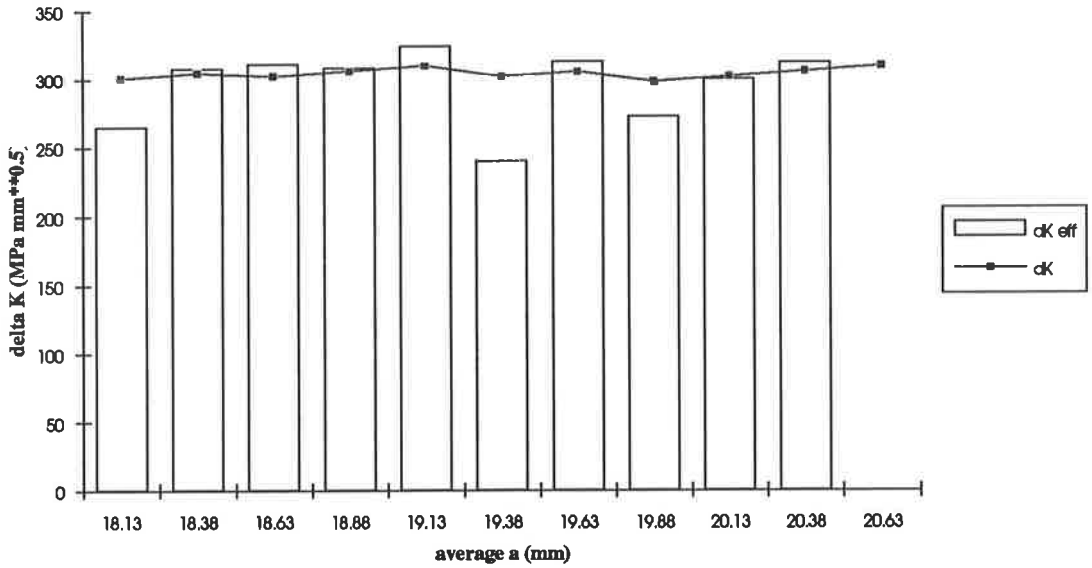

Specimen Gauge		ARL3 3	Overload ratio = delta K =		1.4 300						
W =	74	mm									
B =	10	mm									
i	a	a ave	delta a	P (N)	N actual	dK	da/dN (ARL1)	da/dN ave	dK eff	N (ARL1)	N retarded
1	23.3	23.425	0.25	19300	4360	303.1	4.27742E-05	5.734E-05	334.40158	5844.6406	-1484.6406
2	23.55	23.675	0.25	19300	3332	307.2	4.45396E-05	7.503E-05	365.97341	5612.9793	-2280.9793
3	23.8	23.925	0.25	18700	3080	301.8	4.22291E-05	8.117E-05	375.75831	5920.0825	-2840.0825
4	24.05	24.175	0.25	18700	3830	306.0	4.40099E-05	6.527E-05	349.26361	5680.5436	-1850.5436
5	24.3	24.425	0.25	18700	3380	310.3	4.58871E-05	7.396E-05	364.22139	5448.155	-2068.155
6	24.55	24.675	0.25	18000	4275	303.0	4.27228E-05	5.848E-05	336.61778	5851.6754	-1576.6754
7	24.8	24.925	0.25	18000	2167	307.3	4.45902E-05	0.0001154	422.80296	5606.6105	-3439.6105
8	25.05	25.175	0.25	17250	2204	298.9	4.10173E-05	0.0001134	420.40816	6094.9932	-3890.9932
9	25.3	25.425	0.25	17250							
10	25.55	25.675									
11	25.8										
12	26.05										
13	26.3										
14	26.55										
15	26.8										
16	27.05										
17	27.3										
18	27.55										
19	27.8										
20	28.05										

Key:

i	gauge strand number (1-20)
a	crack length at each strand number (measured before testing)
a ave	average crack length used for all calculations (= $[a_i + a_{i+1}]/2$)
delta a	distance between strands (interval over which average calculations are valid)
P (N)	load applied (if **bold** indicates overload was applied at start of that interval)
N actual	number of cycles for crack to grow through that interval (indicated by LABTECH and recorded by Instron)
ΔK	ΔK calculated using equation 6.1 at crack length = a_{ave}
da/dN (7050)	calculated da/dN at that ΔK value using equation 3.2 fitted to the data shown in figure 6.6
da/dN ave	recorded da/dN = delta a / N_{actual}
ΔK eff	ΔK_{eff} calculated from da/dN_{ave} using equation 3.2 and figure 6.6
N (7050)	number of cycles expected at that ΔK level over delta a using data in figure 6.6
Nretarded	number of cycles crack growth was retarded = N actual - N (7050)

Recorded da/dN compared to da/dN calculated using ARL1 (overload = 1.4)

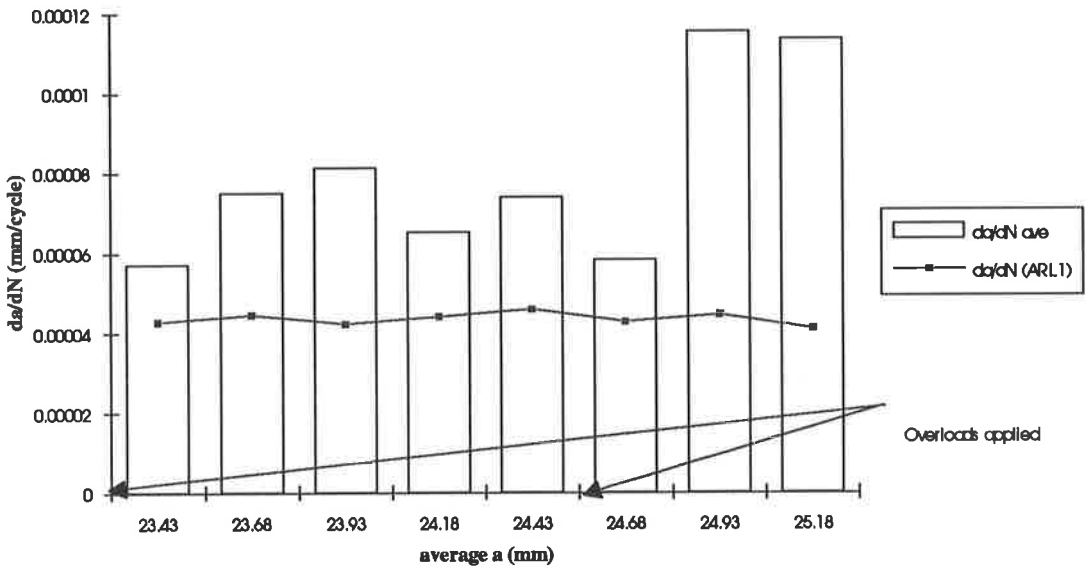

Effective delta K values Specimen ARL3 Gauge 3 (overload = 1.4)

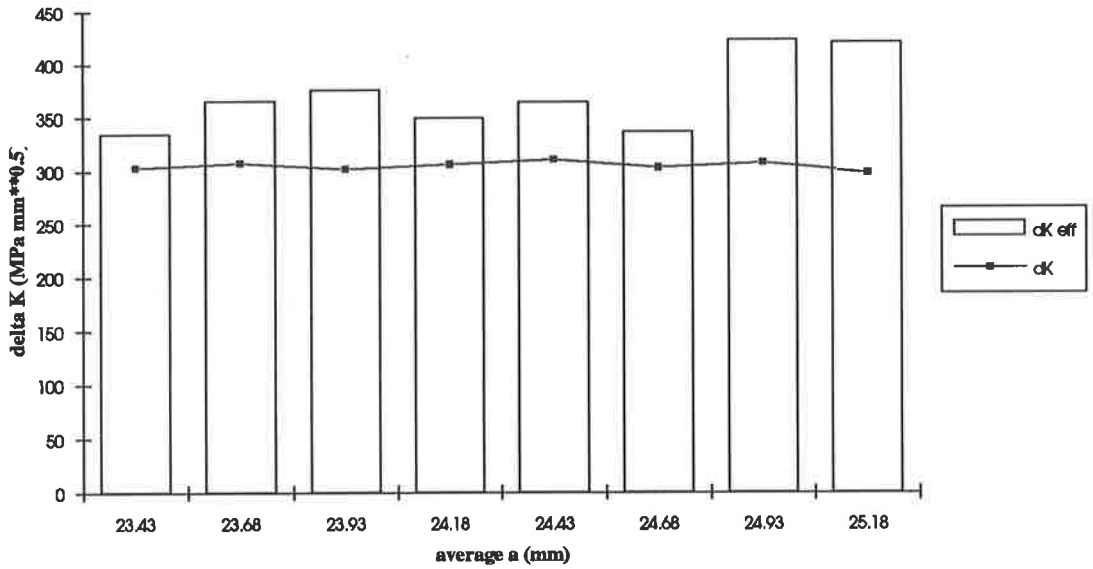

APPENDIX M - COMPENDIUM OF STRESS INTENSITY FACTORS - TABLE 1.3.1

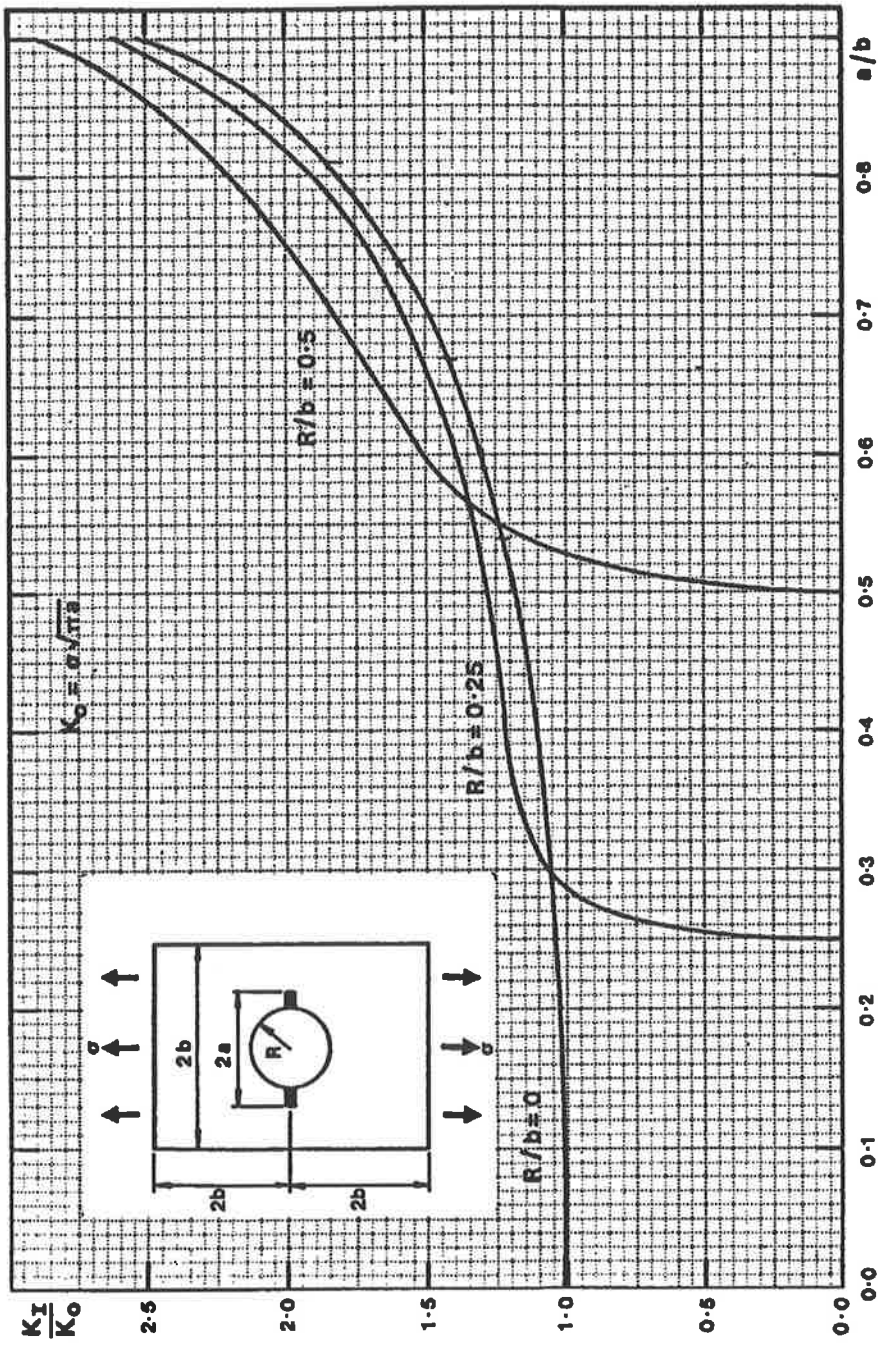

Fig. 105 K_I for two cracks at a circular hole in a rectangular sheet subjected to a uniform uniaxial tensile stress

APPENDIX N - COMPENDIUM OF STRESS INTENSITY FACTORS - TABLE 1.1.1

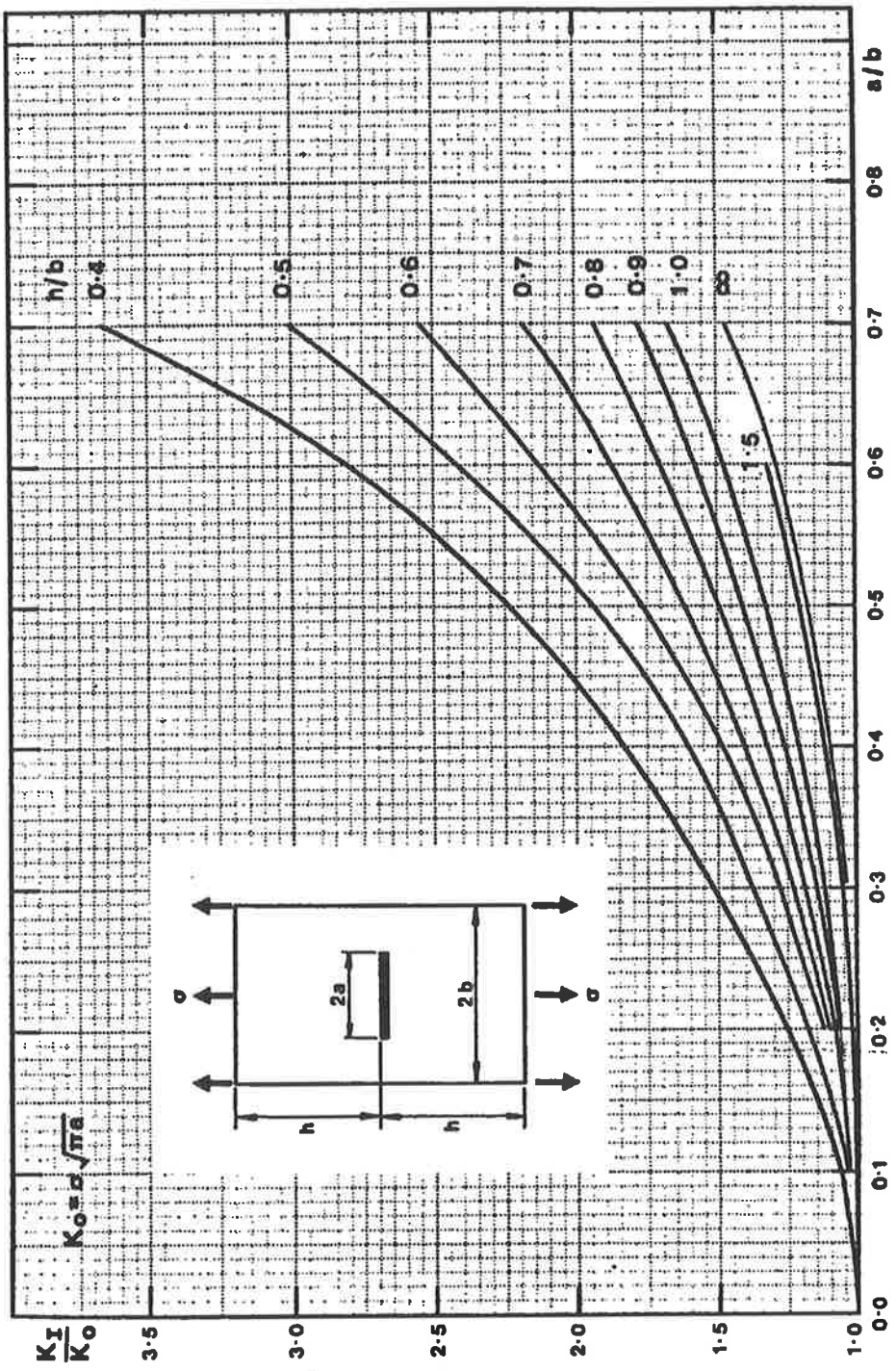

Fig.1 K_I for a central crack in a rectangular sheet subjected to a uniform uniaxial tensile stress